NTNU
Norwegian University of
Science and Technology

Analysis of the Reduced Wake Effect for Available Wind Power Calculation during Curtailment

Including Validation Experiments

Marthijn Peter Cornelis Bontekoning

Wind Energy
Submission date: January 2017
Supervisor: Torgeir Moan, IMT
Co-supervisor: Lars Sætran, EPT
                          Jan Bartl, EPT
                          Gerard Van Bussel, TU Delft

Norwegian University of Science and Technology
Department of Marine Technology

Analysis of the Reduced Wake Effect
for Available Wind Power Calculation
During Curtailment

Including Validation Experiments

Master of Science Thesis

For obtaining the degrees of Master of Science in
Offshore Engineering and Dredging at the Delft University of Technology and
Technology-Wind Energy at the Norwegian University of Science and Technology

by

M. P. C. (Marthijn) Bontekoning

Thesis committee	Prof. dr. G. J. W. van Bussel	TU Delft (chair holder)
	Dr. ir. M. B. Zaaijer	TU Delft
	Dr. ir. E. Lourens	TU Delft
	Mr. S. Sanchez Perez-Moreno, MSc	TU Delft
	Prof. L. R. Sætran	NTNU
	Dipl.-Ing. J. Bartl	NTNU
	Dr. ir. B. C. Ummels	Ventolines BV
	Ir. T. A. Walvis	Ventolines BV

EWEM   TUDelft   NTNU   Ventolines

ACKNOWLEDGEMENTS

Performing experiments on a 144MW wind farm during commercial operation is not standard procedure for a Master thesis, but a lot of fun. I consider this a very special opportunity and I would therefore like to start this report by thanking some of the people that helped me along the way to make it possible.

First of all, I would like to thank Bart Ummels and Ardaan Walvis from Ventolines, who coached me along every step of the project. I am very grateful for their trust and the many discussions on all kinds of topics. I am also grateful to Tonny Kroes and Marcel Gorter, who were available for many weeks to perform the curtailment experiments, and Brendan Williams, who helped me with the technical aspects of the data acquisition. Furthermore, I would like to thank everyone else from the Ventolines team for their collegiality. It has been a very rewarding experience to work with them and to learn so much from them.

At TU Delft, I would like to thank Sebastian Sanchez Perez-Moreno for the many meetings where we discussed the progress of my research. His feedback, guidance and commitment were very important to keep me on the right track. Similarly, I am grateful to Michiel Zaayer, who provided me with very detailed feedback on this report as well, and Gerard van Bussel and Eliz-Mari Lourens for completing my thesis committee.

As part of the European Wind Energy Master (EWEM), I also had the privilege of using the resources of NTNU. Although most of the work of this research was performed at TU Delft, Jan Bartl and Lars Sætran were always ready and accessible to provide feedback and arrange the organisational matters.

I would also like to explicitly thank the organization behind EWEM, especially Linda Gaffel and Marte Broos. Their commitment to overcome all the organizational and administrative challenges of a Master programming, where four universities need to work together, is very impressive and much appreciated.

Finally, on a personal note, I would also like to thank my family and friends for their patience, their support and for helping me put my research in a societal perspective.

Marthijn Bontekoning,
January, 2017

ABSTRACT

With increasing wind power capacity, the impact of wind power on power system operation increases. For a mature integration of large amounts of wind power, controlling wind farm output by temporary curtailment becomes increasingly relevant. Wind farm curtailment provides valuable technical and economic opportunities for balancing the power system. However, quantifying the exact amount of curtailed wind power at the wind farm level is not trivial. This is because curtailment induces a reduction of the wake effects, complicating the determination of the available power in the wind. Understanding the reduced wake effect is important to improve the technical reliability and business case of wind power curtailment, especially for very large offshore wind farms.

The purpose of this research is to present and validate an algorithm to determine the available power of a wind farm during curtailment. Current best practices in available power estimation is to sum the individual turbine available power signals. This leads to an overestimation, as the reduced wake effect is not accounted for. In the algorithm developed in this thesis, existing wake models play a key role in quantifying the reduced wake effect. These wake models have been validated first for wind turbine operation without curtailment and then for operation during curtailment. For the latter, curtailment experiments were prepared and executed on the existing nearshore wind farm Westermeerwind, consisting of 48 wind turbines in commercial operation. Based on that, the developed algorithm has been validated for wind turbines in a straight row and for sub-rated wind speeds.

In the experiments, the first turbine in the row was curtailed and the reduced wake effect was clearly observed at the second turbine. The reduced wake effect led to a power increase of the second turbine of 45% to 80% of the curtailed power of the first turbine. However, it also led to a power decrease for the third turbine in a range of 5% to 40% of the curtailed power. No noticeable structural changes in power production were observed from the fourth turbine onward. The algorithm was shown to perform well in calculating the available power at the second turbine, with the Jensen wake model delivering the lowest error. For the third turbine, the improvement of the algorithm over the current best practice was smaller, due to relatively large errors of the wake models for the third turbine. The Larsen wake model resulted in the lowest error considering the available power of the whole row of turbines.

Overall, it is concluded that the algorithm proposed and validated in this thesis delivers a significantly improved estimation of the available power during curtailment. It is recommended to continue study of the proposed algorithm by testing the performance of other wake models, performing more (types of) curtailment experiments and obtaining higher quality wind data.

TABLE OF CONTENTS

Appendices

1

INTRODUCTION

With increasing installed wind power capacity, the curtailment of wind power as a contribution to power balancing becomes increasingly more necessary. However, determining the available power of a wind farm under curtailment is not trivial, as curtailment changes the wake effects in a wind farm. Yet, this determination is imperative when calculating the net curtailed power. This thesis presents and validates an algorithm to determine the available wind power of a wind farm during curtailment.

1.1 Context of Research

Wind Power

The electricity market is currently experiencing a paradigm shift from a market dominated by generators running on fossil fuels, towards a more varied market with multiple renewable power sources. Wind power plays an important role in this transition for several reasons:

- It is clean in its operation.

- It has an unlimited energy reserve and is thus sustainable.

- It has political benefits with respect to fossil fuel systems.

- It is widely available.

- Its costs of implementation are lowering fast.

Continuing…

1

1

1.1 Context of Research, Continued

Power Production Challenges

Notwithstanding the well-known benefits of the renewable sources, the paradigm shift poses new challenges concerning the grid balance. These challenges are mostly related to its intermittent characteristics and (partly) unpredictable power output. These short-term and long-term uncertainties make it more difficult for the power supply to follow the demand.

Wind Power Curtailment

Taking into account must-run requirements of fossil fuel generators, high wind conditions might lead to a threat of overproduction of electricity, causing a potential power imbalance. This threat leads to the requirement of wind farms to temporarily reduce their power production. [1] This power reduction is referred to as wind power curtailment. The sum of the curtailment at turbine level over a wind farm equals the gross wind power curtailment.

Available Wind Power

The available power of an energy system is the maximum producible power at that moment. For conventional generators this is fairly easy to determine - generally equal to the installed capacity. For wind farms, however, this is more complex, as it depends on both the installed capacity and the wind conditions. The latter determines the production of the turbines directly, but also influences the wake development behind those turbines. This in turn, influences the power production of downstream turbines.

Reduced Wake Effect

The wake losses also depend on the operation of the turbines. When the turbines curtail their power generation, less energy from the wind is extracted and their wakes are reduced. Hence, downstream turbines experience an increase in incoming wind speed. This is referred to as the reduced wake effect during curtailment.

Continuing…

1.1 Context of Research, Continued

Available Power During Curtailment

As soon as wakes influence the power of a wind farm, one cannot simply add the gross curtailed power to the produced power to calculate the available power, which is referred to as the gross available power method. It is imperative to account for the reduced wake effect. It is the main objective of this research to present an algorithm to determine available power during curtailment taking this effect into account.

1

1.2 Research Objectives

Previous
Literature

Previous literature indicates the need of an accurate method for available power determination during curtailment. In a report by Belgian transmission system operator (TSO) Elia [2] the necessity is linked to the possibility of wind power to contribute to the hour-ahead and day-ahead energy balancing market. In the wind farm that was used for the curtailment experiments no large reduced wake effect was found, but it was noted that this effect depends on the wind farm design.

During this research a PhD research by T. Bozkurt [3] was published, that proposes a similar algorithm as this report, which is called the PossPOW algorithm. In the curtailment experiments the reduced wake effect was measured and the algorithm provided good results. The algorithm of this report differs in its implementation and selection of wake models.

Problem
Statement and
Hypothesis

The problem statement is formulated as: *there is currently no methodology to accurately calculate the available wind power during curtailment at the wind farm level.*

Hypothesis

The hypothesis is that estimating the available power on wind turbine level is accurate during curtailment and existing wake models can be augmented to model wakes during curtailment. This allows accurate modelling of the reduced wake effect and leads to an algorithm to determine the available wind power during curtailment, which can be validated using curtailment experiments.

Continuing...

1.2 Research Objectives, Continued

Research Objectives

In order to test the hypothesis the following four objectives are defined for this research:

1. Develop an algorithm to calculate the available wind power during curtailment using wake models.

2. Validate the wake models used in the algorithm.

3. Validate the wake models when applied to curtailed turbines.

4. Validate the complete algorithm.

Westermeerwind

For the last three objectives, measurement data from wind farm Westermeerwind is used as part of a collaboration with Ventolines BV. Experiments have been performed to obtain the right validation data.

Focus

The goal of this research is to test the ability of wake models to incorporate curtailment as an input parameter in order to calculate the reduced wake effect, allowing available power determination during curtailment. The dependency on additional models influencing the accuracy of this algorithm is minimized, while the severity of the wake effect itself - and thus the reduced wake effect - is maximized in the validation procedure. This combination allows to focus on the performance of the algorithm itself and potential errors being the most striking.

1

1.3 Document Outline

Thesis Parts

The structure of this report follows the four research objectives. Each objective is presented in a separate part of this document .

Part I: Algorithm

Part I first elaborates on the research context and rationale leading to the need for the algorithm in chapter 2. The algorithm, with all involved parameters and models, is presented in chapter 3.

Part II: Wake Modelling

Part II discusses the fundamentals about wakes and their properties in chapter 4 and the approach of modelling wakes in chapter 5. The two selected wake models are presented in chapters 6 and 7, including the implementation of curtailment as a modelling parameter. Wake measurements obtained from wind farm Westermeerwind are presented in chapter 8 and the wake models are validated in chapter 9.

Part III: Curtailment

In part III the ability of the wake models to calculate the power of downstream turbines during curtailment is tested with experiments. First, the experiments are introduced in chapter 10 and the results are discussed in chapter 11. Second, the results are used to validate the wake models during curtailment in chapter 12.

Part IV: Validation

In chapter 13 of part IV the algorithm of part I is tested with the experiments of part III using the wake models of part II.

Conclusion & Recommendation

The conclusion of the report is presented in chapter 14. Recommendations for further research and improvements of this research are presented in chapter 15. This report contains a Nomenclature and list of References at the end as well.

I

AN ALGORITHM FOR AVAILABLE POWER ESTIMATION DURING CURTAILMENT

Before the details of the algorithm are presented, first the rationale behind its development will be discussed in chapter 2. The reasons for curtailment are explained and the trends in the curtailment market are studied. Also, the problem is demonstrated when simply adding individual turbine available power signals to get the total available power at the wind farm level. In chapter 3, the algorithm is introduced with all its involved parameters and the uncertainties that need to be tested in this research are discussed.

7

2

RATIONALE FOR ALGORITHM

If wind power is to play a mature role in the electricity generation market, it will have to deliver more power balancing services. This will lead to more wind power curtailment, thus making proper determination of the curtailed volumes increasingly important.

This chapter discusses the rationale for an algorithm calculating the available power during curtailment, that allows this determination. First, the reasons for power curtailment in general are discussed. Second, the power curtailment market is briefly explained. The chapter closes with an example demonstrating the error when simply adding individual turbine curtailments (i.e. the gross curtailment) to obtain the total curtailed power at wind farm level.

2.1 Curtailment

Wind Power Curtailment

In standard conditions, a wind farm operator will exploit its assets at maximum financial optimum, which is to maximize the power production of the wind farm. In certain cases, however, reasons may arise that the operator wants to or is required to limit its production to a sub-maximum level. In these cases the wind farm is considered to be curtailed. This leads to costs of opportunity loss, i.e. the loss in profit from production with respect to the available power. The operator loses part of its revenue, which has an impact on the investment payback time. [4]

Continuing...

9

2.1 Curtailment, Continued

Curtailment Reasons

Many reasons can be identified to (temporarily) curtail wind power, such as:

- Surplus of (national) power production

- Maintaining upward power reserves

- Overplanting [5]

- (Very) low power demand

- Expected rising demand

These reasons will be discussed in the next few sections. The last two reasons are related to the need for and limitations of conventional power systems in the grid.

Surplus of Power Production

The most common reason for curtailment is a surplus of power production. This surplus can be either on a national level or from a specific party connected to the grid. The working of this curtailment market will be elaborated upon in section Curtailment Market. There are two main reasons why wind power is not a favorable choice for curtailment when there is a surplus for several hours:

1. In most European countries renewable energy sources have priority to deliver their power to the grid in order to achieve their sustainability goals. [6]

2. The marginal cost of wind power production are close to zero, whereas conventional systems have operational resource costs, e.g. coal of gas.

Continuing…

2.1 Curtailment, <small>Continued</small>

Upward Reserves   When a wind farm is continuously under curtailment, its curtailed power can act as an upward reserve. Because wind turbines can quickly change their curtailment level, this reserve can be sold as primary or secondary power reserve. [7] These types of power reserve are required to act after an event within several seconds or minutes, respectively. [8] These events can be either unexpected production loss of other power systems connected to the same grid or sudden unexpected consumption increase. Continuous calculation of the amount of curtailed power is essential to determine the volume and value of such a service.

Overplanting   Overplanting refers to the installed capacity of the wind farm being larger than the capacity of the local grid. This leads to compulsory curtailment of the wind farm during high wind speeds. This is the most important reason for curtailment in the United States of America [9].

Very Low Demand   The inertia of conventional systems contributes to the balance of the grid: sudden loss of power systems do not lead to instantaneous frequency changes. Therefore during low demand of power, a grid operator can favor conventional power systems instead of renewable energy sources that do not provide this inertial balancing service [9]. In these cases, despite their small marginal cost, wind farms might need to curtail their production.

Expected Rising Demand   The inertia discussed in the previous section to contribute to the frequency balancing of the grid, also means that the ramp-up time of conventional generators are rather large. Therefore, when demand is expected to rise, but there is a high risk of a reduction of wind power as well, wind power might (temporarily) be curtailed to ensure that the load gradient that must be met by the remaining power plants is within their dynamic capacities. [6]

2.1 Curtailment, Continued

Curtailment
Capability Wind
Turbines

There are two types of wind farm curtailment. One could either completely shut down a certain amount of turbines in the wind farm or curtail each of the turbines by a certain percentage. The latter method is more common and treated in this report. The most common way of curtailing the production a turbine is by blade pitching. [10] The thrust force of the blades is dependent on the pitch angle, so when accurately setting this angle, the power of the turbine can be curtailed precisely and quickly. Other curtailment methods, like overspeeding and yawing are not considered.

2.2 Curtailment Market

The Netherlands For the secondary reserves entities that submit either generation or load schedules are referred to as a power responsible party or PRP. The Dutch TSO TenneT charges these responsible parties a certain price if they deviate from their schedule. However, when the deviation contributes to the balance of the system they will be paid that price instead. [8]

Imbalance When the Dutch TSO TenneT notices a power imbalance in a 15 minute time segment (or power transfer unit, PTU) it is responsible to solve it. Some TSOs of other countries use PTUs of 30 minutes or 60 minutes duration. Two situations can be identified:

1. A surplus is expected and the TSO will ask the responsible parties to curtail their power. (downward adjustment)

2. A shortage is expected and the TSO will approach the responsible parties to ramp up their production. (upward adjustment)

This research considers the first situation only.

Volume Example Figure 2.1 shows the settled imbalance price of TenneT of the last week of 2015 for power curtailment and the power increase. This data can be obtained from the website of TenneT [11] and is updated every 15 minutes. The figure shows that the imbalance price can be very high for some PTUs. In these cases it might be financially interesting for a wind farm operator to curtail its power generation.

Continuing...

2.2 Curtailment Market, Continued

2

Market Trend   Figure 2.2 shows the increase of the total volume of the imbalance
market and the size of the market expressed in Euros. Both of
these values have increased over the last near-decade. Only the
part of the market where the imbalance price was higher than the
feed-in subsidy of the government are considered, as curtailment
would lead to a direct loss of this subsidy. A subsidy of $50\frac{€}{MWh}$
is indicated by the Netherlands Enterprise Agency for wind farms
located in large lakes, like Westermeerwind. [12]
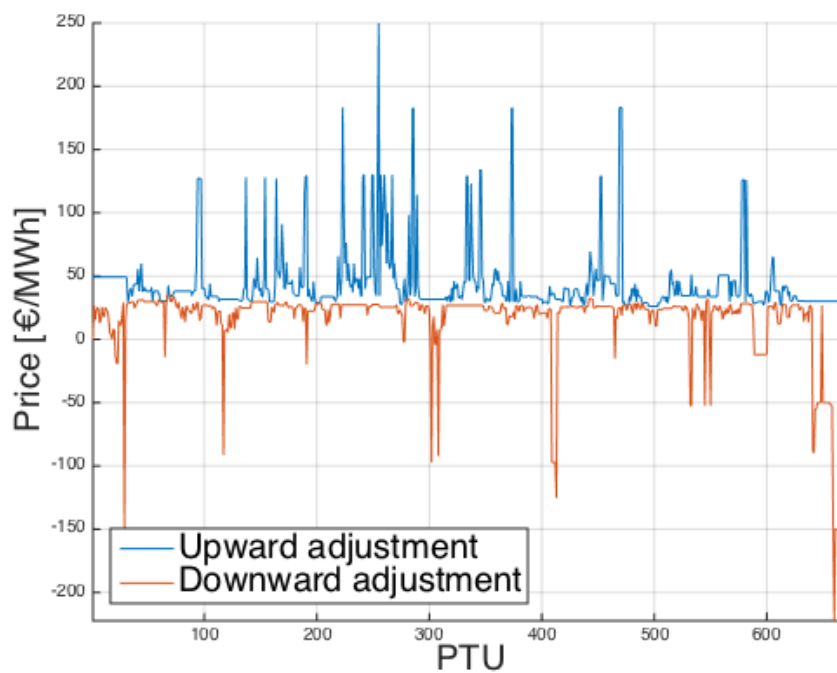
Figure 2.1: Settled prices for imbalance of Dutch TSO TenneT for the last week of 2015. [13]

2.2 Curtailment Market, Continued

Conclusion

Due to the increase of the imbalance market both in volume and in value, it can be expected that wind power curtailment will be performed increasingly more in the future. The only way to calculate how much power is being curtailed at the wind farm level, is to continuously calculate the power that the wind farm would have been producing if it was not curtailing. This supports the need for an accurate algorithm determining the available power during curtailment.

Figure 2.2: Increase in market growth of interesting part of power curtailment market for wind turbines (compensation higher than $50\frac{€}{MWh}$ only) [11][13]

2.3 Error Using Gross Available Power Method

Individual Turbine Curtailment

The curtailment of a individual turbine can be calculated by using the available power estimator (APE) [14]. This APE uses the pitch angle, rotational speed and the measured produced power as inputs to determine what the power production could have been if the turbine was operation in normal operation mode. This estimator was tested and proved to be reliable in the experiments on a individual turbine basis. However, it does not include the reduced wake effect due to curtailment of upstream turbines, when considering the available power of the whole wind farm.
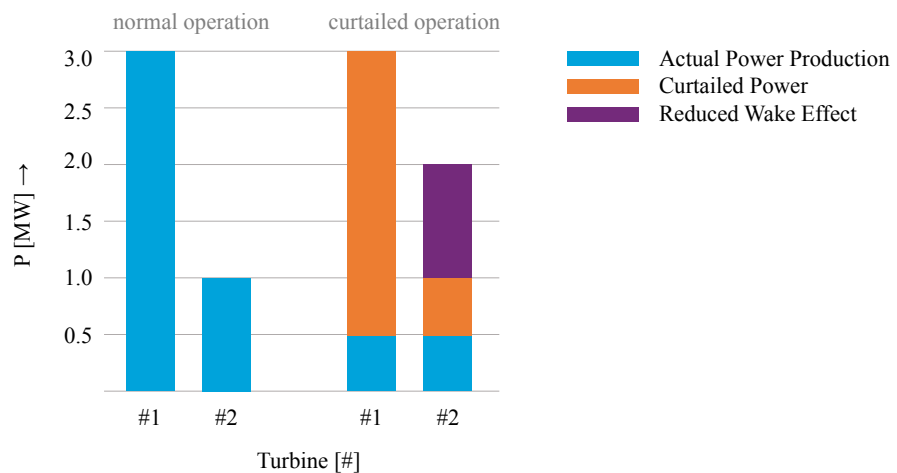
Figure 2.3: Example of the error when using the gross available power method. The height of the bars indicate the available power per turbine, consisting of the different parts.

2.3 Error Using Gross Available Power Method, Continued

Example

The following quantitative example demonstrates the error by simply adding the individual turbine curtailments to obtain the total curtailed power at wind farm level, which is the current best practice, referred to as the gross available power method.

- Consider the two turbines in figure 2.3 standing in line with the wind direction, operating without curtailment, i.e. the power production equals the available power.

- Turbine #1 produces $3MW$, but due to wake losses turbines #2 produces just $1MW$. The total available power therefore equals $4MW$.

- The production of both turbines are now curtailed to $0.5MW$ each. This leads to the gross curtailed power of the wind farm being $2.5 + 0.5 = 3MW$.

- Due to less power extraction from the wind by turbine #1, more wind energy becomes available for turbine #2 due to the reduced wake effect. Assume that this leads an increase in the available power of turbine #2 from $1MW$ to $2MW$.

- If now the total curtailed volume is determined again including the reduced wake effect, by determining the difference of the individual turbine available power and the individual actual production for each turbine, it leads to a gross curtailment of $2.5 + 1.5 = 4MW$. So it seems that the available power using the gross curtailment method depends on the curtailment of the turbines, which it should not.

- The production of the two turbines equals $1MW$ and the total available power therefore appears to have increased from $4MW$ before curtailment to $5MW$ during curtailment without a change in wind conditions.

- The size of this faulty calculated increase of the available power, when using the gross available power method, equals the reduced wake effect of $1MW$.

3

ALGORITHM

Now that the rationale of the algorithm has been established, the algorithm itself can be presented. In this chapter, first the requirements of the algorithm are stated. Second, all relevant involved parameters and required models are discussed. Third, the algorithm itself is presented and the unknowns of the models are identified.

3.1 Requirements Algorithm

Improvement versus Gross Method

Evidently, the algorithm needs to perform better and be more reliable in determining the available power at the wind farm level than the current best practice, which is to the sum the gross curtailed power and the measured power production.

Real time Evaluation

To ensure practical relevance of the algorithm, it is important to perform the calculations of the algorithm fast. Only with real time evaluation potential, the algorithm can be used for wind farm operators and grid operators to establish continuous agreement on the net curtailed wind power. After the PTU they can directly settle on the curtailed volume. This requirement results in advanced, computational heavy wake and power analysis - taking hours to process - not being appropriate elements of the algorithm.

Continuing…

19

3.1 Requirements Algorithm, Continued

Usage Turbine Data Signals

The algorithm needs to be robust enough to determine the available power using turbine data signals only. Using turbine data can have several disadvantages for the algorithm accuracy:

- The data signals can be rough in accuracy.
    - The sensors can be imperfectly calibrated, e.g. North not being exactly North.
    - The measurements can be influenced by the turbine presence.
- The sampling rate of the signals can be limited.
- The data signals are sometimes only valid in normal operation and not during curtailment.

Only Steady State

The purpose of the algorithm is to determine the available wind power of the wind farm for the steady state only. The steady state refers to the different power production values of the turbines due to the change in curtailment settings. This means that although the changing wind conditions are accounted for, the transient response of changing power production due to changing the curtailment settings of turbines is not.

3.2 Involved Parameters & Models

Wake Models   In order to model the difference in wake losses between normal operation and during curtailment existing wake models are used. The accuracy of the wake models are validated first, before implementing them in the algorithm. These wake models generally have the same inputs, which will be discussed in detail in part II:

- Wind speed

- Wind direction and farm layout

- Turbulence

- Turbine specifications, e.g. rotor diameter and thrust curves

Wind Speed   The most important parameter influencing the power of a single turbine is the wind speed. There are two types of wind speed:

- The free stream wind speed is experienced only by the turbines first in line with respect to the wind direction. This turbines are referred to as leading turbines.

- The local wind speed can be different for each turbine. Turbines that experience wake effects of upstream turbines, will have a lower local wind speed than the leading wind turbines.

Measuring Wind Speed   For wind farm Westermeerwind, the mean wind speed is determined using the power production of the turbine in combination with the power curve and not the from the sonic sensor. The method and reasoning behind this will be explained in section 8.2 Data Accuracy .

Continuing…

3.2 Involved Parameters & Models, Continued

3

Wind Direction	The wind direction determines which turbines are leading turbines and which turbines will experience wake effects.

Measuring Wind Direction	To accurately determine the wind direction for wind farm Westermeerwind the wake profile of the turbines are observed as will be explained in section 8.2 Data Accuracy .

Turbulence Intensity	The turbulence intensity is an important parameter that influences the wake development behind all turbines. In general lower turbulence levels lead to slower dissipation of the wake. This makes the need for such an algorithm ever more important for offshore wind farms, atmospheric turbulence is generally lower than onshore. Both the free stream turbulence level and the local turbulence (including the added turbulence from upstream turbines) at each turbine is determined. A hybrid method dependent on both the power production and the sonic sensor of the turbine is used as explained in appendix D.

Turbulence Models	During curtailment the local turbulence might be different than in normal operation mode. In order to determine this difference turbulence models can be used to allow a correction. However, this is outside the scope of this research and measured turbulence intensities are used during validation.

3.3 Proposed Algorithm

Algorithm

The algorithm consists of two parts:

1. The curtailment induced difference in wake loss with respect to normal operation needs to be determined for each turbine.

2. This difference needs to be subtracted from the individual gross available power (excluding the reduced wake effect) of each turbine which can be summed to get the total available wind farm power.

Flowchart

Figure 3.1 shows the flowchart describing the algorithm. It consists of the two parts, which are indicated by the two different colors and discussed in the next few sections. Each of the parameter in figure 3.1 is explained in table 3.1.
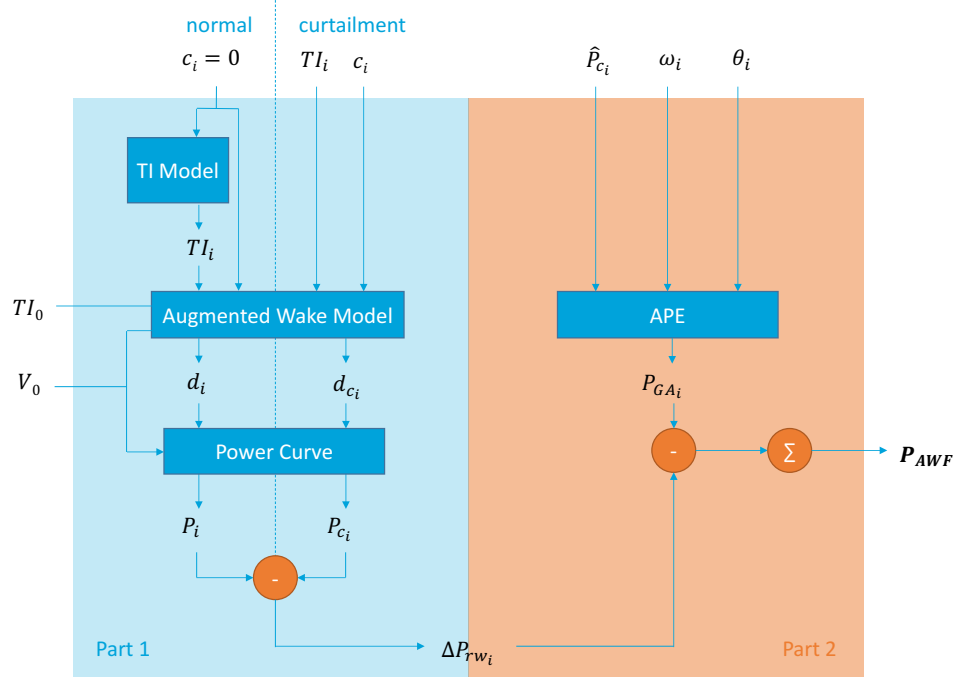
3

Figure 3.1: Flowchart of the Algorithm, see table 3.1 for the explanation of the used symbols

Table 3.1: Parameters of flowchart in figure 3.1

Symbol	Explanation
θ_i	Blade pitch angle of turbine i
ω_i	Rotational speed of turbine i
APE	Available power estimator
c_i	Curtailment factor of turbine i
d_{c_i}	Wind speed deficit at turbine i during curtailment
d_i	Wind speed deficit at turbine i in normal operation mode
ΔP_{rwi}	Reduced power loss of turbine i due to wake reduction
P_{AWF}	Available wind farm power, including the reduced wake effect
P_{GA_i}	Gross available power of turbine i, excluding the reduced wake effect
P_i	Modelled power production of turbine i in normal operation
P_{c_i}	Modelled power production of turbine i during curtailment
$\hat{P}_{c_i}$	Measured power production of turbine i during curtailment
TI_0	Free stream turbulence intensity
TI_i	Turbulence intensity at turbine i
V_0	Free stream wind speed

3.3 Proposed Algorithm, Continued

Algorithm Part 1

For the first part of the algorithm the augmented wake models are run twice:

- First, the augmented wake model is evaluated not taking into account any curtailment of the wind farm. The augmented wake models are expansions of existing wake models to allow the additional input parameter of curtailment, see the next section. This run calculates the value P_i for each turbine as seen in the flow chart.

- Second, the augmented wake model is run with the curtailment factor of each turbine, which can be determined using equation 3.1. This calculates the value P_{c_i} in the flow chart for each turbine.

$$c_i = \frac{\hat{P}_{c_i}}{P_{GA_i}} \tag{3.1}$$

The difference between these two model evaluations calculates the curtailment induced reduced wake (ΔP_{rw_i}), using equation 3.2.

$$\Delta P_{rw_i} = P_{c_i} - P_i \tag{3.2}$$

Augmented Wake Models

Augmented wake models are based on existing wake models, but are combined with several auxiliary models. They have the additional input parameter of curtailment and the output is the wind speed deficit of each turbine, see figure 3.2. The flowchart of figure 3.2 needs to be run stepwise from turbine #1, which has no wind speed deficit ($d_{c_1} = 1$), to the second last turbine. On each run the wind speed deficit of the next turbine is determined.

3
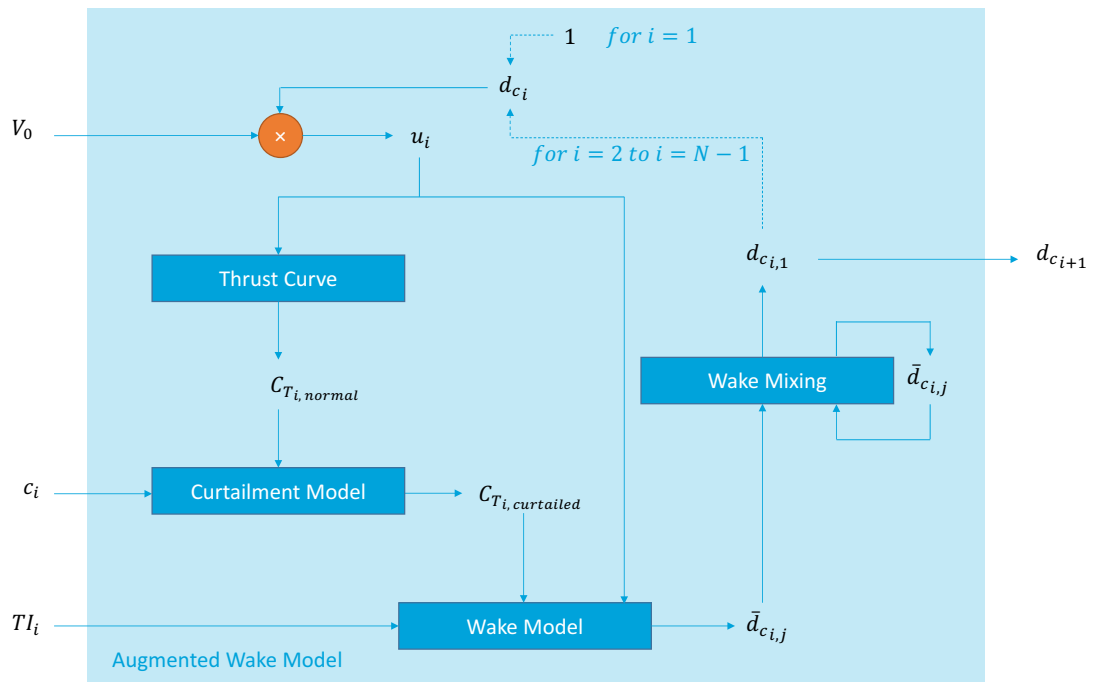
Figure 3.2: The augmented wake model, see tables 3.1 and 3.2 for the explanation of the used symbols. Note that turbine and wind farm constants, like rotor diameter and turbine spacing, are not visualized.

Table 3.2: Parameters of flowchart in figure 3.2 in addition to table 3.1

Symbol	Explanation
$C_{T_{i,normal}}$	The thrust coefficient of turbine i if the turbine would not curtail its power
$C_{T_{i,curtailed}}$	The thrust coefficient of turbine i including curtailment
$\bar{d}_{c_{i,j}}$	Vector of wind speed deficits at downstream turbines j due to turbine i only
$d_{c_{i,1}}$	The wind speed deficit at the turbine directly downstream of turbine i
j	A turbine downstream of turbine i, i.e. $j \in (i+1, N)$
N	Number of turbines
u_i	Wind speed at turbine i

3.3 Proposed Algorithm, Continued

Thrust Coeffient

The incorporation of curtailment could be different for each type of wake model. In section 5.2 Wake Model Auxiliaries it will be explained that using a different thrust coefficient is a method of effectively setting the curtailment factor for the wake models in this research. This coefficient can be determined from the thrust curve when the wind speed at that turbine is known. The thrust curve is specific to each turbine design. However, it describes the thrust coefficient in normal operation, which needs to be altered by the curtailment model to obtain the value during curtailment. Note that an inherent requirement of the curtailment model is that $C_{T_{i_{curtailed}}} \rightarrow C_{T_{i_{normal}}}$ for $c \rightarrow 0$, resulting in normal wake modelling without applying curtailment.

Wake Mixing

During wake mixing the wake effects from all upstream turbines are combined to a single wind speed deficit for turbine $i+1$. Different methods of mixing wakes are known, which will be discussed in section 5.2 Wake Model Auxiliaries . In each run, only the wind speed deficit for the turbine directly next ($d_{c_{i,1}}$) can be calculated additionally, as only for that turbine all the information from its upstream turbines is known. This is due to the feedback relation of the operation thrust coefficient of a turbine on its wind speed, which is determined by the wake effects of upstream turbines. See the dashed line in the flowchart of figure 3.2, where the output of a run ($d_{c_{i,1}}$) is the input for the next run (d_{c_i}).

Continuing…

3.3 Proposed Algorithm, Continued

Algorithm Part 2　　The second part of the algorithm is dependent on the individual turbine available power. This can be determined using the pitch-power and rotational speed-power curves of the turbine. The detailed procedure of this lies outside the scope of this thesis, but for example, by knowing the pitch curve one can determine the deviation from the normal power production using the measured pitch angle. The wind turbines of wind farm Westermeerwind are equipped with an Available Power Estimator (APE) [14], which does this procedure internally and has a high accuracy when disregarding the reduced wake effect. Therefore the APE signal is used in this research. This is a gross available power (without wake reduction) per turbine, referred to in figure 3.1 with symbol P_{GA_i}. Finally, the total wind farm available power can be calculated using equation 3.3.

$$P_{AWF} = \sum_{i=1}^{N} \left(P_{GA_i} - \Delta P_{r w_i} \right) \tag{3.3}$$

3.4 Algorithm Uncertainties

Uncertainties

Although the whole algorithm needs to be validated as it is unknown of the approach itself will yield good results, several elements within the algorithm also introduce uncertainties.

3

Using Wake Models Instantaneously

Wake models are generally used and validated using 10-minute averages. The goal of the algorithm is to provide a real time signal of the available power during curtailment. It needs to be validated if using the wake models instantaneously provides acceptable results. This is done in part II.

Wake Modelling During Curtailment

The wake models are augmented in part II to include curtailment as an input. This approach needs to validated, which is done in part III.

Using Power Curve Instantaneously

The power curve provides a relation between wind speed and power production of a turbine. However, power curves are generally only guaranteed using 10-minute averages and using a long measurement period. It needs to be validated if using the power curve instantaneously yields acceptable results, this is done in section 8.2 Data Accuracy .

Turbulence Model

Although no turbulence model is used in this algorithm to minimize errors and uncertainties, for the full algorithm this will be an integral part. Further study needs to determine the additional uncertainty of the algorithm when the turbulence model becomes part of it.

II

WAKE MODELLING

In this part existing wake models that are part of the augmented wake models of the algorithm are studied. First, the fundamentals of wakes, including their main parameters, and the basics of wake modelling are examined in chapters 4 and 5, respectively. Second, the Jensen wake model and the Larsen wake model, which are used for the algorithm, are reviewed in chapters 6 and 7, respectively. Third, the validation data used for wake model validation without curtailment is studied in detail in chapter 8, including its measurement context and accuracy. Finally, the validation of both wake models without curtailment is performed in chapter 9.

31

4

WAKE FUNDAMENTALS

Before going into detail about modelling wakes, first the wake phenomena itself should be understood correctly. This chapter starts with an overview of the different parts of wake study, which can be skipped by the readers who are familiar with wake modelling. Second, the most important wake properties and the parameters that influence them are discussed.

4.1 The Study of Wakes

Betz Limit

In 1920 Albert Betz introduced a law describing the maximum efficiency of a horizontal axis wind turbine. Using the actuator disk theory, he established the power coefficient as in equation 4.1. The parameter a refers to the induction factor, which is a ratio of wind speed before and after the turbine. The theoretical maximum power coefficient can be found as $C_P(\frac{1}{3}) = \frac{16}{27}$, which is referred to as the Betz (or Betz-Joukowski) limit. [15]

$$C_P(a) = 4a(1-a)^2 \tag{4.1}$$

Continuing...

33

4.1 The Study of Wakes, Continued

Inevitability of
Wakes

Equation 4.2 [16] calculates the wind speed in the far wake u_1 of a wind turbine using the induction factor a and the free stream wind speed V_0. This equation is primal and does not include wake dissipation or turbulence, but is a mathematical result of the momentum theory of William Froude. Using the optimal induction factor for power generation as found in the previous section ($a = \frac{1}{3}$), results in a wind speed deficit factor of $\frac{u_1}{V_0} = \frac{1}{3}$. So, although wakes cause negative effects on downstream turbines, they are inevitable for power generation.
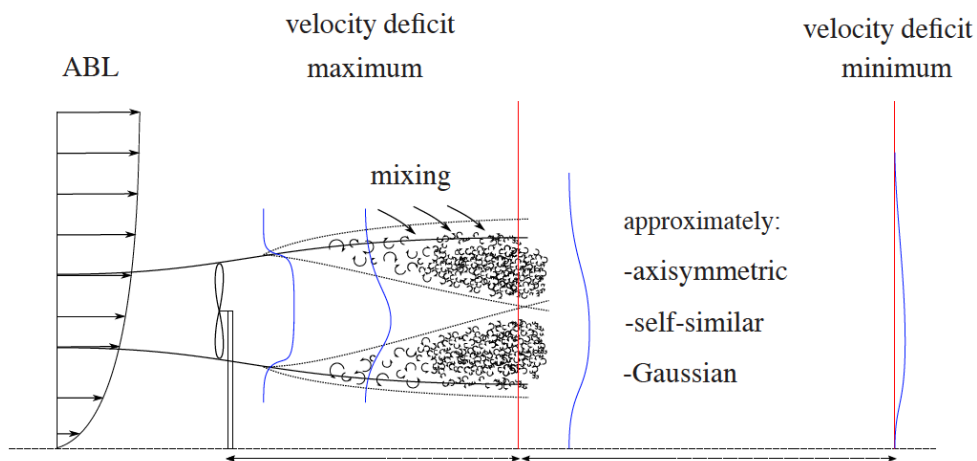
$$u_1 = (1 - 2a)V_0 \tag{4.2}$$

Figure 4.1: Wake expansion[17]

4.1 The Study of Wakes, Continued

Wake Regions

When studying wakes, two regions with different characteristics can be defined, as shown in figure 4.1.

- Directly behind the turbine (the near wake) the wake profile has an almost rectangular shape. The exact shape and size of the wake profile are highly complex and depend heavily on the aerodynamics of the blade.

- Further downstream the deficit profile morphs into a Gaussian-like shape due to the increasing turbulent air as a result from the tip vortex. [18] At a certain downstream distance the whole air can be considered turbulent. This is where the second region starts (the far wake).

The border between the near and far wake is often taken to be at around three times the diameter ($3D$) downstream of the turbine. [3][17][19] However, there is still a debate on the transition zone and where it stops exactly. As most often turbines, and definitely those considered in this report, are spaced further apart, **only the far wake is considered in this research**.

Symmetry

Wakes cannot develop axisymmetrically for two reasons:

1. The ground limits the wake to expand vertically at a certain distance downstream. At that distance the wake can only absorb free stream momentum from above.

2. When the wakes of two neighbouring turbines meet, they cannot absorb free stream momentum anymore. They can therefore not grow across the interaction plane. However, due to the limitation of only straight line turbines in this research, this assymmetry does not occur.

4.2 Parameters Influencing Wake Development

Wake Parameters   It is important that all the relevant parameters are measured and
                   simulated correctly in order to validate the algorithm proposed in
                   this research. The following parameters can influence the wake
                   development significantly, which are discussed in this section:

- Free stream wind speed

- Free stream turbulence

- Wind shear

- Curtailment

Free Stream   At higher wind speeds the turbine will extract more power from
Wind Speed   the wind and therefore cause a larger wind speed deficit. The rela-
                   tion between power extraction and wind speed is described by the
                   power curve. At wind speeds higher than rated wind speed, how-
                   ever, this statement is no longer true. Therefore, in this research
                   only wind speeds below rated power are considered.

Free Stream   The wind speed deficit of the wake fluid dissipates as it interacts
Turbulence   with the free stream fluid that has a higher momentum. The rate
                   of momentum transfer into the wake depends on the turbulence
                   of these two fluids. At higher turbulence levels this rate is higher
                   and the wake therefore dissipates faster. [20] Proper quantification
                   of the turbulence is therefore essential in wake analysis.

Continuing…

4.2 Parameters Influencing Wake Development, Continued

Wind Shear

The wind shear is the phenomena describing the wind speed profile in zenith (upwards) direction. This relation is commonly expressed by the expression in equation 4.3 with $m \in [0.1, 0.25]$, where $u(z)$ is the wind speed at elevation z and u_{hub} is the wind speed at the hub, which is located at altitude z_{hub}. Due to the wind shear the wind speed is higher at the top of the wake than at the bottom, effectively tilting the wake forwards. Due to the complexity and small effect on the mean wind speed and power production **the effect of the wind shear is neglected**.

$$u(z) = u_{hub} \left(\frac{z}{z_{hub}} \right)^m \tag{4.3}$$

Curtailment

The focus of this research is on the effect of curtailment on the wake effect. This effect is expected to be twofold.

1. Due to less power extraction from the wind during curtailment, the wind speed deficit is expected to be lower.

2. Due to the decrease in blade-flow interaction during curtailment, the turbine induced increase of turbulence intensity is expected to decrease.

4.3 Wdake Influencing Power Production

Wind Speed Deficit

The most important and direct wake property influencing the power production of a turbine is the wind speed reduction due to upstream turbines. This deficit gradually dissipates over time and distance behind the turbine, but it can still be noticeable for downstream turbines.

Increased Turbulence

The second most important - but indirect - wake property influencing the power production of a wind farm is the local turbulence at each turbine. The effect of turbulence on wake development is discussed in the previous section, but besides the atmospheric turbulence for free standing turbines, in a wind farm every turbine adds turbulence for its downstream turbines as well. This phenomenon is referred to as turbine induced turbulence (or increased turbulence).

Curtailment Induced Increased Turbulence

It is expected that the increased turbulence is dependent on the curtailment setting of the turbine. This is confirmed by [21], where the increased turbulence at a distance $3D$ downstream drops from 27% to 15% by pitching the blade 5°. However, insufficient literature was found to draw conclusions, so this phenomenon will be described in more detail after the experiment in section 11.2 Experimental Results .

Angular Position Farm Layout

The wind speed deficit depends on the downstream angular (out of straight line) position. This depends on both the wind direction and the farm layout. To keep wake model implementation manageable and allow the focus of this research to be on curtailment and not on flexible wake model implementation, **only turbines in a straight row are considered for this research**.

Continuing…

4.3 Wake Influencing Power Production, Continued

Meandering

Wake meandering is the phenomena describing the stochastic pattern of wake propagation. Due to changing wind directions and turbulent eddies larger than the size of the rotor, the wake does not propagate over a straight line, but has a rather stochastic path. This effect has a significant effect on downstream rotor loading, as the blades can experience very turbulent low wind speed flow, quickly interspersed with low turbulent free stream flow. This also loads to a fluctuating power production, but considering average power generation **this effect is not significant**. [22]

4

5

MODELLING WAKES

Now that the most important parameters and properties describing the wake development of wind turbines are known, the principle of wake modelling can be explored. This chapter covers the fundamentals of wake modelling and the required auxiliary models, which can be skipped by readers who are familiar with wake modelling. These additional models are needed to upgrade the single wake model to the augment wake model, which includes multiple turbines and implements curtailment. Finally, two wake models are selected to be incorporated in the algorithm. The next two chapters will discuss these two wake models in more detail.

5.1 The Study of Wake Models

Model Types

In general two types of wake models can be distinguished, which are discussed in this section:

- The first type uses **computational fluid dynamics** (CFD) to accurately calculate the motion of the flow particles around and behind the rotor. This models are called field models.

- The second type only has a few input parameters to calculate only the main parameters of the wake. These models are referred to as **engineering wake models** or kinematic models.

Continuing…

41

5.1 The Study of Wake Models, Continued

CFD Models

CFD models are based on the highly complex Navier-Stokes equations. Different models make different simplifications to reduce the computational time to weeks or days. The advantage of these kind of models can mostly be attributed to the high accuracy of the calculations. However, this approach also has some disadvantages:

- The computational time is too high for (near) real time calculations.

- The high accuracy of the output can only be achieved with accurate input signals. Using the relatively rough data from the turbines partly mitigates this high accuracy advantage.

- The calculations depend on the detailed (and often proprietary) design of the wind turbine blades and its environment.

Mainly due to the first disadvantage, **CFD based wake models are not considered in this research**.

Continuing…

5.1 The Study of Wake Models, Continued

Engineering Models

Engineering wake models often have a more phenomenological background. They are less accurate than the CFD models, but are focused on calculating only the parameters of interest with acceptable accuracy. The most important advantages for this research include:

- Very low computational effort

- Many validations in literature

- Ease of implementation

- Relative ease to include curtailment

A disadvantage of engineering models is that they depend on premade thrust curves and might require to be both interpolated and extrapolated to cover all regions of curtailment, see the next section.

5.2 Wake Model Auxiliaries

Augmented Wake Models

As shown in the flowchart of figure 3.2, the wake models to calculate the wake behind a single turbine are augmented with a wake mixing method and a method to insert curtailment, which are discussed in the next two paragraphs.

Wake Mixing Methods

Engineering wake models generally only describe the flow behind a single turbine. When a turbine experiences a wind speed deficit from its upstream turbine it will produce a different wake itself. These two wakes have a combined effect on downstream turbines, etc. There are several ways to combine different wakes [21], which is referred to as wake mixing, see table 5.1. The symbol d_i is the ratio of the wind speed at turbine i versus the free stream wind speed V_0, referred to as the wind speed deficit. During the wake model validation, it was found that the root mean square (RMS) method performs best. Katic et al [23] confirm this result.

Table 5.1: Several wake mixing methods. The symbol u_j refers to the wind speed at upstream turbine j and u_{ij} refers to the wind speed at turbine i including only the wake effect due to turbine j

Method	Description	Governing Equation for d_i
Geometric sum	Multiplication of all deficits	$\prod_j \frac{u_{ij}}{u_j}$
Linear superposition	Reduction of each deficit	$1 - \sum_j \left(1 - \frac{u_{ij}}{u_j}\right)$
Energy balance	Reduction of energy from deficits	$1 - \sqrt{\sum_j \left(\frac{u_j}{V_0}\right)^2 - \left(\frac{u_{ij}}{V_0}\right)^2}$
Root mean square	Quadratic summation	$1 - \sqrt{\sum_j \left(1 - \frac{u_{ij}}{u_j}\right)^2}$

5.2 Wake Model Auxiliaries, Continued

Curtailment
Model

Another model is required to include the curtailment configuration. Thrust curves of the turbines in wind farm Westermeerwind are known for several curtailment settings. Therefore, using these curtailed curves allows a method of curtailment implementation. Figure 5.1 shows a qualitative example of this method. From the known curves, it was found that the curtailment factor (c_i) was a good interpolation factor to calculate the curtailed thrust coefficient with respect to the default thrust coefficient without curtailment (C_T). As a lower interpolation bound a small dependency of the wind speed was used (γ) to better fit the actual curves, see equation 5.1. Note that this relation is specifically for the turbines at Westermeerwind, presented in section 8.1 Measurement Context .

$$C_{T_{curtailed}}(u_i, c_i) = \left[1 - c_i \cdot \gamma(u_i)\right] \cdot C_T(u_i) \tag{5.1}$$

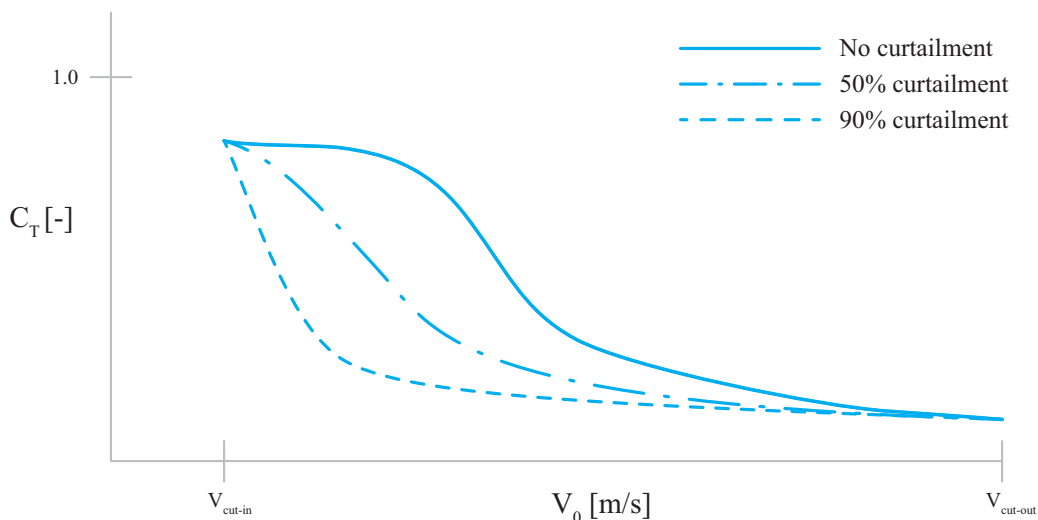$$\gamma(u) = 1 + \frac{u + 5.0}{100.0} \tag{5.2}$$

Figure 5.1: Qualitative example of thrust curves for different curtailment settings. The curve without curtailment is the default thrust curve of the wind turbine. The percentage of curtailment is relative to nominal power in this figure.

5.3 Wake Model Selection

Engineering
Wake Models

As mentioned in the previous section only engineering (or kinematic) wake models are considered. Several of these type of wake models exist, but in many comparative (validation) studies [15][21][24] the four wake models treated in the next four sections are discussed.

Jensen

The Jensen wake model [25] is one of the most popular wake models, due to its simplicity, practicality and robustness. [24] It is based on the conservation of mass and a linearly expanding wake profile. An other important advantage is its ease of implementation. [15]. This allow the focus of the research to be more on testing the algorithm instead of the implementation.

Ainslie

The Ainslie wake model [26] was developed considering a two dimensional field model with axis symmetry to reduced computational effort. [15] It is based on the time averaged Navier-Stokes equations. Several implementations of the Ainslie wake model exist, like GH WindFarmer and FLaP. [21]

Larsen

The Larsen wake model has several versions, but in this research the 2009 version [27] is considered. The model is based on the Ainslie model and the solution of the Reynolds Averaged Navier-Stokes (RANS) equations with Prandtl's mixing length theory. The result is a simple set of explicit equations. The implementation of the equations are fairly easy, considering that only straight a row of turbines is considered in this research.

Continuing…

5.3 Wake Model Selection, Continued

Frandsen

The Frandsen wake model [28] is a relatively more advanced model that consists of three regions. The goal of this model is to include both small and large scale flow features and it is more focussed on larger (offshore) wind farms. The development of this wake model has stagnated [15]

Conclusion

Considering that the implementation of the Frandsen wake model requires the programming of three regimes and as it is more focussed on large wind farms it is decided to not use this model for this research. The Larsen and Ainslie wake model are both based on the Navier-Stokes equations, but with the more recent development of the Larsen wake model in combination with the empirical calibration, it is preferred over Ainslie, following the argument of [15]. **This leads to the Jensen and Larsen wake models being implemented in the algorithm in parallel.** The wake models will be compared against each other in order to find if one model performs better than the other.

5

6

N. O. JENSEN WAKE MODEL

This chapter reviews the most known and used wake model, developed by N. O. Jensen in 1983. The Jensen wake model is widely used, due to its simplicity, robustness and performance. [29] First, his initial publication [25] and governing equations are studied. Second, the model is augmented to include curtailment as a parameter. In chapter 9 the model will be tested against measurement data.

6.1 Literature Review

Usage
Boundaries

In order to keep computational effort to a minimum, Jensen defined some clear boundaries and assumptions for his model.

- It should only be used to calculate the mean velocity deficit in the far wake.

- The only fundamental governing equation is the equilibrium of mass, so it does not model turbulent fluctuations. Therefore it can be used for power calculations, but is not recommended for load or fatigue calculations as for the latter small pertubations have a much more significant effect.

Continuing...

6.1 Literature Review, Continued

Main
Assumptions

In the Jensen wake model it is assumed that:

- The velocity profile has a clear sharp boundary and top-hat shape.

  – This is not an issue for this research as it assumes a straight row of turbines.
  – An off-axis modulation can be added to the model other cases.

- The wake expands linearly and axisymmetrically.

  – This is unrealistic as the ground prohibits expansion at around $4D$ to $6D$ downstream. It is up to the results of the validation to see if this assumption is acceptable.

- No increased turbulence is introduced.

  – In this research, the measured local turbulence intensity will be used for each turbine, so added turbulence is accounted for.

- The wake effects are instantaneous.

  – In order to validate this model with measurement data, in which there is a time delay for wind conditions marching over the wind farm, an artificial delay is introduced, see section 8.3 Data Post-Processing .

Governing
Equations

The governing equation of the Jensen wake model is equation 6.1, which calculates the wind speed deficit d_i of turbine i, where R is the radius of the rotor. For its detailed derivation see Jensen's original publication [25].

$$d_{i+1}(x) = 1 - 2a_i \cdot K(x) \quad with \quad K(x) = \left(\frac{R}{R + k_i \cdot x} \right)^2 \qquad (6.1)$$

Continuing…

6.1 Literature Review, Continued

Wake Decay
Factor

In equation 6.1, parameter k_i is referred to as the wake decay (or wake expansion) constant of turbine i. Jensen suggested a value of 0.01 himself, but generally 0.075 (onshore) or 0.04 (offshore) is used. In order to determine this value, equation 6.2 can be used, where TI_i is the turbulence intensity of the incoming wind of turbine i. [3] However, Choi and Shan [29] developed a more detailed relation, see figure 6.1. This relation is tested in the validation of this wake model in chapter 9.
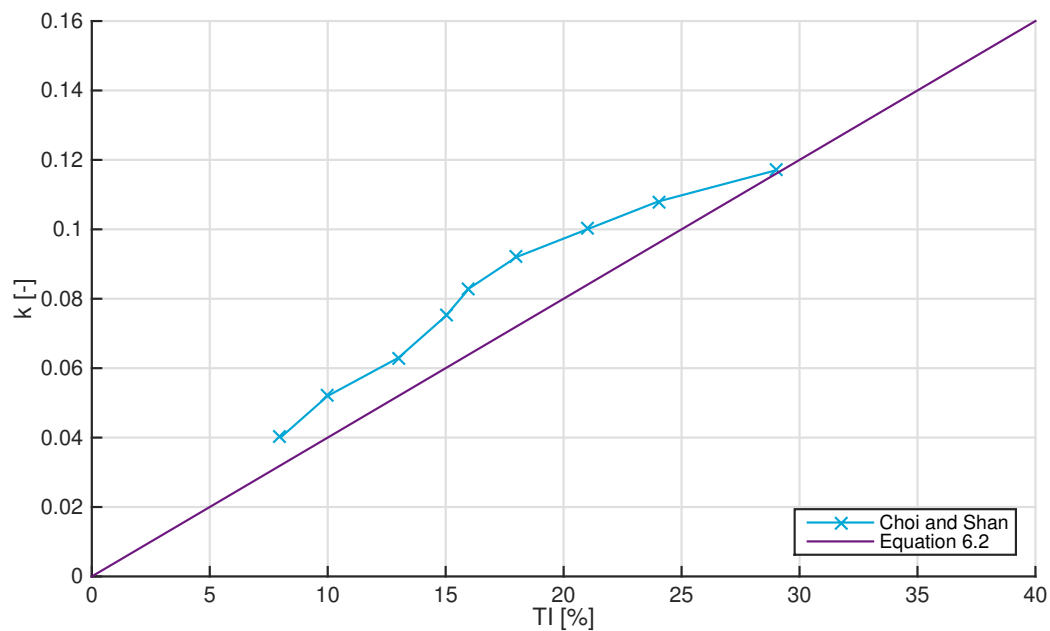
$$k_i = 0.4 \cdot TI_i \tag{6.2}$$

6

Figure 6.1: Wake decay parameter k dependency on the turbulence intensity for both alternatives.

6.2 Augmented Jensen Wake Model

Curtailment
Dependent
Parameters

When studying the parameters in equation 6.1, it can be found that only the induction factor a_i is directly dependent on the curtailment of turbine i. The wake decay factor k_i is dependent on the turbulence of the incoming flow and can therefore be considered to be dependent on the curtailment of upstream turbines.

Induction Factor

As proposed in the the augmented wake model of figure 3.2, curtailment will be implemented by expressing curtailment dependent parameters as a function of the thrust (coefficient). This allows curtailment to be a control variable of the wake model. The only relevant parameter for this procedure is the induction factor and its dependence on the thrust coefficient is shown in equation 6.3 [23].

$$a_i = \frac{1 + \sqrt{1 - C_{T_i}}}{2} \tag{6.3}$$

7

C. G. LARSEN WAKE MODEL

C. G. Larsen used the work of Prandtl - describing a turbulent boundary layer with the Navier-Stokes equations - to develop a set of less computationally expensive equations for wake analysis. This chapter will first study this wake model and its most important parameters. Second, the method of implementing curtailment as a control variable will be discussed.

7.1 Literature Review

Model Fundamentals

The Prandtl turbulent boundary equations are a set of differential equations. In order to solve this set of equations, Larsen used Prandlt's mixing length theory for the width of the wake and proposed both a first-order and second-order solution. [21] The results of the actuator disk theory are used as input for these differential equations. [15] Generally only the first-order solution is used.

Usage Boundaries

The aim of the model was to study the wake meandering effect and its effect on local turbulence at the turbine. The main output of the model is a function for the velocity deficit dependent on the downstream distance and off-axis distance. The latter is zero at the center of the downstream turbine for this research, as the turbines are located in a straight line and only the wind direction along that line is modelled.

7.1 Literature Review, Continued

Main
Assumptions

Larsen made the following assumptions to develop his model:

- The flow is incompressible.

  – This assumption is mentioned as it is a requirement in order to continue on Prandtl's work. However, all wake models have this assumption. It is more than reasonable for wind speeds up to even fifty of meters per second.

- The flow is stationary.

  – This is similar to the Jensen wake model. The wake effects are not depending on any historical wind conditions.

- The wake is semi-axisymmetric.

  – The wind shear of the flow is neglected, but the ground boundary is accounted for. It is up to the results of the validation to conclude if this assumption is acceptable.

Continuing…

7.1 Literature Review, Continued

Equation 7.1 is a easy to implement version of the governing equation, where the parameters D, R, A and x are respectively, the rotor diameter, rotor radius, swept area of the rotor and the downstream distance behind the turbine. It depends on two internal parameters, c_1 and x_0 as defined in equations 7.2 and 7.3 respectively. Parameter c_1 is related to the Prandtl mixing length and x_0 to the position of the rotor in the used coordinate system. [21] $R_{9.6D}$ is the wake radius at a downstream distance of $9.6D$.

$$d_{i+1}(x,r) = 1 - \frac{1}{9} \sqrt[3]{\frac{C_T A}{(x+x_0)^2}} \left(\frac{r^{\frac{3}{2}}}{\sqrt{3c_1^2 C_T A (x+x_0)}} - \frac{\left(\frac{35}{2\pi}\right)^{\frac{3}{10}}}{243 c_1^{10}} \right) \tag{7.1}$$

$$c_1 = \left(R_{eff}\right)^{\frac{5}{2}} \frac{\sqrt{\frac{2\pi}{105}}}{(C_T A x_0)^{\frac{5}{6}}} \quad with \quad R_{eff} = R \sqrt{\frac{1 + \sqrt{1-C_T}}{2\sqrt{1-C_T}}} \tag{7.2}$$

$$x_0 = \frac{19.2R}{\left(\frac{2R_{9.6D}}{D_{eff}}\right)^3 - 1} \quad with \quad R_{9.6D} = 2R \cdot a_1 \left(b_1 TI + 1\right) e^{a_2 C_T^2 + a_3 C_T + a_4}$$

$$\tag{7.3}$$

As can be seen in equation 7.3 part of the Larsen wake model depends on five unkown parameters (a_{1-4}, b_1). Larsen determined the values of these constant parameters emperically using the Vindeby wind farm, see table 7.1. [3] It might prove to be neccesary to determine these parameters specifically for Westermeerwind.

In equation 7.1, symbol r is the off-axis distance, which is used to integrate over the rotor area of the downstream turbines.

Table 7.1: Larsen wake model constant parameters [27]

a_1	a_2	a_3	a_4	b_1
0.435449861	0.797853685	-0.124807893	0.136821858	15.6298

7.2 Augmented Larsen Wake Model

Main Parameters   Most of the parameters in Larsen's wake model are either con-
stants, turbine specific (e.g. R, A) or wind farm specific (e.g.
x). The parameters that depend on operation conditions are the
turbulence intensity (TI) and the thrust coefficient (C_T). Cur-
tailment can therefore be implemented in the augmented Larsen
wake model directly as shown in the flowchart of figure 3.2.

7

8

VALIDATION DATA

In order to determine which of the wake models performs best they need to be validated and compared. This chapter focuses on validation data to test the wake models in default operation without curtailment. Only if the models perform well without curtailment they can be considered for implementing curtailment as an additional control variable. First, the context of the measurements are discussed. Second, the accuracy of the used data signals are scrutinized. Finally, the results are presented. In the next chapter the wake models will be tested against these results.

8.1 Measurement Context

Wind Farm

The measurements are obtained from the wind farm Westermeerwind in The Netherlands, see the green turbines in figure 8.1. It consists of three rows of a total 48 turbines located in the lake IJsselmeer, see figure 8.2. The numbering of the turbines used in this report is shown in figure 8.3. The shore directly next to Westermeerwind also contains wind turbines. However, these have no effect on the measurement data as long as no easterly winds are considered.

Continuing...

57

8.1 Measurement Context, Continued

Turbine Selection   All experiments have been performed on the northern (inclined) row with wind from the south south west (SSW, 210°). The validation data for the wake models are therefore also obtained for those turbines and in that wind direction. The distance to shore for these turbines is $1100m$, which is more than 10 times the diameter.
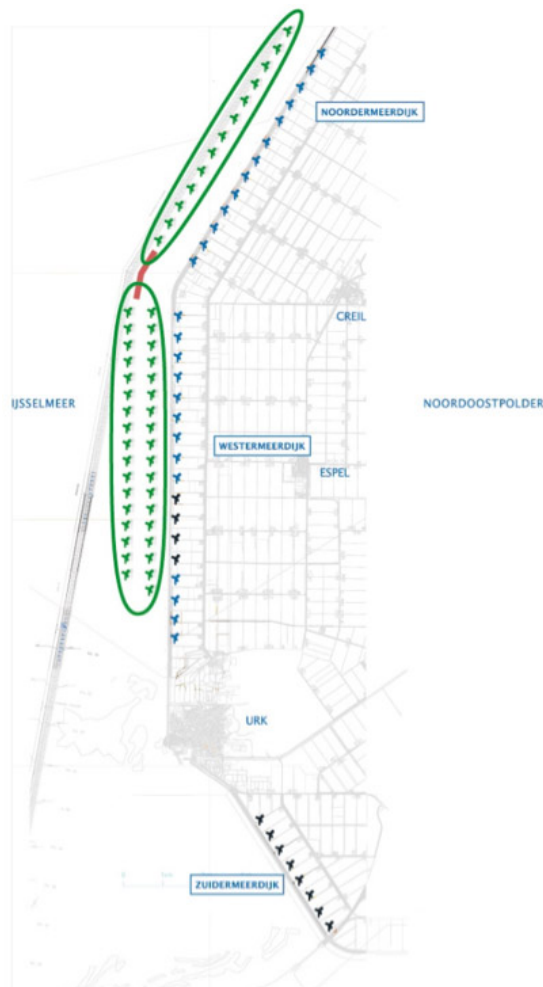

Figure 8.1: Farm Layout Westermeerwind (only the green turbines are part of wind farm Westermeerwind)

8.1 Measurement Context, Continued

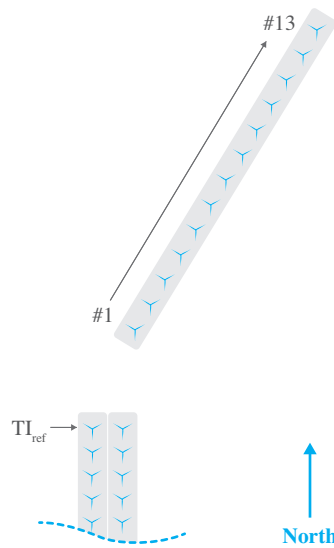Figure 8.2: Location Westermeerwind indicated by the dark lines (©2016 GeoBasis-DE/BK (©2009), Google)

Figure 8.3: Turbine numbering of northern part of wind farm Westermeerwind

8.1 Measurement Context, Continued

Turbine
Specification

Westermeerwind consists of 48 Siemens Wind Power 3.0 MW D3-108 wind turbines. The relevant turbine specifications for this research can be found in table 8.1.

Table 8.1: Wind turbine specifications SWT 3.0 MW D3-108 [30]

Specification	Value
Rated power	$3000\,kW$
Cut-in windspeed	$3\frac{m}{s}$
Cut-out windspeed	$25\frac{m}{s}$
Rated windspeed	$12\frac{m}{s}$
Rotor diameter	$108\,m$
Hub height	$95\,m$

Turbine spacing

The turbines are in a straight row and are spaced $520\,m$ apart. which equals 4.8 times the rotor diameter.

Measurement
Frequency

A custom program was written that connected with the SCADA system from Siemens. This allowed a sampling frequency of $1\,Hz$ for obtaining the data signals from the turbines.

8.2 Data Accuracy

Error Wind
Speed Signal

Considering the goal of validating the wake models, the most interesting signal to measure from the turbines is the wind speed. However, there are two disadvantages in using the sonic anemometer sensor of the turbine to determine the wind speed.

1. The datasheet of the sonic wind sensor that is installed on the turbines states an accuracy of $\pm 0.5 \frac{m}{s}$, see figure 8.4 [31]. This error is considered too large to be useful for wake model validation.

2. The wind sensor is located behind the rotor and corrections are applied by the turbine controller to determine the wind speed in front of the turbine. An additional error is therefore introduced. In the recalibration document it was also mentioned, that this adjustment is only valid under normal operation mode, so it is not guaranteed to work during curtailment. It was not possible to quantify the error of this recalibration.
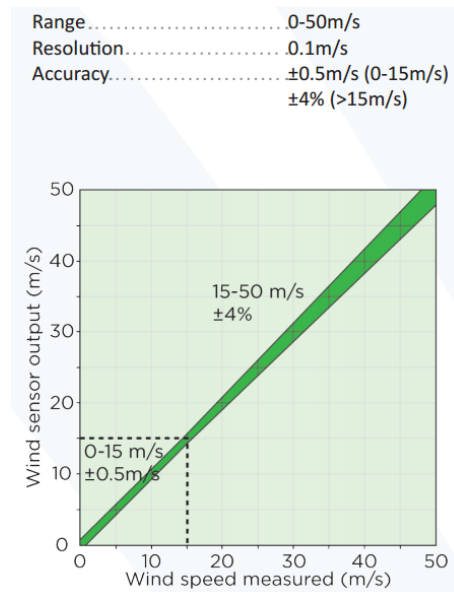

Figure 8.4: Accuracy of sonic wind sensor [31]

8.2 Data Accuracy, Continued

Method for
Determining
Wind Speed

As the sonic sensor does not provide the required accuracy to determine the wind speed, an alternative method needs to be used. The signal with the highest accuracy (99.8%) is the produced power. The power that a wind turbine produces is related to the wind speed by the power curve.

Power Curve
Method

Using the data from table 8.1 the power curve of the turbine is visualized in figure 8.5. Note that this is not the actual confidential power curve of the turbine that is used in the analysis. In the region between cut-in wind speed and rated power, the curve has a one-to-one relation between the wind speed and the power production. In that region equation 8.1 is tested to determine the wind speed, where $\mathscr{P}^{-1}$ is the inverse of the power curve function.
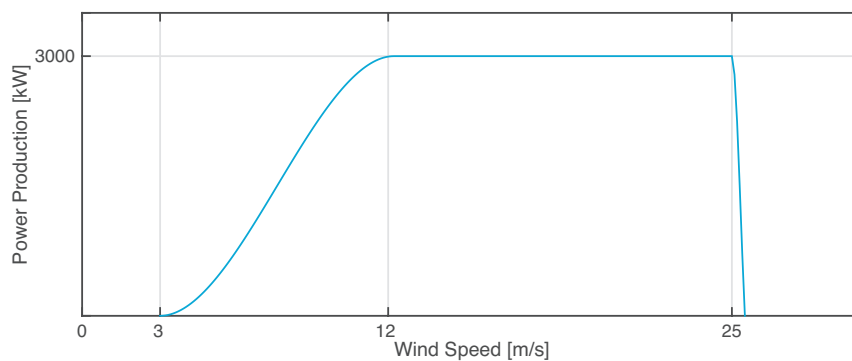
$$u = \mathscr{P}^{-1}(P) \tag{8.1}$$

Figure 8.5: Qualitative representation of the power curve

8.2 Data Accuracy, Continued

Figure 8.6 shows the result of using the power curve for determining the wind speed versus the sonic sensor when using an increasing amount of data points.

- In figure 8.6a the coefficient of determination (R^2) of the linear regression is shown versus the amount of points taken per average before comparison. This amount refers to how many power data points are converted to wind speed - using equation 8.1 - averaged and than compared to the average of the wind speed measurements. It rises quickly to 0.99 when using 46 data points. At 300 data points $R^2 = 0.993$ and at 600 data points $R^2 = 0.994$. This high fit level is confirmed by the boxplots of figure 8.6c, where it can be seen that both the whiskers are smaller and the amount of data points between the whiskers is higher for an increasing amount of data points used.

- In figure 8.6c the intercept between the sonic sensor and the power curve method is shown. This converges to about $0.3\frac{m}{s}$. This is confirmed by figure 8.6d where it can be seen that there is a small (nearly constant) difference between the wind speeds of the two methods. This difference falls in the error margin of the sonic sensor.
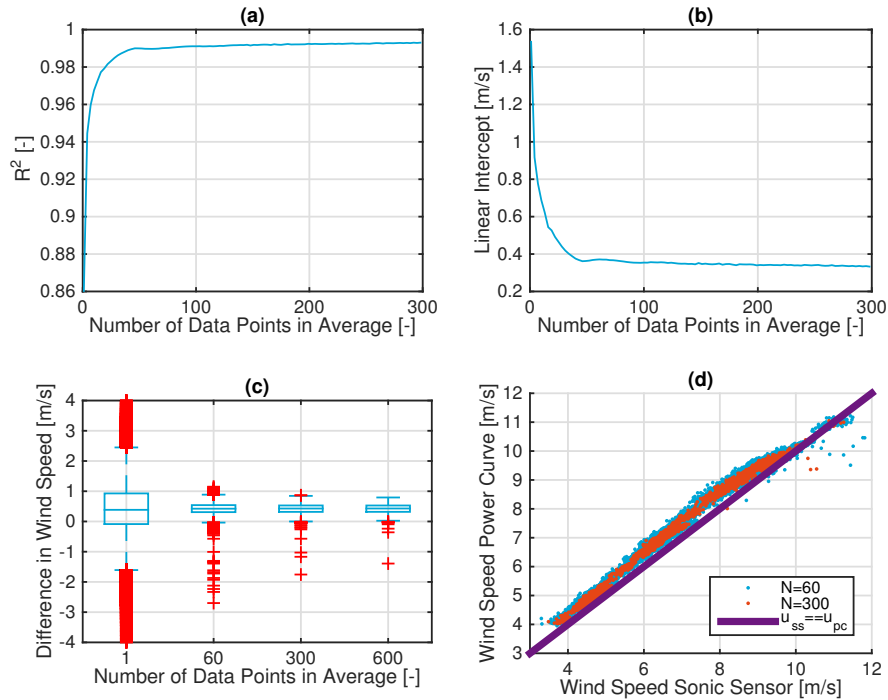
8

Figure 8.6: Accuracy of using the power curve to determine the wind speed with respect to the sonic sensor. The *number of data points in average* refers to how many power data points are converted to wind speed - using equation 8.1 - averaged before comparing it to the average of the wind speed measurements. In a and b the coefficient of determination and the linear intercept are shown for the linear regression. In c and d the convergence is visualized with boxplots and the data points themselves for different number of data points in the average. The red points in figure c indicate outliers.

8.2 Data Accuracy, Continued

Conclusion Power Curve Method	Considering the high fit of the regression of the power curve method versus the sonic sensor method and taking into account the higher accuracy of the power signal from the documentation (99.8%), it is concluded that using the power curve method is the best way of determining the wind speed. The error of determining the wind speed this way is lower than $0.16\frac{m}{s}$ as is shown in appendix D.

Continuing…

8.2 Data Accuracy, Continued

Air Density Correction

The power curve is specified for default air density ($\rho = 1.225\frac{kg}{m^3}$). An air density correction has been applied by using the temperature measurements of the turbines and the pressure and relative humidity measurements from the Royal Netherlands Meteorological Institute (KNMI) (metmast Lelystad). Equation 8.2 [32] is used to calculate the air density from the three data signals, based on the equation of state. The symbols T, p and ϕ refer to the absolute temperature, pressure and relative humidity of the air, respectively. p_w is the pressure of the water vapour in the air and R_0 and R_w are the gas constants for air and water vapour, respectively. The density correction per data point is calculated using equation 8.3. This correction changed the calculated wind speed with a maximum of 1%.

$$\rho = \frac{1}{T}\left(\frac{p}{R_0} - \phi \cdot p_w \left(\frac{1}{R_0} - \frac{1}{R_w}\right)\right) \quad with \quad p_w = 0.0000205 e^{0.0631846T}$$

(8.2)

$$\mathscr{P}_{corrected}(u) = \mathscr{P}(u) \cdot \sqrt[3]{\frac{\rho}{1.225}}$$

(8.3)

8

Error Turbulence Intensity

The error of the turbulence intensity due to the error of the sonic sensor is more difficult to determine. In appendix D a maximum error is derived of $2.5pp$ (percentage points) for low turbulence levels at wind speeds higher than $8\frac{m}{s}$. In the next chapter it will be studied how sensitive the wake models are to this error.

Relevance Wind Direction

The wind direction is not used directly to determine the wind speed deficits, as this research only focusses on a straight line of turbines with the wind direction in the same line. However, it is important to determine if the wind direction is in parallel with the turbines as in the implementation of the wake models.

Continuing…

8.2 Data Accuracy, Continued

Availability Wind
Direction Signal

For Westermeerwind, there was no data of the wind direction available directly. The turbines do, however, provide a signal for their yaw direction. This signal is not suitable as the instanteneous wind direction, but as the turbine always tries to point in the direction of the wind, it is suitable as an average of a larger time span.

Quality Yaw
Direction Signal

It was found that the yaw direction signal from the turbines were not perfectly calibrated. Figure 8.7 does, however, show a relative constant mean offset in the different yaw direction signals versus the yaw direction of turbine #1. Especially for the closer wind turbines (#2 and #3) the fit of this constant offset is good judging on the standard deviation around this mean, namely 1.9° and 2.5°. For turbines further away this fit is worse, namely a standard deviation of 3.7° for turbine #5 and 6.1° for turbine #11. This decrease of fit has two reasons.

1. As the wind travels over the row of turbines, the wind conditions can change, due to either the increased turbulence or just in general.

2. As the distance between two turbines increases, it takes longer for the wind to reach the second turbine. This time delay is unaccounted for in figure 8.7, so rapid changing wind directions disturb the quality of this analysis for long distances. This time delay is discussed in the next section.
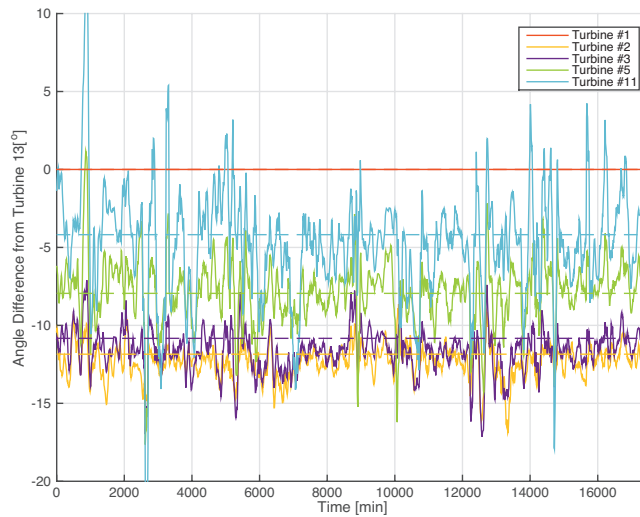
Figure 8.7: Error of the yaw direction signal for 10-minute averages, smoothed over 10 points for visibility, using a moving average, for about 10^6 data points per turbine.

8.2 Data Accuracy, Continued

Determining Wind Direction

As the absolute wind direction is difficult to determine, a more qualitative approach was used. Figure 8.8 shows the wake effect of turbine #1 on turbine #2 versus the yaw direction signal of turbine #1. It can be seen that this wake effect is the highest at $211° \pm 1°$. It is therefore concluded that the yaw direction of turbine #1 provides a good determination of the wind direction. When the wind direction of turbine #1 is mentioned from now on a correction of $-1°$ is applied to align with the actual turbine row orientation.
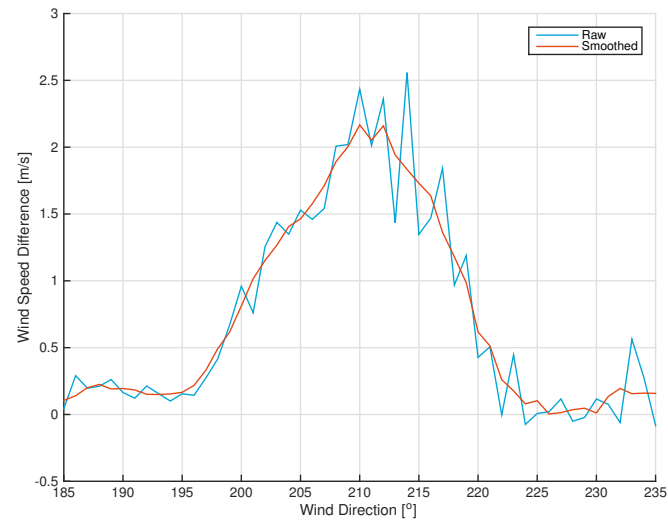
8

Figure 8.8: Wake effect between turbine #1 and #2 versus wind direction of turbine #1 for an average number of 8.500 data points per degree. The smoothed curve is a moving average over 5°.

8.3 Data Post-Processing

Time Delay

In order to compare the wind speeds of different turbines, one needs to account for the time delay for wind conditions to travel over the wind farm. When studying the experiments in the next chapter this will be done manually for every turbine for every experiment. However, in order to validate the wake model more than $16,500$ data points per turbine were used and a more scalable approach was used.

Time Delay Adjustment

A time variant approach would be the most suitable as the propagation of the wind (and wake) is not only dependent on the instantaneous wind speed. However, Gebraad et al [33] achieved good results using the mean of the wind speed behind the first turbine and the wind speed at the direct downstream turbine, as in equation 8.4, where Δx is the turbine spacing. Note that they calculated the wind speed behind the first turbine by using the induction factor from the actuator disk theory as in equation 4.2. For this analysis it is assumed that the turbines are all operating optimally, so $a_i = \frac{1}{3}$. It was found that this method provided good results in this research as well.

$$t_{delay} = \frac{\Delta x}{\frac{1}{2}\left(u_i \cdot (1 - 2a_i) + u_{i+1}\right)} \xrightarrow[a_i = \frac{1}{3}]{\Delta x = 520m} \frac{520}{\frac{1}{6}u_i + \frac{1}{2}u_{i+1}} \quad (8.4)$$

8.4 Overview Validation Data

Overview
Validation Data

In the previous section it was explained why it is important for the wind direction to be around 210° when performing the validation. In this section an allowance will be set to filter the data on the wind direction. Also, in section 4.2 Parameters Influencing Wake Development it was discussed that the most important parameters influencing the wake development are wind speed and turbulence intensity. An overview of this data filtered on wind direction will be presented, which will be used in the next chapter for validation of the wake models.

Wind Direction
Dependency

Figure 8.8 showed a dependency of the wake at turbine #2 versus the wind direction. Figure 8.9 shows this dependency per turbine expressed as the relative wind speed with respect to turbine #1. An allowance of ±2° is used to account for the non-instantaneous behaviour and possible inaccuracy of the wind direction signal. This leads to a maximum difference between the mean and the highest or lowest values of less than 3% as can be seen in figure 8.9, and leaves more than 45,000 data points per turbine available for validation.
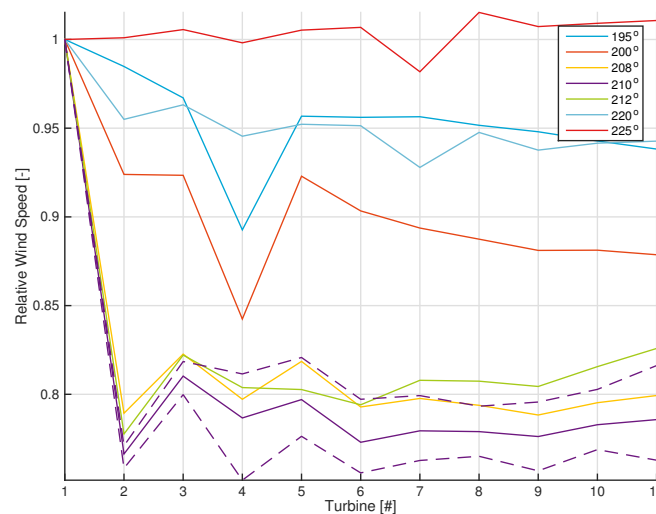

Figure 8.9: Wake effect for different wind direction. Per wind direction an average is calculated for ±2° over at least 30,000 data points per turbine. The dashed line indicates the mimimum and maximum wake effects within the ±2° for 210°

8.4 Overview Validation Data, Continued

Wind Speed Dependency

Figure 8.10 shows the time-averaged wind speed, calculated using the power curve method at the first ten turbines with the wind direction $210° \pm 2°$, i.e. from turbine #1 to #10 see figure 8.3. From this visualization of the wake effect several conclusions can be drawn.

- The largest difference in wind speed is between the leading turbine (#1) and the direct downstream turbine (#2).

- After the second turbine the wind speed profile is very flat, which is referred to as the spatial steady state wind speed value.

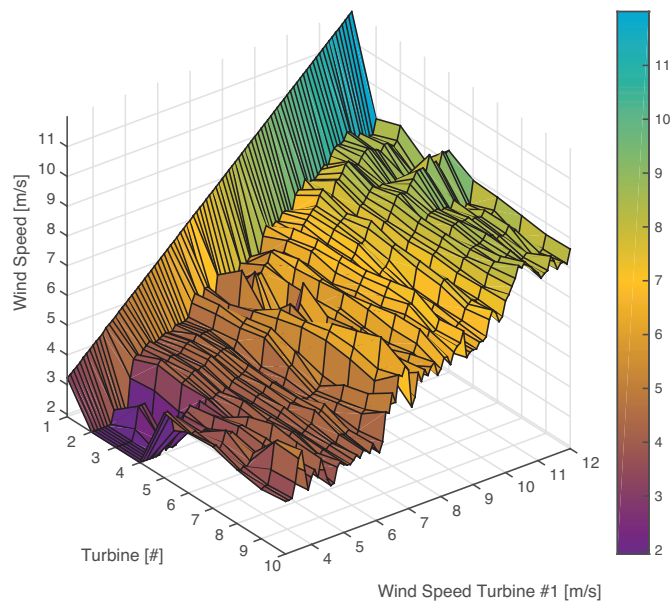- The steady state wind speed increases with wind speed.

8

Figure 8.10: Measured local wind speed at the turbines for the wind direction $210° \pm 2°$ for free stream wind speeds per $0.1 \pm 0.05 \frac{m}{s}$ at turbine #1, with more than 150 data points per value between $4.6 \frac{m}{s}$ and $11 \frac{m}{s}$ except between $6.2 \frac{m}{s}$ and $7.1 \frac{m}{s}$

8.4 Overview Validation Data, Continued

Wind Speed
Dependency
Relative Wake

Figure 8.11 shows the relative wind speed deficit of the down-stream turbines in percentage of the wind speed at turbine #1. Again, several conclusions can be drawn.

- The wake development over the turbines appears to be relatively flat.

- In figure 8.12a the average is taken per wind speed. Except from the two peaks in the curve of $8\frac{m}{s}$ the maximum deviation of the mean wake loss of 22.8% is only 4%.

- This is confirmed by the boxplots of figure 8.12b for $6\frac{m}{s}$ and $10\frac{m}{s}$, where the mean of 22.8% is always in the span of the data points, often between the 25th and 75th percentile and - especially in the deep wake - near the mean as well.

- The direct downstream turbine #12 shows a structural higher wind speed deficit of 24.5% on average

---

Peaks in Relative
Wake

A peak can be observed around $7\frac{m}{s}$. This is partly due to the low amount of data points in that region. However, a more significant error could be due to the way the wind speed is calculated. As the wind speed drops below the cut-in wind speed, this method is not valid any more. It is likely that this happens for the third turbine in the row around these wind speeds. Data from the curve of $7\frac{m}{s}$ is not taken into account when calculating the mentioned averages.
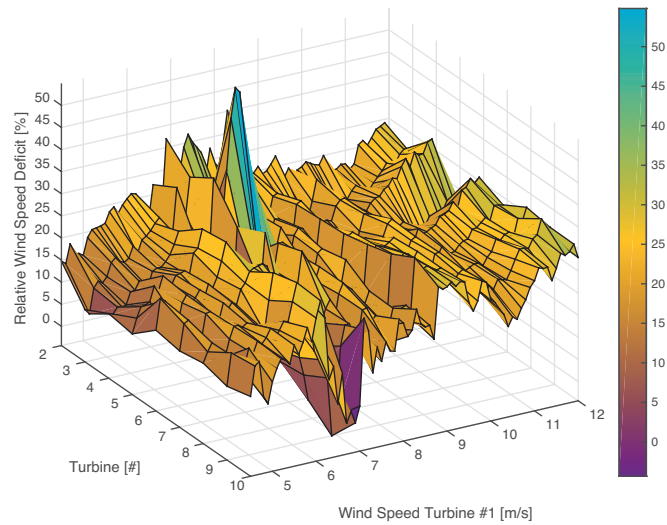

8

Figure 8.11: Relative wind speed deficit calculated as the wind speed in percentage of the wind speed at turbine #1, similar to figure 8.10.
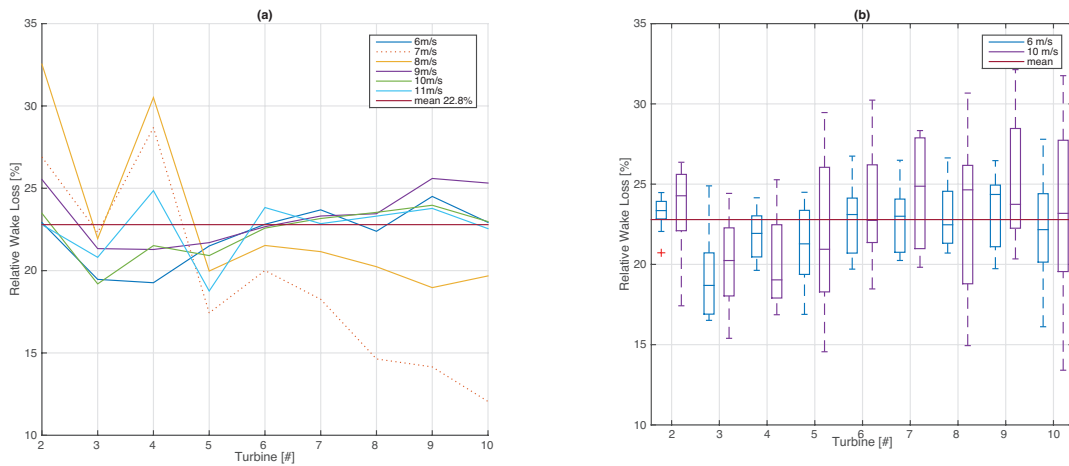

Figure 8.12: (a) Relative wake loss averaged over differend wind speeds. The curve of $7\frac{m}{s}$ is discarded due to the low amount of data points. (b) Box plot equivalent of (a) for two wind speed averages. The red point in figure (b) indicates an outlier.

8.4 Overview Validation Data, Continued

Turbulence
Intensity
Dependency

The last wind condition parameter to study is the turbulence intensity. Figure 8.13 shows the calculated average turbulence intensity at turbine #1 for different wind directions. For this calculation both the sonic sensor and the power production are used, which is explained in appendix D. Several conclusions can be drawn based on this figure.

- Around 30° there is a significant increase in the turbulence level. This is due to the fact that from this wind direction turbine #1 is actually the last turbine in the wake, instead of the leading wind turbine, see figure 8.1 for the wind farm layout.

- Between 45° and 90° the turbulence is higher than between 205° and 270°, which can have two reasons.

    1. The wind is coming from land instead of from the lake, see figure 8.2, which causes a higher turbulence [34]

    2. From that wind direction wind turbines from another wind farm are in front of turbine #1, see figure 8.1, so it could be a residual of the added wake from that wind farm.

- Between 150° and 205° the turbulence level is also significantly higher, which is due to the turbines located south of turbine #1.

- Between 205° and 270° the turbulence level is the lowest. In this region the wind is coming from the lake undisturbed. The reference average free wind stream wind speed for this wind farm is there taken to be between 8% and 10%, see figure 8.2.
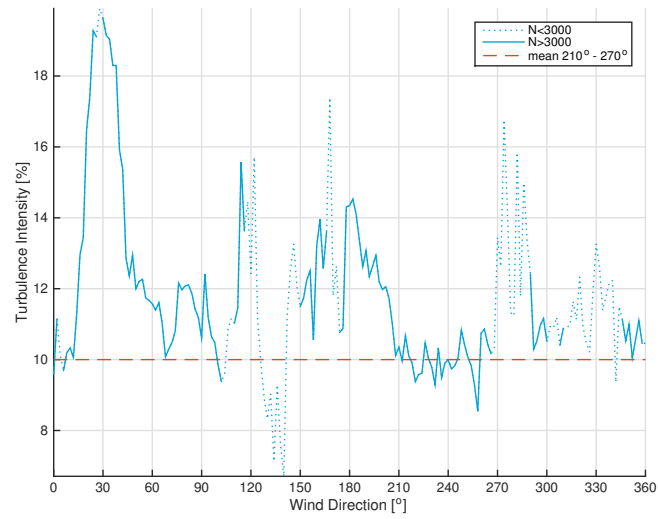
Figure 8.13: Average turbulence intensity at turbine #1 for different wind directions based on 1.6 million data points, using a $\pm 30s$ window per data point. The dashed lines indicate the parts where less than $3,000$ data points were available.

8.4 Overview Validation Data, Continued

Dependency TI
on Time Span

In order to calculate the turbulence intensity, the standard deviation and mean of the wind speed over a certain time span needs to be calculated. Figure 8.14 shows the effect of increasing the time span per data point, equivalently to figure 8.13. Several conclusions can be drawn, excluding the region around 30° and 180°.

- A trend can be recognized, as the calculated turbulence intensity increases when larger time spans are taken.

- The maximum increase is about $0.3pp$ (percentage points) for a time span increase of $60s$.

- The maximum increase is about $2pp$ for large time spans.

- Taking into account that for larger time spans not only the turbulence can change, but the mean wind speed as well, it is considered that taking a time span between $60s$ and $120s$ is optimal to calculate the turbulence intensity.
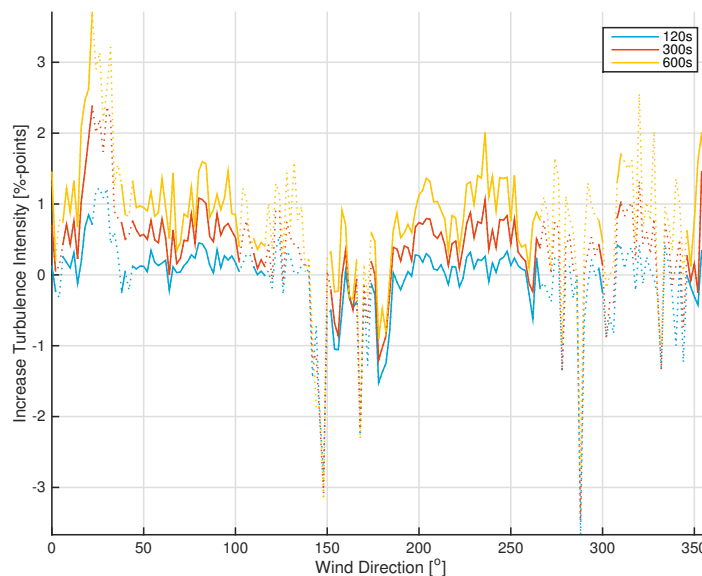

Figure 8.14: Difference of several time spans vs taking a time span of $60s$. The dotter parts of the line indicate that there were not enough data points available.

8.4 Overview Validation Data, Continued

Now that both the wind speed and the turbulence intensity are studied, their relation can be studied as well. Figure 8.15 shows the free stream turbulence intensity for several wind speeds.. Interestingly enough, it can be concluded that between $5\frac{m}{s}$ and $12\frac{m}{s}$ there is no significant relation between the turbulence intensity and the wind speed and the stated average of 10.0% holds for all wind speeds.
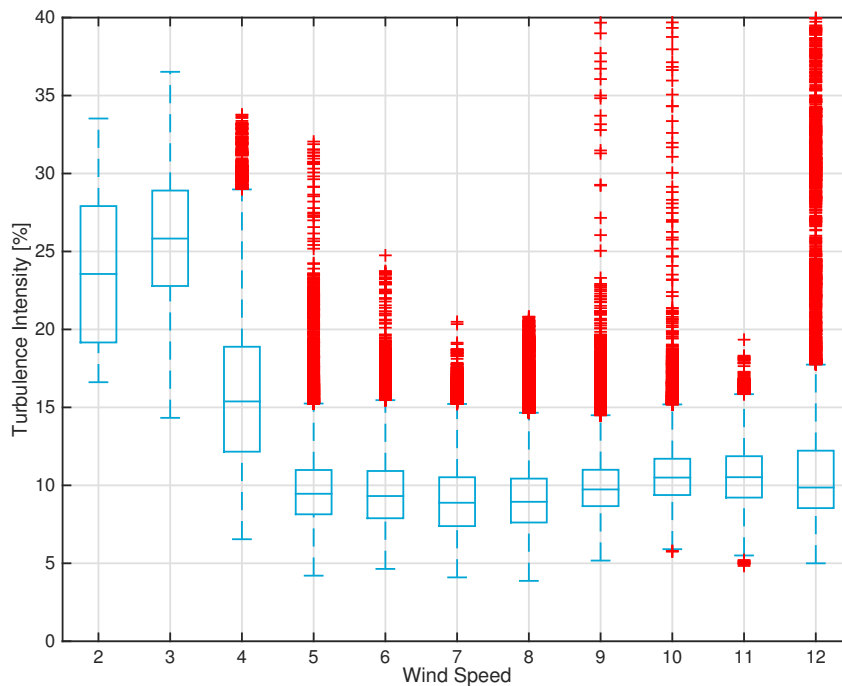
8

Figure 8.15: Box plots of free stream turbulence intensities per wind speed for wind directions between 205° and 227°, measured at turbine #1. The bin width is $1\frac{m}{s}$, every box plot holds at least $11,000$ data points and the maximum percentage of outliers (indicated by the red points) is 5%.

8.4 Overview Validation Data, Continued

Turbine Induced
Turbulence

The last analysis is on the turbine induced turbulence. Figure 8.16 shows the turbine induced turbulence for the downstream turbines of turbine #1. It is calculated as the difference of the turbulence at the turbines with respect to the turbulence at turbine #1, which is equal to the free stream turbulence in the considered wind direction, see equation 8.5. It can be seen that the turbine induced turbulence is the highest at the direct downstream turbine (#2). After some fluctuating behaviour, it averages to about 10%.

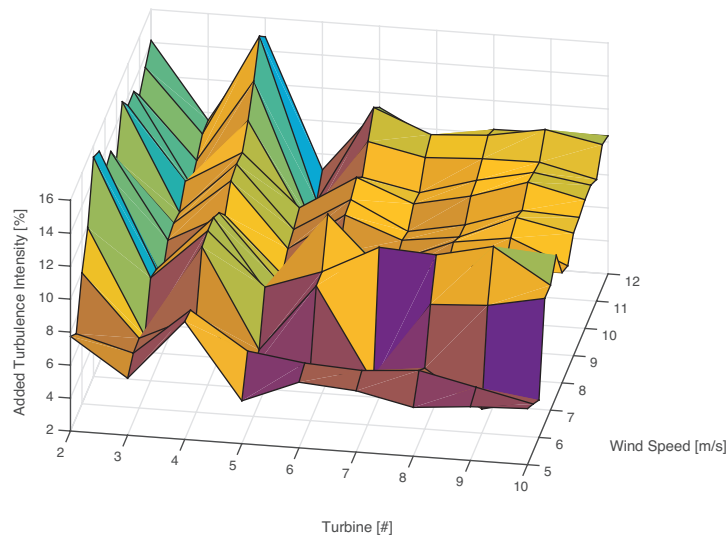$$TI_{induced} = TI_{measured} - TI_{free-stream} \tag{8.5}$$

8

Figure 8.16: Turbine induced turbulence for the downstream turbines for different wind speeds when the wind direction is in the range $210 \pm 2°$.

8.4 Measurement Results, <small>Continued</small>

Normal Distribution Turbulence

It was found that the turbulence intensities has a probability behaviour very close to a normal distribution. In figure 8.17 the probability distribution for three turbines is shown with the Gaussian distribution based on the mean and standard deviation of that data. Figure 8.18 shows the mean and standard deviation for all ten turbines. This behaviour is assumed to be partly due to the error of the sonic sensor and the method of calculating the turbulence intensity. Therefore it is considered to be appropiate to use the mean turbulence intensity for validation purposes.
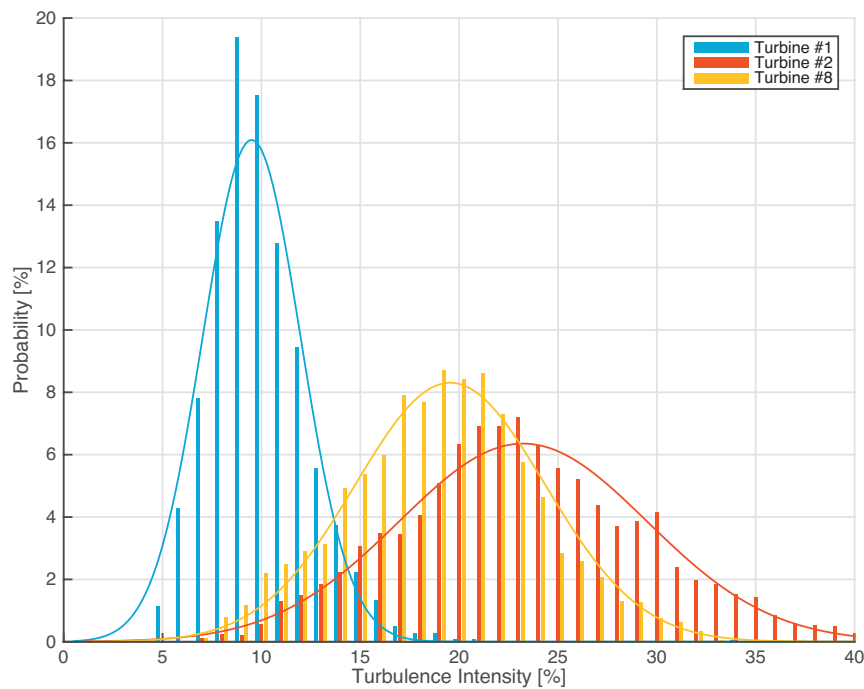
8

Figure 8.17: Normal probability behaviour of the total local turbulence intensity for different turbines. Note, the curves have been slightly moved to match the bar locations.

8.4 Overview Validation Data, Continued

Overview
Uncertainties

Table 8.2 shows the overview of all data uncertainties that will
be present in the next chapter to validate the wake models. The
derivation of the uncertainties of the wind speed and turbulence
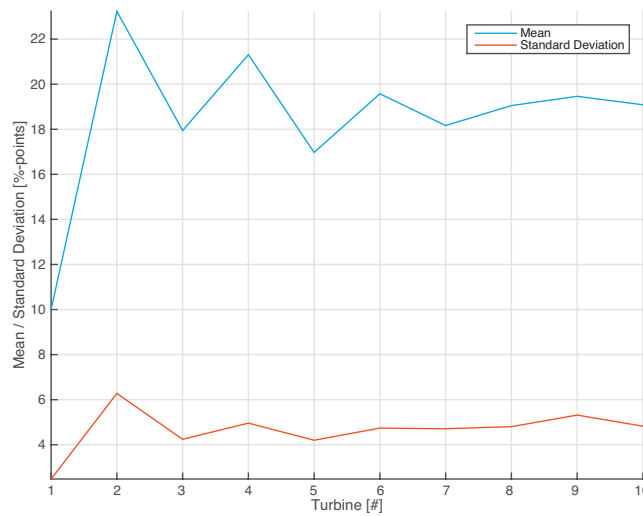intensity can be found in appendix D.

Figure 8.18: Gaussian distribution parameters of turbulence intensity over the turbines.

Table 8.2: Overview data accuracies, where V_0 is the free stream wind speed.

Allowance / Uncertainty	Condition	Value
Allowance Wind Direction		$\pm 2°$
Uncertainty Wind Speed	for $V_0 < 11\frac{m}{s}$	3%
Uncertainty Turbulence	for $V_0 = 8\frac{m}{s}$	$< 3.5 pp$
	for $V_0 = 10\frac{m}{s}$	$< 2.5 pp$

9

WAKE MODEL VALIDATION

The first section of this chapter tests the models as they are documented in literature. However, in the previous chapters several calibration possibilities have been suggested. The second section will present the selected corrections to optimize the wake models and tests if it indeed improves the results of the models.

9.1 Validation without Optimization

Modelling Approach

The wake models are tested for several free stream wind speeds. For each of these wind speeds the mean turbulence intensity is determined for nine downstream turbines, as in figure 8.17. The distance between each turbine is set to $520m$ as in Westermeerwind. The upper and lower boundaries of the error bands of the models are determined by running the models with the error in turbulence intensity as derived in appendix D.

Data Approach

In order to determine the representative measurement results, filters were applied on both the free stream wind speed and wind direction. The wind speed filter has a bandwidth of $\pm 0.25 \frac{m}{s}$. The wind direction filter has bandwidth of $\pm 2°$. Changing these bandwidths by a factor $\frac{1}{2}$ or 2 did not yield any significant differences in results. The error bands of the data are determined based on the error in measuring the wind speed as visualized in figure D.1.

Continuing...

9.1 Validation without Optimization, Continued

Results

Figure 9.1 shows the results of running the wake models and the measurement data without any wake model alterations.
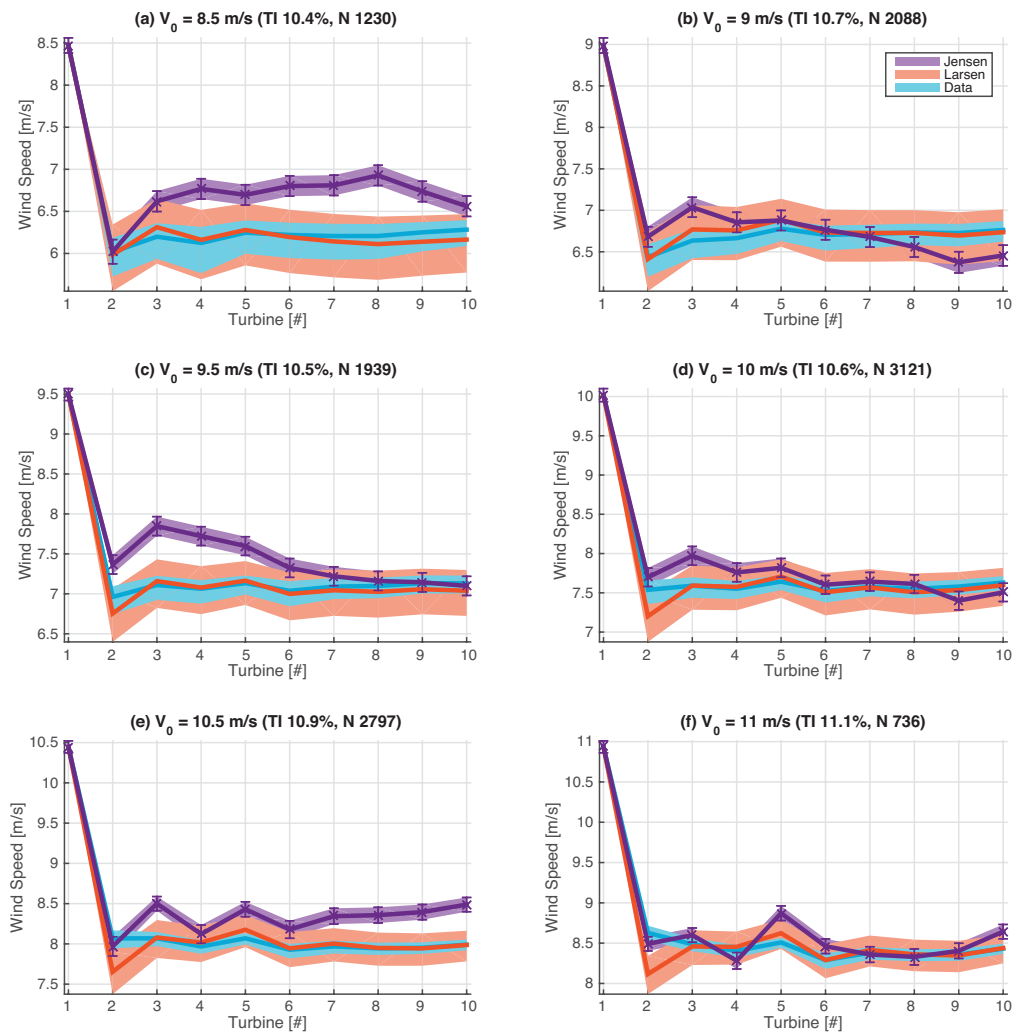

Figure 9.1: Wake model results without alteration and measurement data for several wind speeds. Above the graphs it is indicated which mean free stream turbulence intensity was used to run the wake models and how many data points (N) are used to determine the data curve. The shaded areas show the respective error bands of the data and wake models.

9.1 Validation without Optimization, Continued

Jensen versus Larsen

When comparing the two wake models in figure 9.1 it can be seen that the error bands of the Larsen wake model are wider than those from Jensen. This means that Larsen is more sensitive to the uncertainty in the turbulence than Jensen. Their results, however, are very comparable for almost all wind speeds and turbines.

Accuracy Second Turbine

The largest wake loss difference occurs between the first and the second turbine. The amount of wake loss on the second turbine is almost always overestimated by the wake models.

Accuracy Spacial Steady State

In general the wake models are good in calculating the wake loss of the spatial steady state, i.e. turbines #8 − #4, for these large datasets.

9

9.2 Wake Model Optimization

Optimization Jensen

The Jensen wake model does not contain many parameters that allow model optimization. Only the determination of the wake decay parameter k can be altered. It was found that using equation 6.2 performed better than the emprical relation that Choi and Shan found, see figure 9.2.

Optimization Larsen

Larsen has several parameters that are emperically determined from the Vindeby wind farm, see table 7.1. A multi-parameter optimization was performed to find parameters that better fitted the data from Westermeerwind. As an initial approach the data was not partitioned into a fit and test data set. In the single fold cross validation, many sets of parameters were found with equal errors, but the set differing the least from Larsen's original publication was chosen. This optimization changes only parameter a_3 to -0.50. Although, this does improve the results for some wind speeds, as can be seen in figure 9.2, no structural improvement was achieved. The optimization process was therefore discontinued and k-fold cross validations were not performed. For the rest of the report the original constants from Larsen, as in table 7.1 are used.
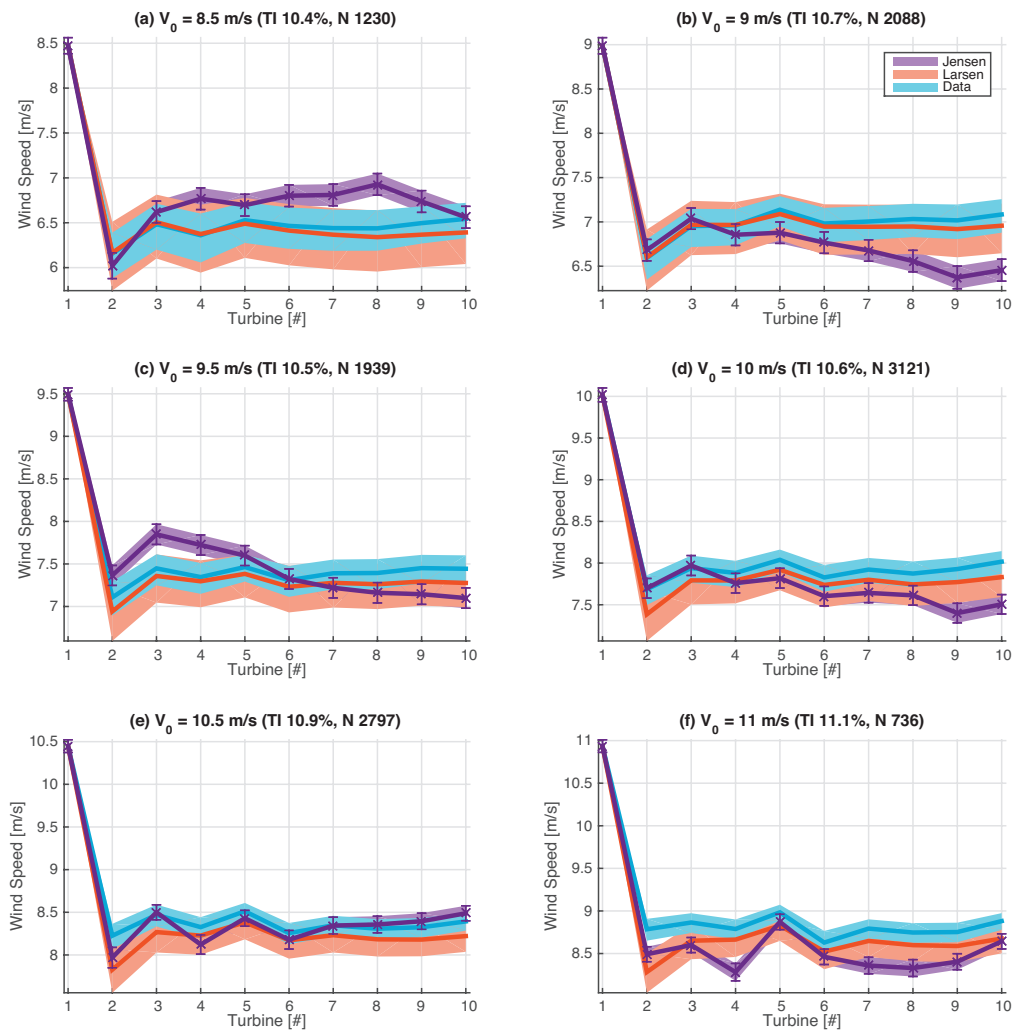
9

Figure 9.2: Wake model results with optimization versus measurement data for several wind speeds. Above the graphs it is indicated which mean turbulence intensity was used to run the wake models and how many data points (N) are used to determine the data curve. The shaded areas show the respective error bands of the data and wake models.

Continuing...

9.2 Wake Model Optimization, Continued

Error

The errors of the wake models versus the measurement data are shown in figure 9.3. Several observations can be made.

- For the higher wind speeds the maximum mean error is between $-0.4\frac{m}{s}$ and $+0.4\frac{m}{s}$.

- For the lower wind speeds the maximum mean error is between $-0.6\frac{m}{s}$ and $+0.8\frac{m}{s}$.

- The optimized Jensen wake models performs specifically well for the second turbine (#12) at higher wind speeds.

- The band where the data is outside of the models is larger for the Jensen wake model. However, in figure 9.2 it can be seen that the band width of Jensen is also smaller than Larsen.

Error All Wind Speeds

Figure 9.4 shows the root mean square error for all wind speeds between $5\frac{m}{s}$ and $11.5\frac{m}{s}$. It can be seen that for lower wind speeds Larsen performs much better, but at higher wind speeds the two wake models are very comparable.
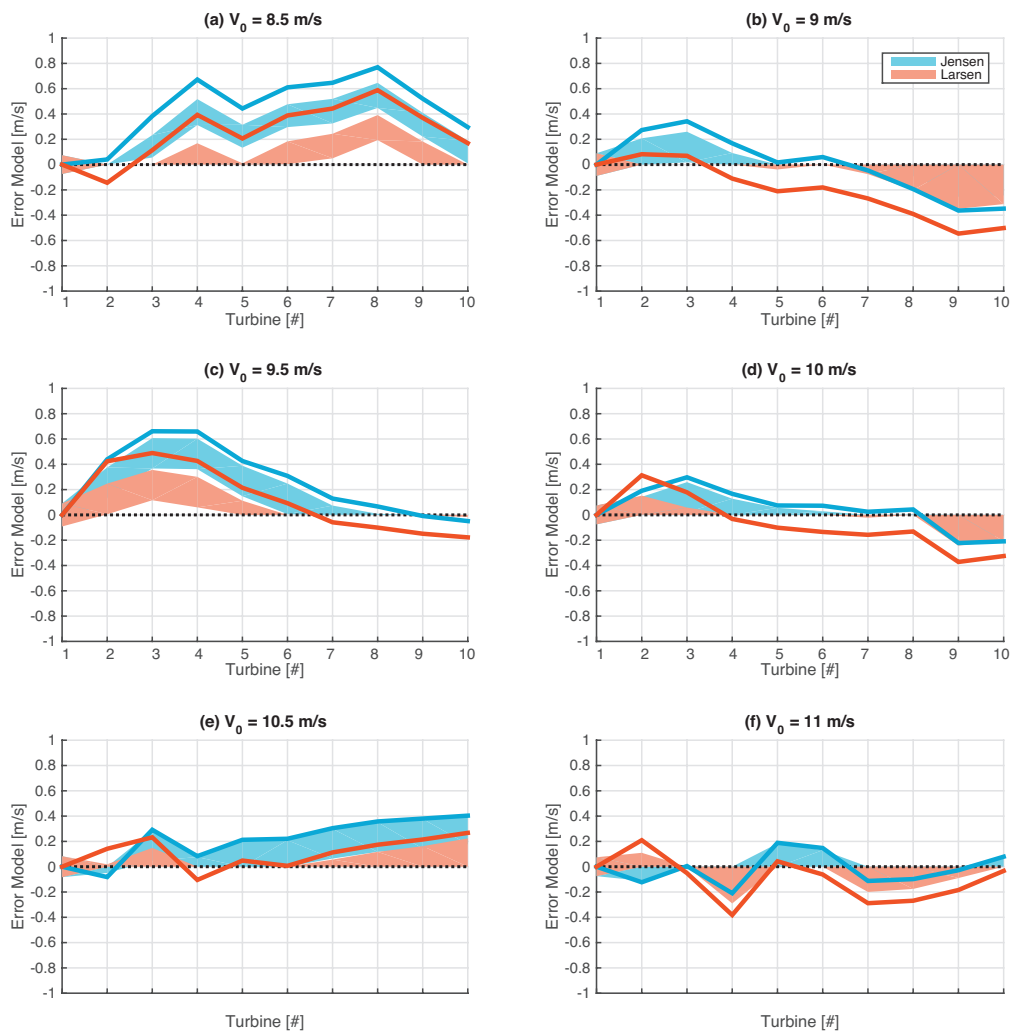
9

Figure 9.3: Errors of wake models versus measurement data. The lines indicate the mean error of the model with respect to the measurement data. The shaded areas indicate the part of the error bands of the wake models outside of the error band of the data.
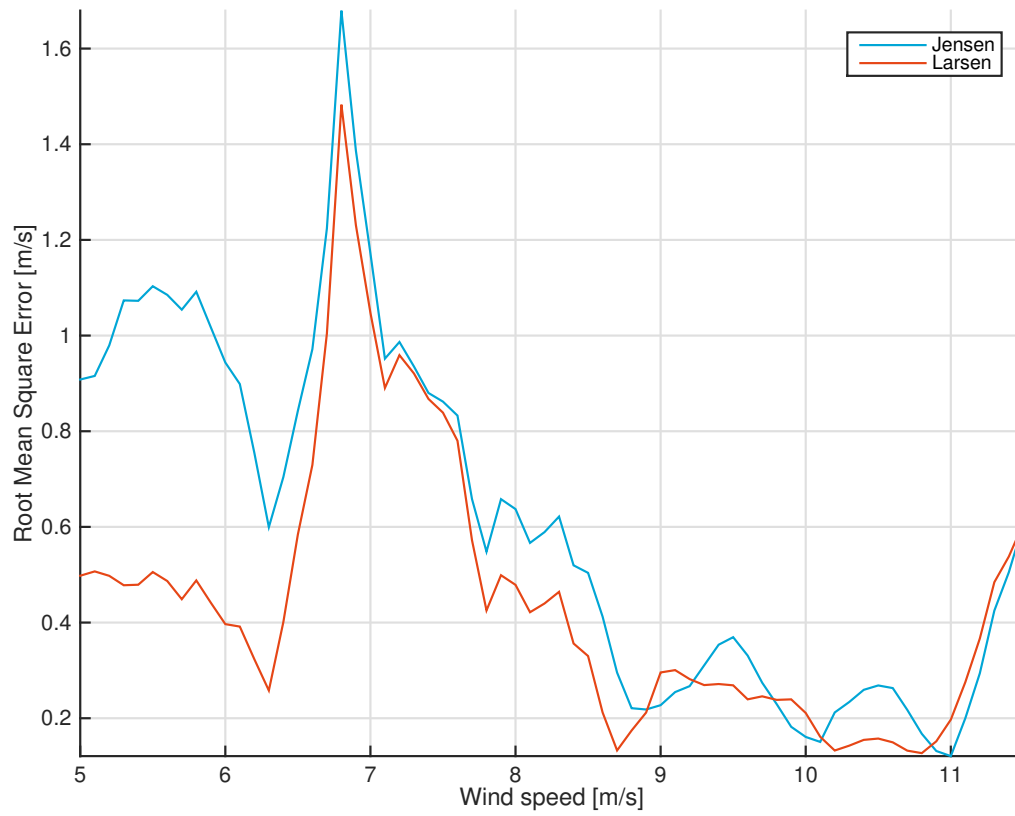
Figure 9.4: Root mean square error of wake models with respect to the measurement data.

9

9.3 Conclusion

Summary

In this part two wake models were presented, discussed, compared and tested against validation data from Westermeerwind. Due to the origin of the data signals a lot of attention was paid to the uncertainty quantification of the wind speed and turbulence intensity. The wake models were tested against measurement data from specific wind speeds and wind directions.

Jensen versus Larsen

In was found that in the region of interest - at wind speeds between $8\frac{m}{s}$ to $11\frac{m}{s}$ - the two wake models have comparable accuracy lower than $0.6\frac{m}{s}$. Both models are therefore judged to be acceptable for the purpose of modelling the wake development of a row of turbines.

9

III

WAKE MODELLING DURING CURTAILMENT

The last step before the algorithm can be validated is to test the capability of wake models to model the wakes behind turbines that are under curtailment. It is also important to test how well the wake models can be used to determine the power that the turbines would produced without curtailment, while the wind turbines are being curtailed. First, the experiments are introduced in chapter 10. Second, in chapter 11 the results are studied and stability criteria are applied to ensure high quality data during the validation process. Finally, the validation is performed in chapter 12.

10

EXPERIMENTAL METHOD

Before the results of the experiments can be discussed in the next chapter, first the experimental set-up is presented. This chapter discusses the turbines and method of curtailment, the method of data acquisition and the experimental design.

10.1 Technical Set-up

Row Selection
The wind farm layout is shown in figure 8.3. The wind direction determines which turbine row can be used for an experiment. All accepted experiments have been performed on the Northern row by curtailing turbine #1 and observing turbines #2 to #13.

Turbine Details
Most of the important parameters are stated in table 8.1 in section 8.1 Measurement Context . Additionally it is mentioned that the turbines curtail their power production by pitching their blades to feather. Also, the turbines have a variable rotational speed. It often occurred that the rotational speed of the rotor changed due to pitching of the blades.

Continuing…

10.1 Technical Set-up, Continued

Curtailing
Turbines

During the curtailment experiments it was not the pitch angle of the blades that was controlled directly. The turbine of interest was set to manual operation mode by detaching it from its automatic power controller and a set-point value was sent to the turbine. This set-point is treated as the new power production limit and the turbine automatically pitches its blades accordingly if power production would otherwise be higher than the set-point. The curtailment experiments are therefore not performed with a fixed curtailment factor, but with a fixed power production. The curtailment factor changes depending on the available power, see equation 3.1.

10.2 Data Acquisition

10-Minute Averages

The wind farm management and data analysis software of Ventolines BV allows exporting 10-minute averages of the measurement data. However, there are several disadvantages when using 10-minute averages:

- Experiments have to last exactly 10 minutes to allow proper comparison, otherwise only part of the average is affected by the experiment.

- It only gives a single data point per 10-minute experiment.

- Turbine variables cannot be monitored closely during the experiment, which is crucial to ensure that the experiment is performed at the right wind conditions.

- It is impossible to calculate the turbulence intensity, using only 10-minute data points.

Siemens SCADA

In order to obtain data with the required frequency a custom program was written in Python, to communicate with the SCADA from Siemens directly. This allowed a data sampling frequency of $1Hz$. This is in accordance of the IEC61400 [32], an international standard for design requirements regarding wind turbines of the International Electrotechnical Commission.

Experiment Dashboard

Next to saving the measurements in a file, every new measurement was also sent to a Firebase real time online database through a secure internet connection. This allowed the development of a custom monitoring web application - or experiment dashboard. In this application all data signals could be monitored in real time per turbine during the experiments, enabling continuous judgement of the right wind conditions and checking correct handling of the curtailment settings by the turbines.

10

10.3 Experiment Design

Practical Limitations

Although more experiments were planned, not all have been executed due to unfortunate wind conditions in the experimental phase of this research. Over the course of two months (September and November, 2016) only a few days allowed experiment execution. The experiments were designed in accordance with the wind farm layout and wind rose, but the most unfortunate wind condition appeared to be the wind direction. During the two months the wind was mostly not aligned with the turbine row. This indicates, that although the reduced wake effect might be significant, it only occurs during specific wind conditions and depends on the wind farm layout.

Realized Experiments

Table 10.1 shows all planned experiments, including their goal and whether or not they have been executed. This combination of experiments is designed to obtain a complete understanding of the reduced wake effect for a straight row of turbines. These experiments can be repeated for different wind directions if research is extended to encompass all possible wind conditions. Each of these experiments will be discussed in the next few sections.

10

Table 10.1: Planned experiments to fully understand the reduced wake effect (RWE). Deep wake refers to the fifth turbine and further downstream.

Reference	Name	Goal	Executed
1	**Curtailing Leading Turbines**	Study pure RWE	
$1a$	Curtailing first turbine		✓
$1b$	Curtailing second turbine		.
2	**Curtailing Multiple Turbines**	Study superposition RWE	
$2a$	Curtailing first two turbines		.
$2b$	Curtailing first five turbines		.
3	**Curtailing Deep Wake Turbines**	Study effect deep wake	
$3a$	Curtailing turbine in near deep wake		.
$3b$	Curtailing turbine in far deep wake		.
$3c$	Curtailing both deep wake turbines		.

10.3 Experiment Design, Continued

Curtailing Leading Turbines

In the previous part of this report it was found that the highest power difference between two neighboring turbines is between the first and the second turbine. In other words, the wake from the leading turbine causes the largest direct wake loss without curtailment. All turbines downstream of the second turbine experience multiple wakes. Curtailment of this first turbine is therefore expected to result in the largest change of wake effects for the most turbines.

Curtailing Multiple Turbines

Compared to curtailing a single turbine, a more probable commercial application would be the curtailment of multiple (if not all) turbines. When the first turbine is being curtailed, the second turbine will experience a reduced wake effect. When curtailing that second turbine as well, the following two reduced wake effects are expected:

1. A reduced wake effect on downstream turbines due to the curtailment of the production of turbine #2 during normal operation

2. A reduced wake effect of curtailing the available power increase of turbine #2, due to curtailment turbine #1

Curtailing Deep Wake Turbines

Besides experiencing a lower wind speed, turbines in the deep wake (from the fifth downstream turbine) also experience a much more turbulent incoming wind. Therefore, it is expected that the wakes of these turbines dissipate quickly, which would result in a smaller reduced wake effect when curtailing these turbines. Moreover, the curtailment of the fifth turbine should not show a significant effect on the tenth turbine and further downstream as not a lot of power relative to the first turbine is available for curtailment.

10.3 Experiment Design, Continued

Experiment
Duration

Each experiment is repeated several times for different curtailment levels. Each experiment had a duration of four minutes initially. In between each experiment, at least four minutes was waited without curtailment. This allowed monitoring of the normal free stream wind conditions and normal wake effects and served as a reference period for the experiments. During the data processing of the first few experiments it was found that the transient response of the wake effect could take up to two minutes. Experiments duration was therefore expanded to fifteen minutes and pauses to ten minutes, to allow better steady state analysis of both the experiment and the reference period.

10

11

EXPERIMENTAL RESULTS

This chapter presents the results of the performed curtailment experiments. First, the stability criteria are presented, which are applied to the performed experiments to ensure only high quality data for the quantitative analysis in the next part of this report. Second, the results of the accepted experiments are presented and discussed. Some interesting findings that are outside the scope of this report are presented in appendix C.

11.1 Stability Criteria

Criteria

The results from the curtailment experiments are only relevant when the experiments are performed under the right stable conditions. The following criteria were set to ensure meaningful results on top of all the research boundaries stated in previous chapters:

1. As the curtailment is determined by the difference of the available power and a fixed set-point for each experiment, the wind speed cannot reduce to the point that less than $200kW$ is being curtailed.

2. The wind direction cannot change to the extend of changing the wake profile over the turbines.

Continuing…

11.1 Stability Criteria, Continued

Monitoring Wind
Speed Condition

In order to monitor the first criterion, the wind speed could be measured directly. However, the required pitch angle of the blades to maintain a constant power is very sensitive to wind speed and is therefore also a good indicator of experiment quality.

Example Wind
Speed

Figure 11.1 shows the measurement data of five experiments performed right after each other. The following observations are made:

- In the first experiment the power was only curtailed $300\,kW$, while the wind speed was reducing. During this experiment the wind speed was also quite intermittent, observable by the changing pitch angle. This led to the actual curtailment often being lower than $200\,kW$.

- For the second experiment the wind speed was not intermittent, but gradually increased $1\,\frac{m}{s}$ during the experiment. This increase is also visible by the pitch angle data signal.

- In the third experiment the wind speed before and after the experiment are within a $0.5\,\frac{m}{s}$ difference and the flat pitch angle data indicates a constant wind speed during the experiment as well.

- The fourth and fifth experiment, experienced an intermittent wind speed, visible by the pitch angle. However, as the curtailment is more than $200\,kW$ on average these experiments can still be accepted.

From these five experiments, only the first is rejected due to its too small average curtailment.
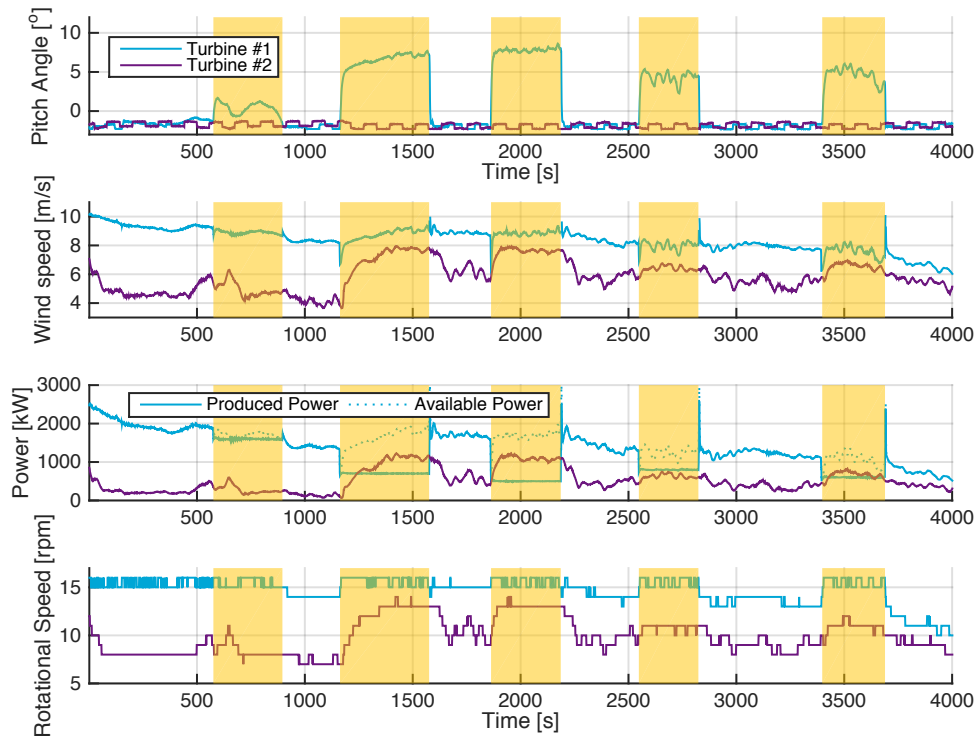
11

Figure 11.1: Five curtailment experiments performed consecutively. The yellow shaded areas indicate the moments when turbine #1 was being curtailed. In the first experiment the curtailment is often lower than $200kW$ which leads to the rejection of that experiment. The other experiments are all accepted.

Monitoring Wind Direction Condition

As mentioned in part II, the wind direction itself could not be measured directly. A better way of monitoring the wind direction is to look at the wake profile of the turbines. As was shown in figure 8.9 the wind speed deficit has a strong dependency on the wind direction. Therefore, heaving a stable wake profile means that the wind direction is also stable.

11

Continuing...

11.1 Stability Criteria, Continued

Example Wind Direction

Figure 11.2 shows an example of three other experiments than figure 11.1 performed right after each other as well. The first experiment has a difference in wind speed of $1\frac{m}{s}$ before and after the experiment, while the wind speed at turbine #1 is constant - note the constant pitch angle of turbine #1 as well. It is therefore concluded that the wind direction changed during the experiment. Although this experiment definitely confirms the reduced wake effect qualitatively, the experiment was rejected for quantitative analysis. The other two experiments, do not show this behavior and are accepted for quantitative analysis.
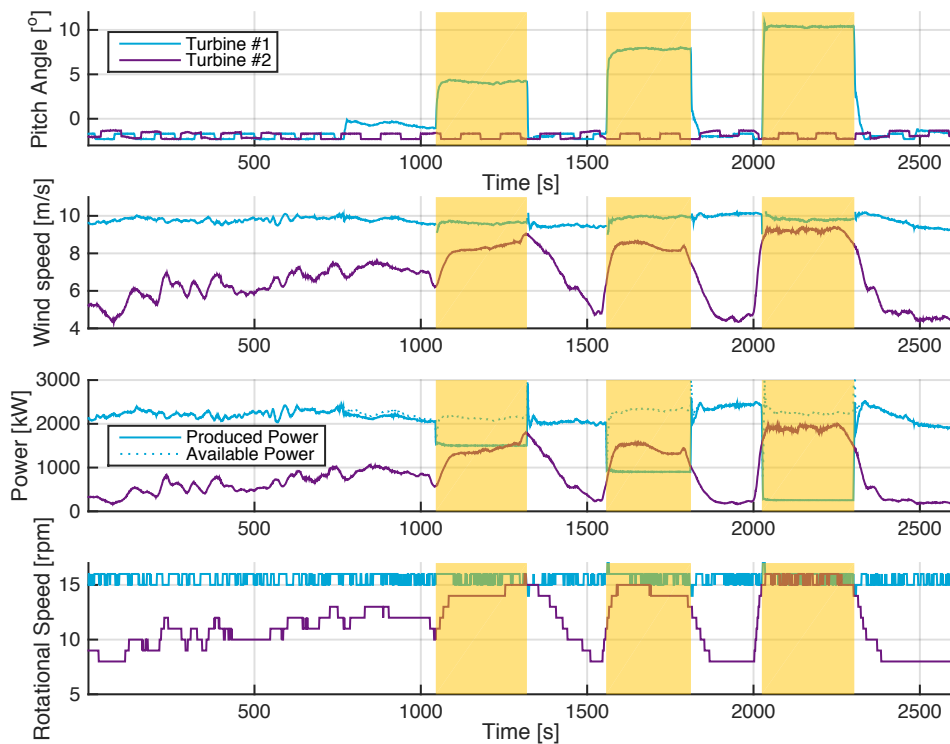

Figure 11.2: Three curtailment experiments performed consecutively. The yellow shaded areas indicate the moments when turbine #1 was being curtailed. The first experiment shows a changed wind direction due to the difference in wind speed before and after the experiments. Note that just before the first experiment the blades were also pitched slightly. This is due to curtailment setting of only 5%, which appeared to be impossible to maintain at all with the changing wind conditions. This experiment is therefore discarded completely.

11.2 Experimental Results

Using the stability conditions of the previous section, many experiments were rejected. From the sixteen experiments performed with turbine #1 eleven were rejected:

- Three experiments were rejected because the curtailment was less than $200kW$ on average. This resulted in very inconsistent curtailment varying between $200kW$ and $0kW$, see for example figure 11.1.

- Two experiments were rejected because they were performed while the first turbine was operating at rated power, making calculation of the wind speed impossible with the hybrid method discussed in part II.

- Six experiments were rejected because the wind direction changed during the experiment or because the wind direction was not aligned sufficiently with the turbines, i.e. more than 2° offset effectively.

Table 11.1 shows an overview of the accepted experiments. The results of first experiment will be presented and discussed in detail over the next sections, the other results and discussions can be found in appendix A.

11

Table 11.1: Overview accepted experiments

Experiment	$V_0 \left[\frac{m}{s}\right]$	$P_{1_{normal}}[kW]$	$P_{1_{curtailed}}[kW]$	**Curtailment**
1	10.0	$2,400$	900	65%
2	9.3	$2,400$	250	85%
3	8.9	$1,700$	700	40%
4	8.8	$1,700$	500	70%
5	8.4	$1,400$	800	60%
6	7.8	$1,100$	600	45%
7	10.3	$2,600$	$1,200$	55%

11.2 Experimental Results, Continued

Experiment 1   Figure 11.3 shows the data signals of the power produced by the
                            first seven turbines. The dotted line is the signal provided by the
                            available power estimator for turbine #1. At $57s$ a signal is sent to
                            turbine #1 to set its power level to $900kW$. This is reached within
                            a few seconds by pitching the blades to 8°. The following observa-
                            tions are made:

- The available power signal of turbine #1 shows a value
  higher than the power before the experiment, while only a
  few seconds have past. This is expected to be a small over-
  estimation of the available power estimator.

- It takes 1 minute for turbine #2 to reach its new steady state.

- The steady state of turbine #2 varies between $1,300kW$ and
  $1,550kW$.

- This steady state of turbine #2 is $1,200kW$ more on average
  than its power production during normal operation.

- It takes 2 minutes for turbine #2 to go back to is normal pro-
  duction after the experiment

- The production of turbine #3 drops during the experiment
  from an average of $700kW$ to $250kW$.

- On average turbines #4 to #7 do not to change more than
  $250kW$ during the experiment and all mean values of the
  production during curtailment fall between the minimum
  and maximum value in normal operation and vice versa.

- The variation of the power production of turbines #4 to #7 is
  higher in the reference periods than during the experiment.

Figure 11.4 shows an overview of the mean power production of all
turbines. This figure confirms the mentioned observations. Tur-
bines #4 to #13 do not change significantly due to the curtailment
of turbine #1; turbine #2 sees the largest increase in power and tur-
bine #3 the largest decrease, which is three times smaller than the
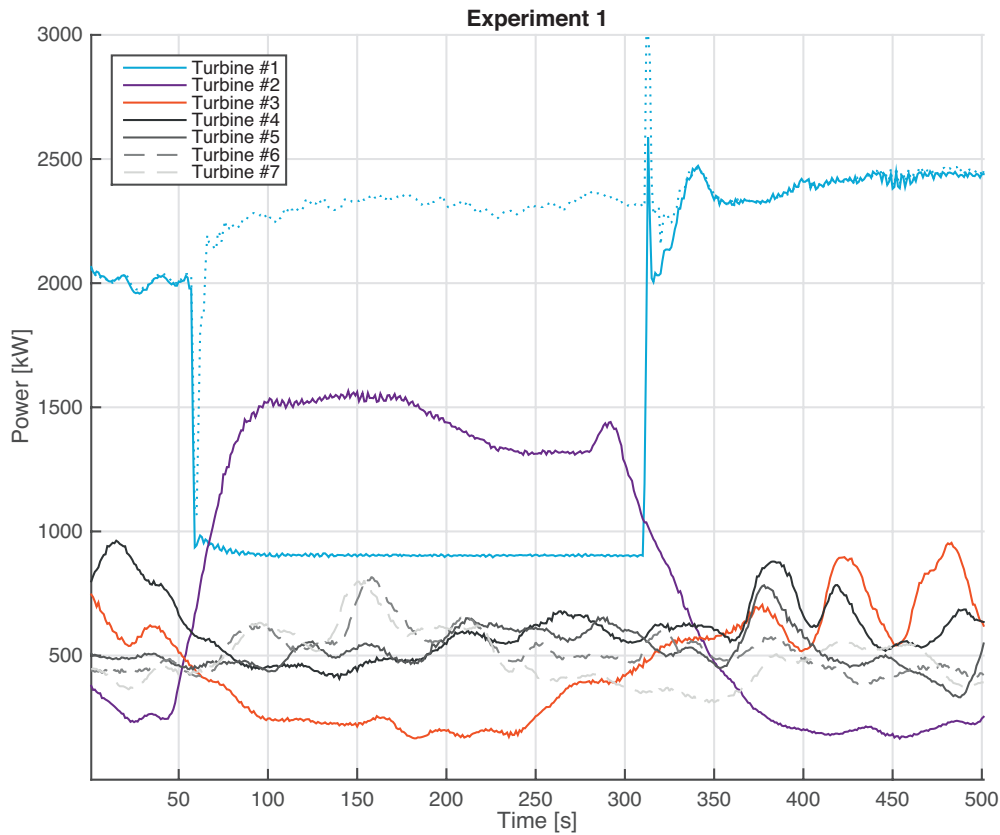power increase of turbine #2.

11

Figure 11.3: Power production signal of the first seven turbines as measured during and around curtailment experiment 1. The dotted line shows the available power of curtailed turbine #1.
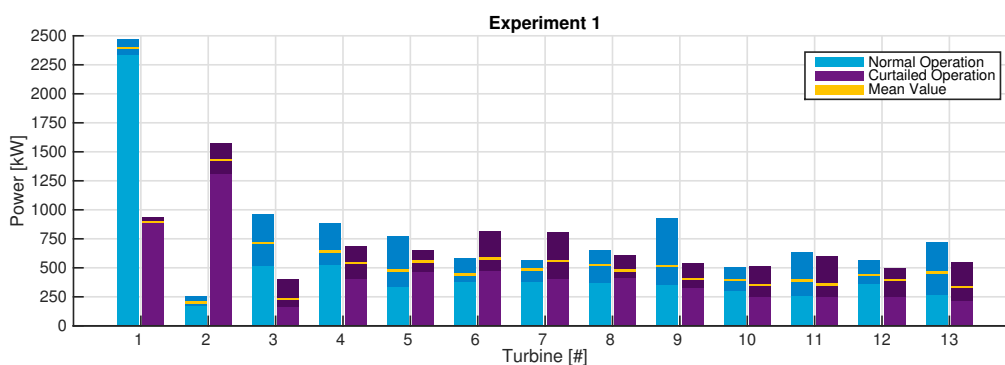

Figure 11.4: The power production of all thirteen turbines for the reference period (normal operation) and during curtailment experiment 1. The dark shaded areas indicate the minimum and maximum measured values, while the yellow line shows the mean value.

11.2 Experimental Results, Continued

Other
Experiments

The other experiments are discussed in a similar fashion in appendix A. The following additional remarks are made:

- For some experiments the curtailment factor changed during the experiments, but the curtailed volume was always more than $200kW$.

- During some experiments the first turbine operated at rated wind speed, as this is not allowed by the research boundaries and only the time segments in which this was not the case are used for validation purposes.

Increased
Turbulence

Figure 11.5 shows the measured turbulence intensities averaged over the reference period and during curtailment for a time span of $60s$. It can be seen that the largest drop in increased turbulence at turbine #2 is for the experiments where the most volume is being curtailed, i.e. experiments 1 and 2. But for all experiment counts that the turbulence intensity at turbine #2 approaches the free stream turbulence.

The mentioned free stream turbulence is determined from a reference turbine, see TI_{ref} in figure 8.3. Not that the values agree with figure 8.2. The added turbulence of turbine #1 provides an indication of the wake effect turbine #1 observes from the Southern turbines. It can be concluded that this wake effect is small for all experiments, as the added turbulence of turbine #1 is significantly lower than the added turbulence of turbine #2, which is in the wake of turbine #1.
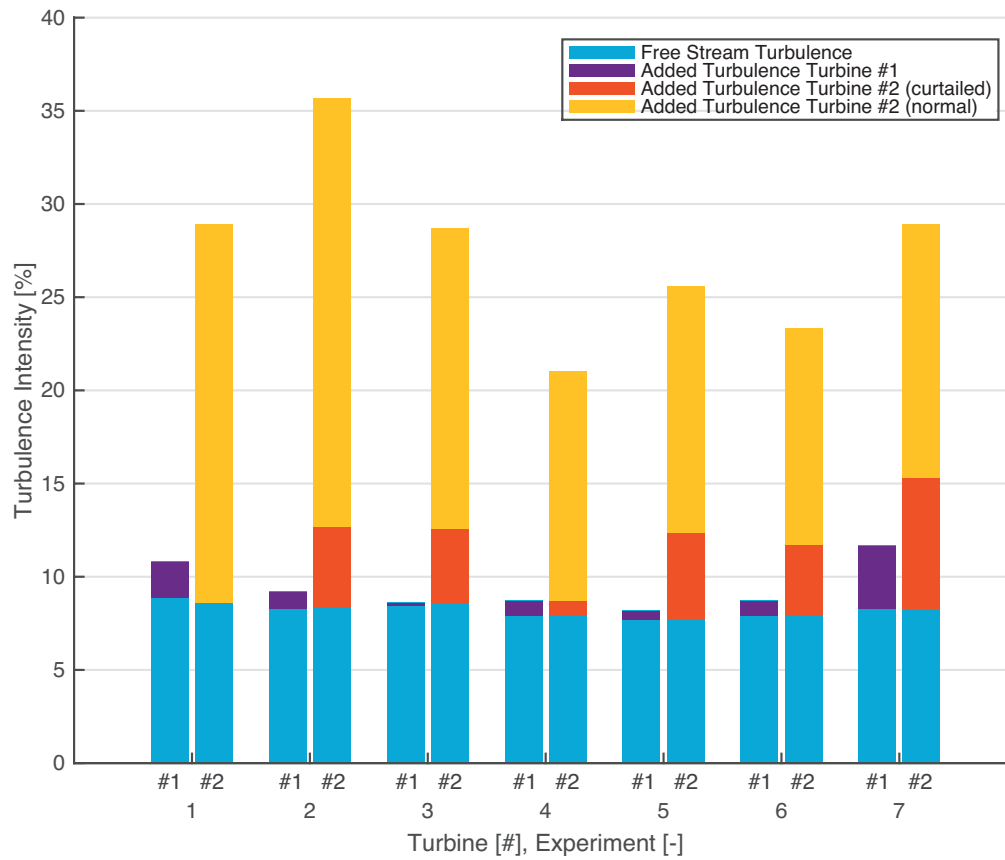
Figure 11.5: The turbulence intensity for each experiment for the first and second turbine. For example, for experiment 1 the turbulence at turbine #1 was 10.8% when the free stream turbulence intensity was 8.9%, i.e. the increased turbulence equals 1.8%. In the same experiment turbine #2 had a turbulence intensity of 28.9% in normal operation and 8.6% during curtailment.

11.3 Conclusion & Discussion Experiments

Experiment
Result Overview

Figure 11.6 provides an overview of all experiments by showing the difference of mean power produced during the experiment and in the reference period. On this figure one of the main findings of this research is based: **When curtailing a leading turbine, the second turbine will experience an increase in power production; the third turbine will have a decrease in power production smaller than that increase and all further downstream turbines will have no significant change in power production**.
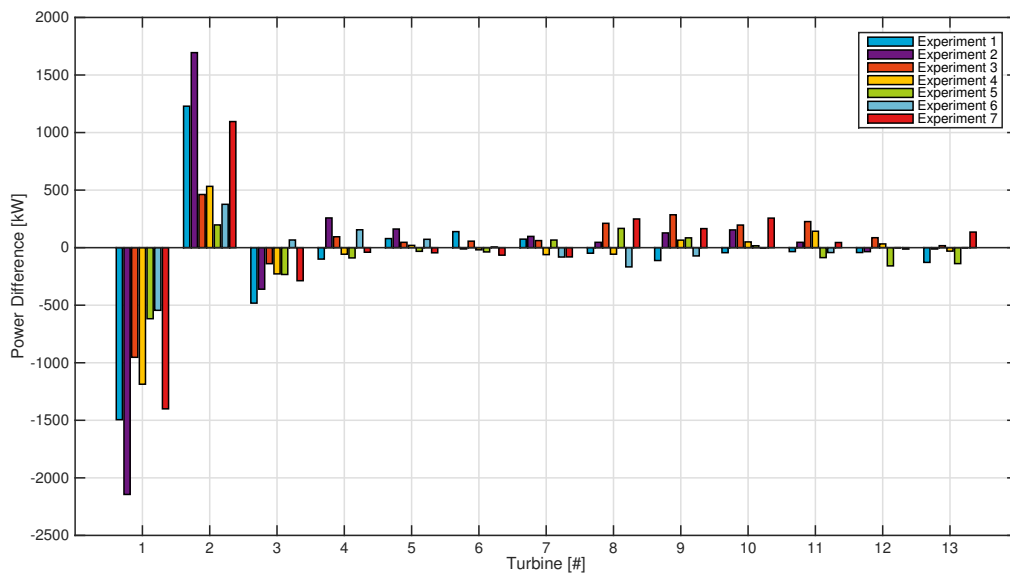

Figure 11.6: Mean power differences between curtailment and normal operation.

11.3 Conclusion & Discussion Experiments, Continued

Turbine #2

Figure 11.7 shows the difference between normal and curtailed operation for the first three turbines. The reduced wake effect is clearly visible on turbine #2. The power that is not extracted from the wind by turbine #1 becomes partly available to turbine #2 for 45% to 80%. In none of the experiments turbine #2 had a larger increase in power than the curtailed power of turbine #1, which seems to correspond with the results of other the pitching experiments by Bartl and Sætran [35].
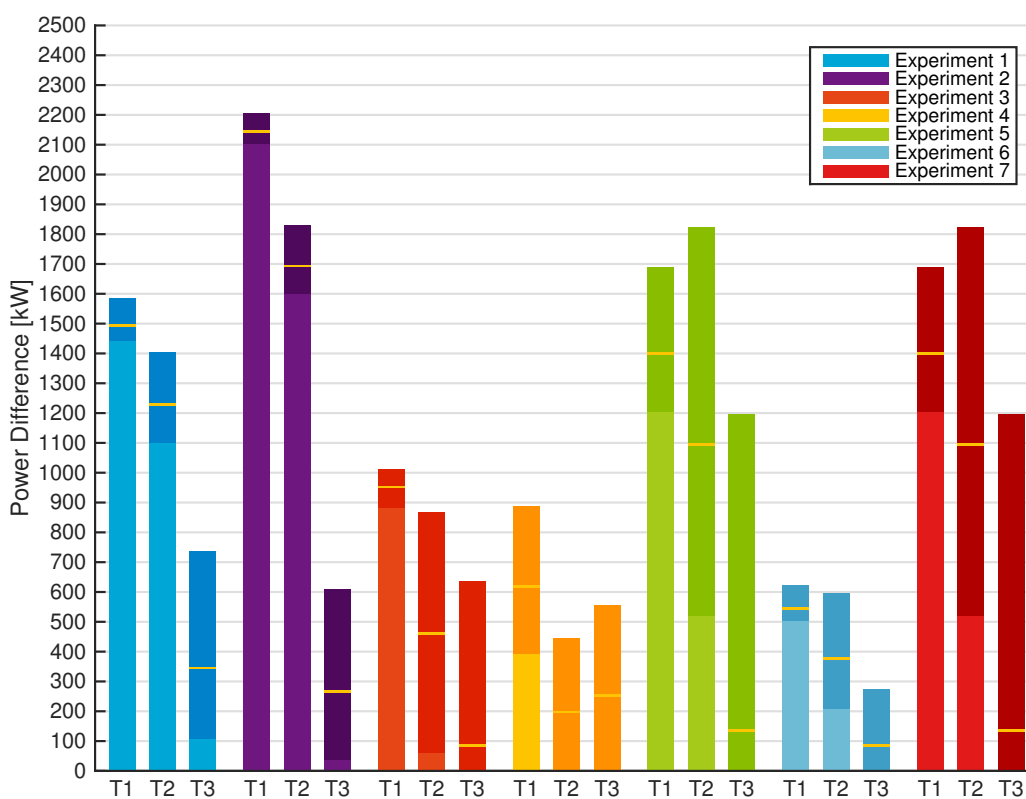

Figure 11.7: Absolute difference in power production between normal operation and curtailed operation of the first three turbines for each experiment. The shaded areas indicate the minimum and maximum values with respect to the mean, which is indicated by the horizontal line in the shaded area.

11.3 Conclusion & Discussion Experiments, Continued

Turbine #3

Turbine #3 does not show a reduction in wake effect. In contrast, turbine #3 often shows a reduction in power production in the range of 5% to 40% of the curtailed power of turbine #1. This can be explained by the increasing thrust force of turbine #2 resulting in a more significant wake development.

Turbine #4

The reduction in power of turbine #3 could have meant that turbine #4 showed an increase in power due to reduced wake of turbine #3. However, the change in power of turbine #3 is smaller than $300kW$ for all experiments, yielding in a reduced wake effect too small to measure at turbine #4.

Downstream
Turbines

For turbines #4 and further downstream no structural change in power production is observed. The non-zero values in figure 11.6 can be attributed to:

- Small differences in wind conditions (e.g. wind speed, wind direction) during curtailment and the reference period.

- Errors in the method shifting the times of downstream turbines, especially for far downstream turbines.

11

12

VALIDATION WAKE MODELLING DURING CURTAILMENT

The seven experiments presented in the previous chapter are used to validate wake modelling during curtailment. By monitoring the wind conditions during the experiments and in the reference periods, it can be tested if the augmented wake models based on the existing wake models of chapters 6 and 7 are accurate. This chapter will first state the modelling approach of the augmented wake models. Thereafter, the validation results are presented and the main conclusions are drawn.

12.1 Modelling Approach

Turbines

In the analysis of the previous chapter it was found that, when curtailing the first turbine, the second turbine experiences the largest difference in power production. This chapter therefore focuses mainly on validating the modelling for the second turbine.

Continuing…

111

12.1 Modelling Approach, Continued

Time Series
Inputs

The augmented wake models using the Jensen and Larsen wake models are applied as discussed in chapter 9. In order to calculate the time series response, the following time series are used as an input:

- Free stream wind speed

  – In order to determine the free stream wind speed the power method of section 8.2 Data Accuracy is applied. During curtailment the *APE*-signal of turbine #1 is used as input for this method.

- Free stream turbulence intensity

  – For the turbulence intensity of turbine #1 a single value for the whole experiment is used, as the sonic sensor data required for the calculation is not valid during the experiments according to the documentation. This value was determined by taking the mean of the turbulence intensity in the reference period of each experiment.

- Curtailment factor

  – The curtailment factor is determined as the ratio between the *APE*-signal and the active power signal of the first turbine, as in equation 3.1.

- Density correction

  – The density correction is continuously determined using the method described in section Air Density Correction.

12

Continuing...

12.1 Modelling Approach, Continued

Steady State

As stated in the requirements of the algorithm in section 3.1 Requirements Algorithm , only the steady state response will be studied. Per turbine it is determined when this steady state has been established.

Modelled Values

The wake models are used to calculate two values:

- The active power signal of turbine #2 during the reference period and the curtailment experiment.

- The active power signal of turbine #2 if no curtailment is applied to the model. This can be understood as the power that turbine #2 would have produced if turbine #1 would not have been curtailed.

The difference between these two values equals the reduced wake effect.

12

12.2 Results for Turbine #2

Experiments 1 and 2

Experiments 1 and 2 were performed right after each other. In figure 12.1 the modelling of the Jensen and Larsen augmented wake models are compared to the measurement data. The following observations are made:

- During both experiments the wake models approach the active power signal of turbine #2.

  - The Jensen augmented wake model has errors of 19% and 1.4% for the two experiments, which are overestimations.

  - The Larsen augmented wake model has errors of -10% and -6.5% for the two experiments, which are underestimations.

- The wake models do not model the power production of turbine #2 outside of the curtailment experiments well: there is an offset of $700\,kW$ to $900\,kW$ between the models and the measured data. Therefore the modelled normal operation during curtailment has a large error as well.
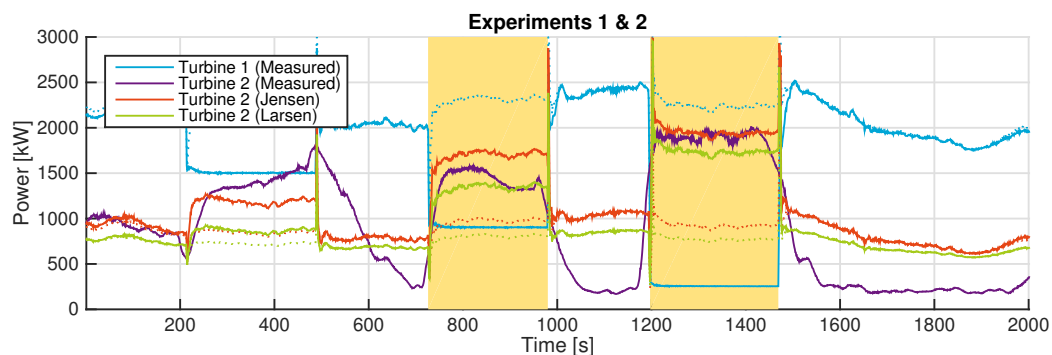

Figure 12.1: Power production signal of turbine #1 and #2. The dotted line of turbine #1 indicates the APE-signal. The dotted line of the wake models indicate the power production modelling if no curtailment is applied to the models. The experiments are indicated by the yellow shaded area.

12.2 Results for Turbine #2, Continued

Explanation Mismatch

It was investigated why the wake models failed to estimate the power production of turbine #2 with better accuracy. When comparing the yaw angle of turbine #2 with the yaw angle of turbine #1, it was found that at around $400s$ turbine #2 started to yaw. It is not known why the turbine changed its yaw angle, as turbine #1 had a constant yaw angle, thus indicating that the wind direction did not change. After these two experiments the turbine yawed to its original position and the model matched better with the turbine measurements. It is therefore concluded that the mismatch is likely to be explained by a yaw misalignment.

Using Experiments 1 and 2 for Validation

When comparing the wake loss of turbine #2 with figure 9.1 it can be seen that for a production of turbine #1 between $2000kW$ and $2500kW$, the production of turbine #2 can be expected to be between $800kW$ and $1,300kW$. The conditions leading to the value of $200kW$ in the reference periods of experiment 1 and 2 can therefore be assumed to be not regular. These experiments will therefore not be used for validation of the algorithm.

Continuing…

12

12.2 Results for Turbine #2, Continued

Experiment 3

In experiment 3 the wind speed gradually increased during the experiment, see figure 12.2. The following observations are made:

- The wake models do not match the measured data before the experiment, both have an error between $150kW$ and $300kW$.

- The APE provides a reasonable signal as it stays between the values before and after the experiment.

- During the experiment the two wake models follow general shape of the measurement data.

  - The Jensen based augmented wake model has an error of 7.5%, which is an overestimation.

  - The Larsen based augmented wake model has an error of -22%, which is an underestimation.

- The modelling of the normal operation during curtailment is reasonable, as it stays between the normal operation before and after the experiment.

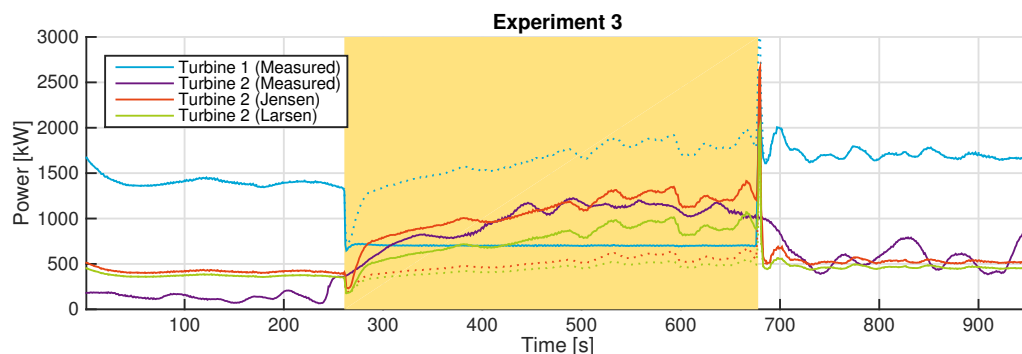- The gradually changing wind speed does not seem to introduce additional errors of the wake modelling.

Figure 12.2: Power production signal of turbine #1 and #2. The dotted line of turbine #1 indicates the APE-signal. The dotted line of the wake models indicate the power production modelling if no curtailment is applied to the models. The experiments are indicated by the yellow shaded area.

12.2 Results for Turbine #2, Continued

Other
Experiments

The modelling results for the other experiments can be found in appendix B. Similar behaviour as in experiment 3 was found for the other four experiments.

Overview

Figure 12.3 shows the performance of the two wake models for all experiments. It shows the mean modelled power for turbine #2 against the mean measured power. It also shows the mean difference of the models with the measurements.
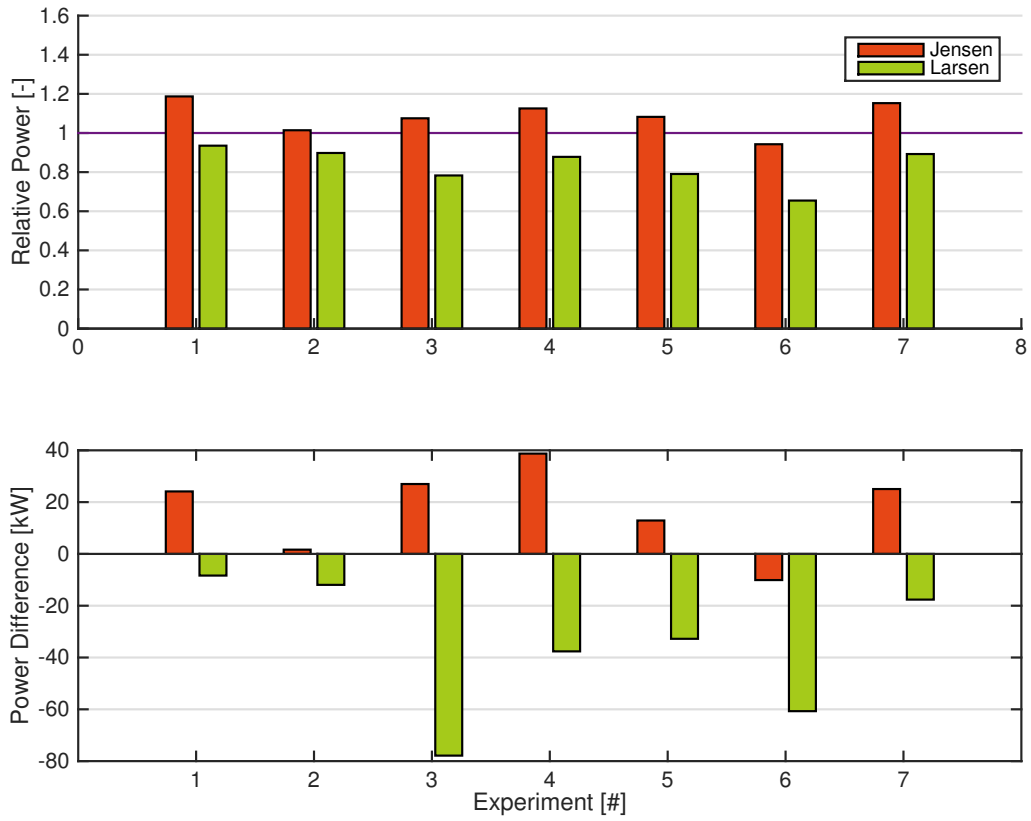
12

Figure 12.3: An overview of the mean performance of the two augmented wake models during curtailment for turbine #2 for all seven experiments. The upper figure shows the ratio between the models and the measurements, while the lower figure shows the difference between the models and the measurements.

12

12.3 Results for Downstream Turbines

Modelling Without Curtailment

Before the wake modelling during curtailment is presented for the downstream turbines, first the performance of the modelling during the reference period (without curtailment) is shown in figure 12.4. This is done in the same way as for turbine #2. The figure shows the error of the wake model with respect to the measurement data. Several observations are made:

- The error of modelling is considerable for all experiments.

- The error generally grows for each downstream turbine.

- The error for turbine #2 for experiments 1 and 2 as discussed in the previous section are clearly visible.

Modelling With Curtailment

In figure 12.5 the results of the wake modelling during curtailment of all turbines can be found. The figure shows the error of the wake model with respect to the measurement data. It can be seen that in most cases the error of the wake models is considerable: in only a few cases the error is less than 30%.
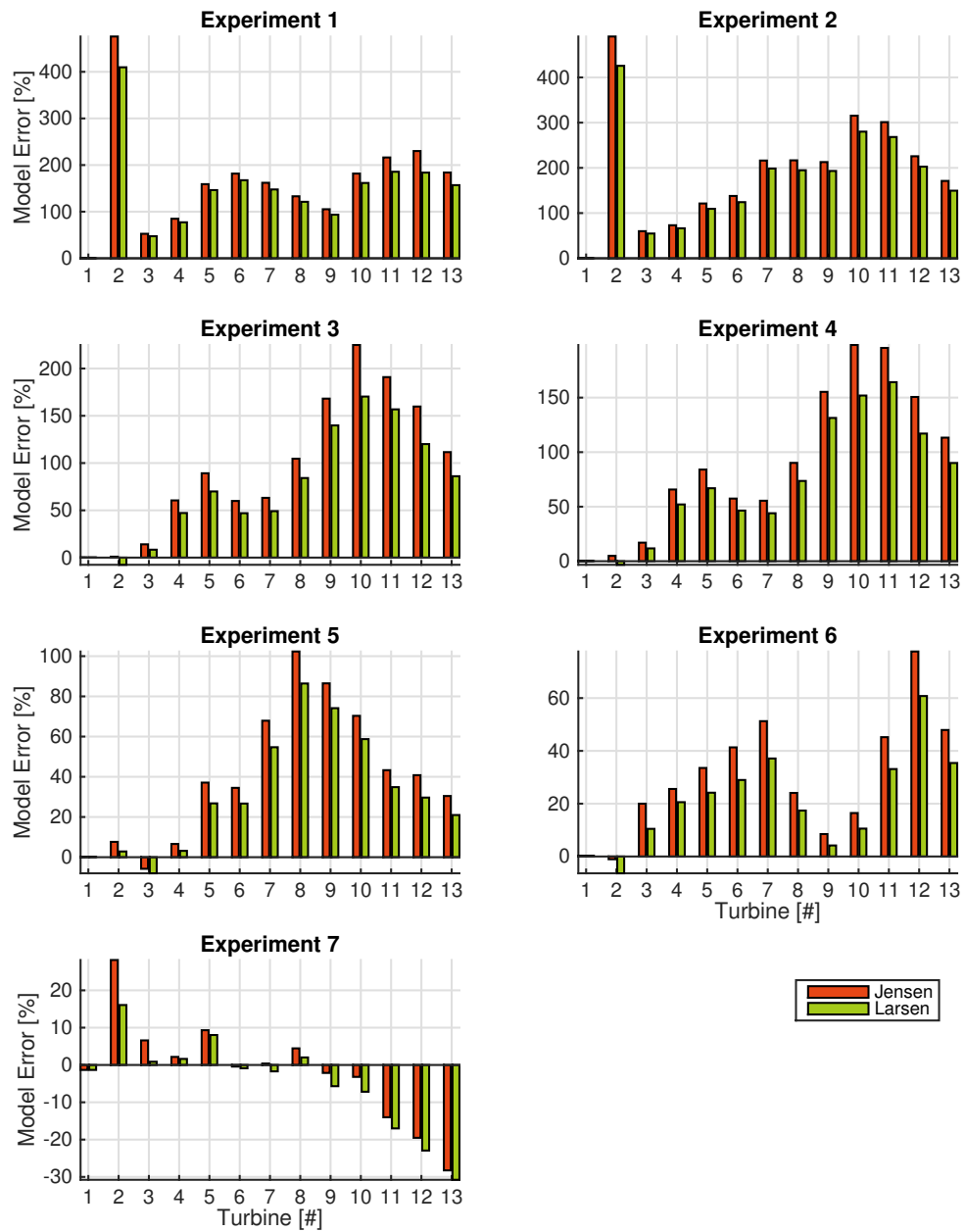
12

Figure 12.4: An overview of the mean performance of the two wake models during the reference period (without curtailment) for all turbines for all seven experiments. The figure shows the error calculated per turbine.
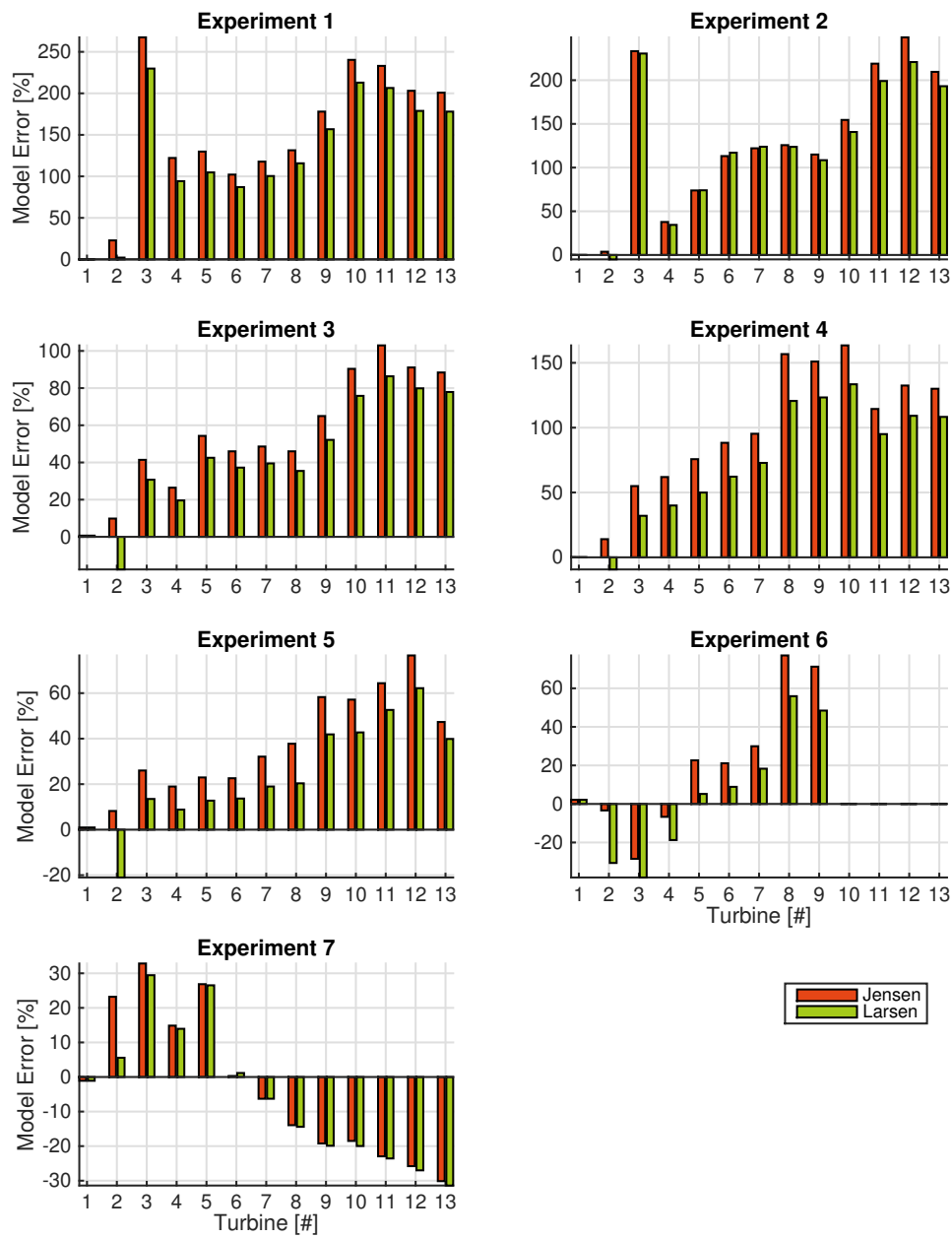
Figure 12.5: An overview of the mean performance of the two wake models during curtailment for all turbines for all seven experiments. The figure shows the error calculated per turbine.

12.4 Conclusion

Turbine #2

Based on the performed analysis the following conclusions are drawn for turbine #2.

- In experiments 1 and 2 the wake models did not match the measurement data of turbine #2 outside of the experiment. These experiments are therefore not used to validate the algorithm in the next chapter, but do indicate that this approach does not work for turbines operating unexpectedly.

- For turbine #2 the curtailable wake models performs well in the other five experiments.

- Using the Jensen based augmented wake model a maximum absolute error of $40kW$ and a maximum relative error of 19% was found.

- The Larsen based augmented wake model lead to an maximum absolute error of $80kW$ and a maximum relative error of 35%.

- In most cases the Jensen based augmented wake model overestimated the power production of turbine #2, while the Larsen based augmented wake model always underestimated that power.

Downstream Turbines

The current approach does not seem suitable to use for turbines further downstream than turbine #2, due to the specific implementation of the wake models in this research.

12

IV

VALIDATION ALGORITHM

In this part the algorithm introduced in part I, using the wake models discussed and validated in part II, is validated using the experiments studied in part III. In this part it will be determined if the algorithm performs better than the gross available power method.

13

VALIDATION ALGORITHM

All the unknowns of the algorithm defined in section 3.4 Algorithm Uncertainties have now independently been tested and (partially) successfully validated. The last step of this research is to validate the complete algorithm and test its improvement with respect to simple summation of individual turbine available power signals, i.e. the gross available power method. First, the procedure of algorithm validation is presented. Second, the validation results are discussed.

13.1 Validation Approach

Algorithm Application

In the five valid experiments on which this validation is based, only turbine #1 has been curtailed. It was found in part III that the reduced wake effect was only noticeable at turbine #2 and #3. However, the wake models have large errors at turbine #3, so the current best usage of the algorithm is to only apply it to determine the available power of turbine #2.

Validation Turbines

In part III it was found that from turbine #4 and further downstream the difference between the curtailed and normal operation has a random behaviour. In order to exclude this noise in the validation process, the sum of the available power of the first three turbines is taken to be validated, considering the validation of the whole row of turbines.

13.2 Validation Results

Reduced Wake
Effects

Before the validation of the available power calculation of the algorithm, first the results of determining the reduced wake effect (RWE) are presented. Figure 13.1 shows the RWE for turbine #2 and #3. It can be seen than for turbine #2 the algorithm using the augmented Jensen wake model overestimates the RWE, while using the augmented Larsen wake model results in an underestimation. However, the algorithm performs poorly for turbine #3. In figure 13.2 it can be seen that error of both models is larger than 50%, except for experiment 4.
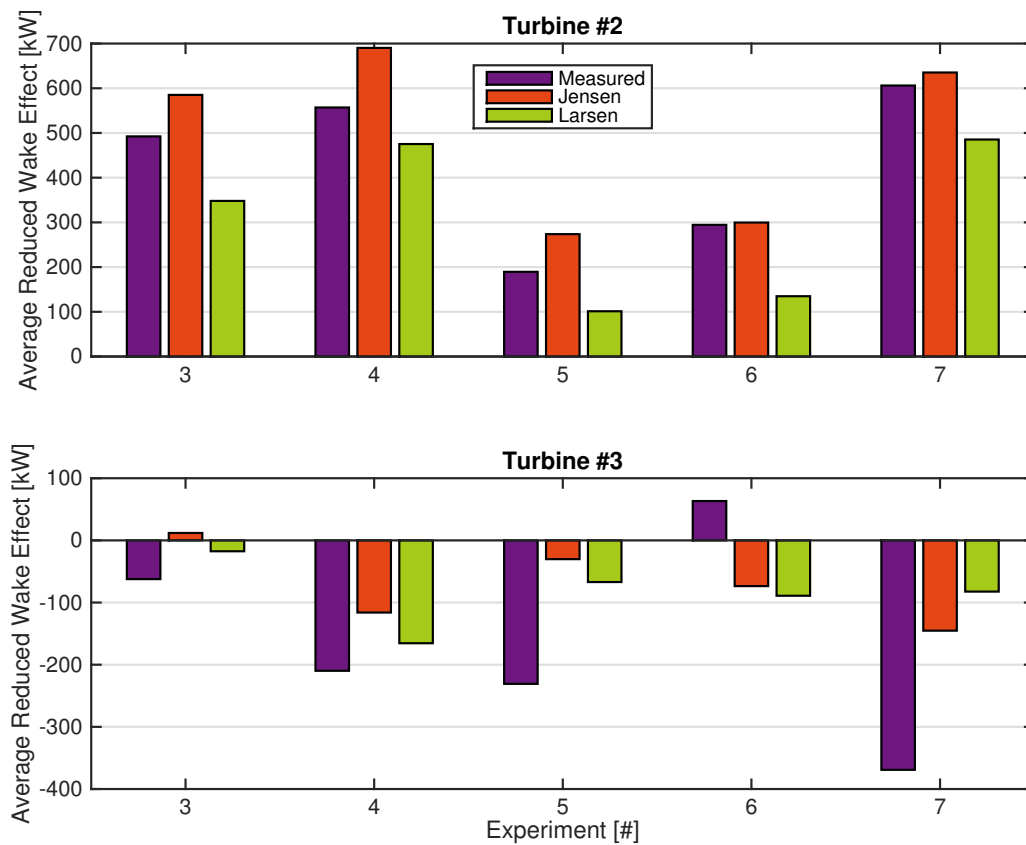

Figure 13.1: Reduced wake effect of turbine #2 and #3 as measured and as determined by the algorithm using the two augmented wake models
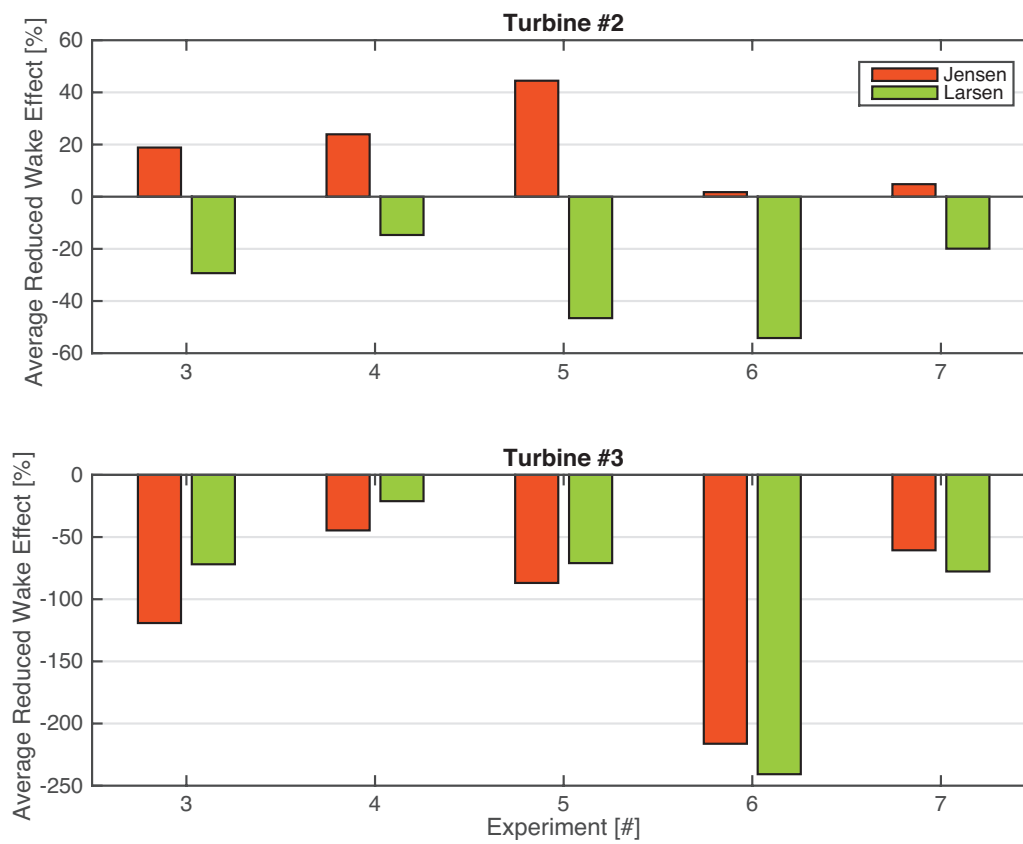
13.2 Validation Results, Continued

Figure 13.2: Error of determining the reduced wake effect by the algorithm using the two augmented wake models

13.2 Validation Results, Continued

Validation
Results

Figure 13.3 shows the average available power of turbine #2 for each experiment. It consists of four bars per experiment:

- The measured available power equals the production of turbine #2 in the reference period, which is the value to be calculated by the methods.

- The gross available power method refers to simply adding the gross curtailed power to the produced power. As turbine #2 was not curtailed in any experiment, this value equals the average measured power of turbine #2 during the experiment.

- The other two bars are calculated with the algorithm using the two augmented wake models.
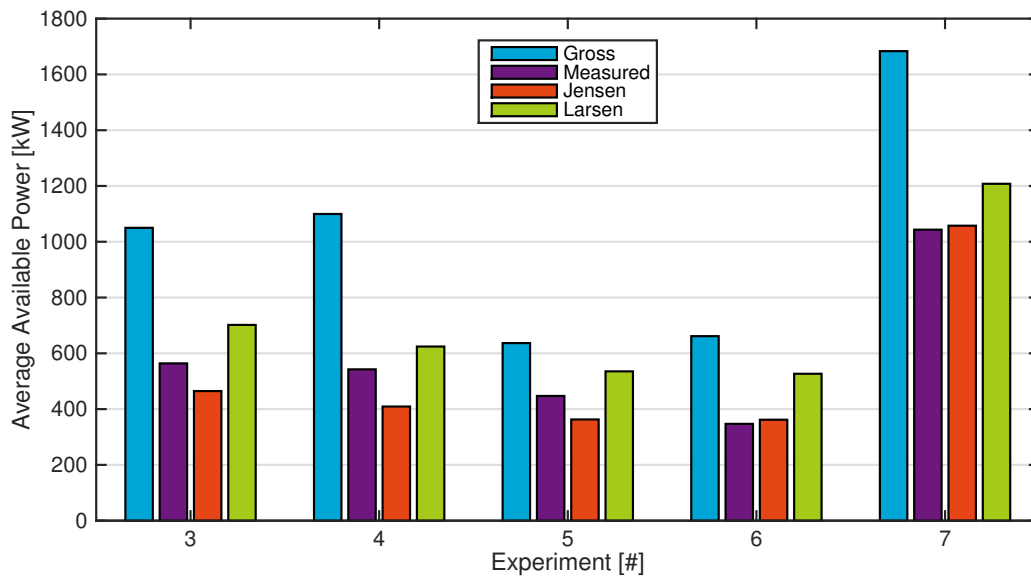

Figure 13.3: Average available power of turbine #2 for gross available power method, measured as the difference between normal and the reference period and the algorithm with the two augmented wake models.

13.2 Validation Results, Continued

Error Turbine #2 In figure 13.4 the error of the algorithm with respect tot he gross available power method is shown. For all experiments the algorithm performed better than the gross available power method with an error reduction between 20% to 80%.
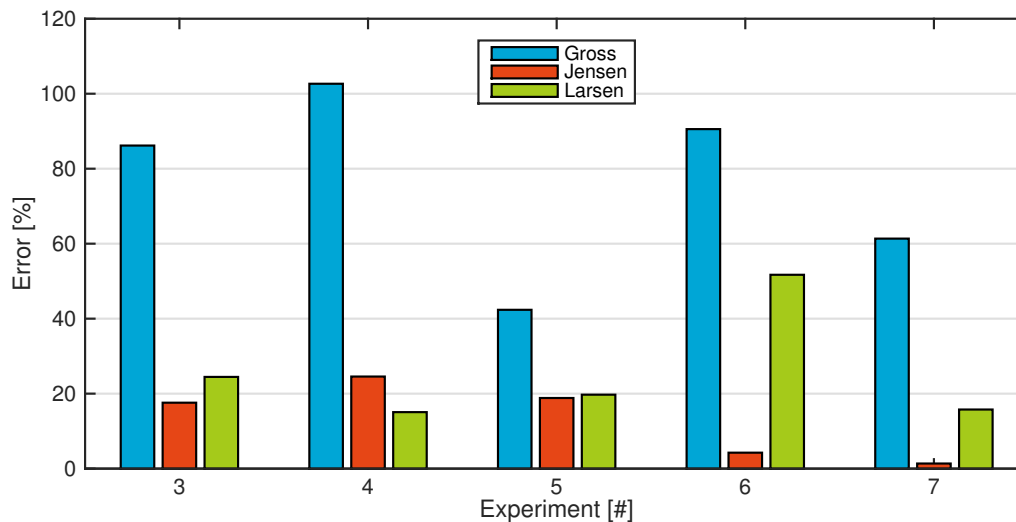

Figure 13.4: Absolute error of the average available power of turbine #2 for gross available power method and the algorithm with the two augmented wake models.

13

13.2 Validation Results, Continued

Three turbines The last validation study is on the available power of the whole row of turbines. To calculate the error only the first three turbines are considered. Considering the large errors of the wake models for turbine #3, current best practise of using the proposed algorithm is to only use it to determine the available power of turbine #2, see figure 13.5. For turbine #3 the change in wake loss is thus ignored. This is known to be underestimation for most experiments, as turbine #3 often had a small power reduction during the experiments. Further study is required to optimize the algorithm for turbine #3 to enable its full potential.
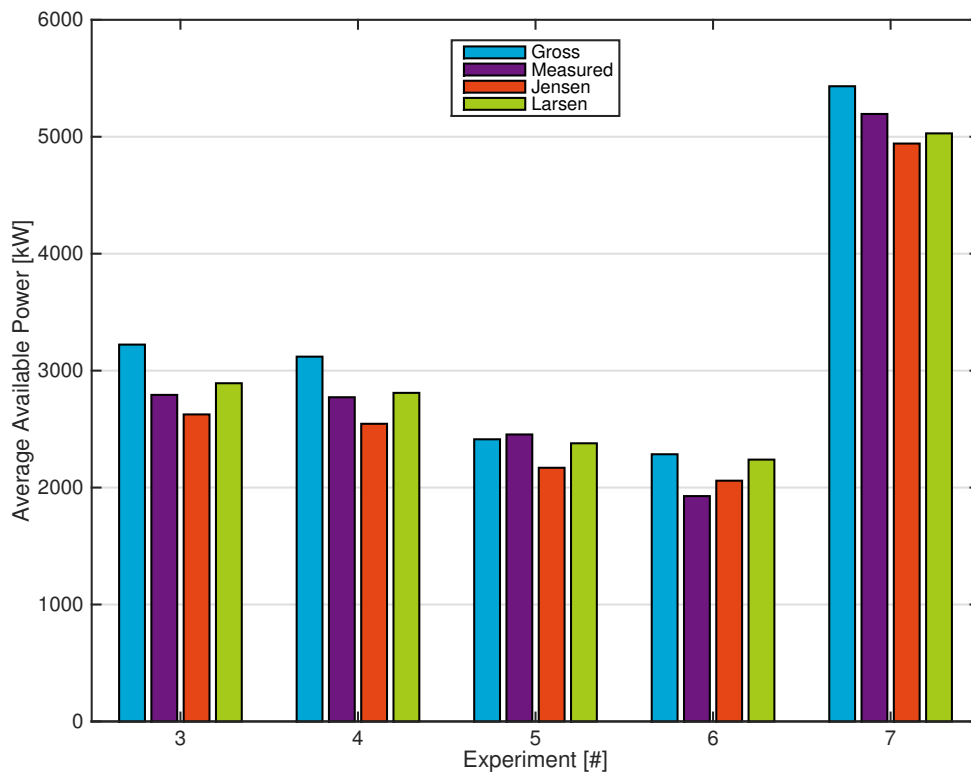

Figure 13.5: Sum of average available power of turbine #1, #2 and #3 for gross available power method, measured as the difference between normal and the reference period and the algorithm with the two augmented wake models.

13.2 Validation Results, Continued

Error Three
Turbines

The error is calculated over the total available power of the three turbines, see figure 13.6. It can be seen that the improvement of the algorithm over the gross available power method is smaller than considering turbine #2 solely. The error of the algorithm is lower than the gross method for four experiments. In experiment 5 both augmented wake models, especially the Jensen based, have a significant larger error.
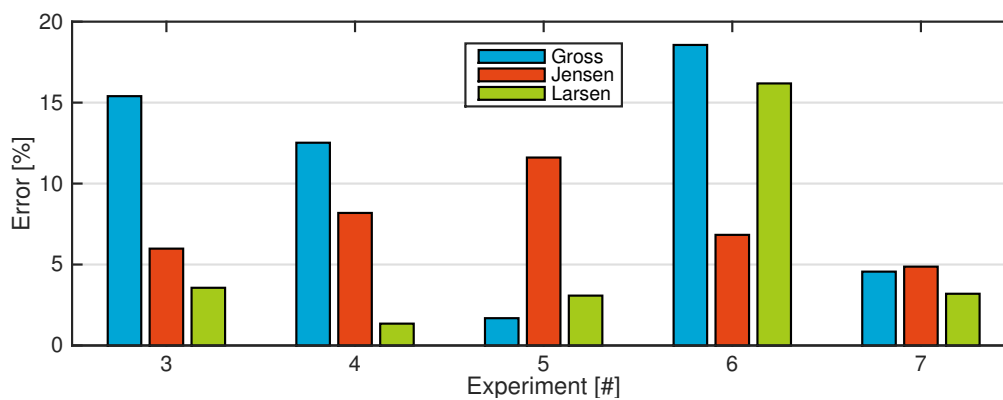

Figure 13.6: Absolute error of the average available power of turbine #1, #2 and #3 for gross available power method and the algorithm with the two augmented wake models.

13

13.2 Validation Results, Continued

Conclusion

Using the algorithm with any of the two augmented wake models reduces the error of calculating the available power of turbine #2 significantly. Using the Jensen based augmented wake model performed better than the Larsen based augmented wake model in three (experiments 3, 6 and 7) of the five experiments and in experiment 5 the methods were comparable. However, when determining the available power of the set of three turbines, the algorithm did not always perform better than the gross available power method. This leads to the recommendation of continuing the development of the algorithm to be accurate for all turbines, see chapter 15.

13

14

CONCLUSION

This chapter provides an overview of the main results and conclusions of this research. First, an overview research focus is briefly repeated, followed by an overview of the main results and the evaluation of the research hypothesis. The recommendations for further research are discussed in the next chapter.

14.1 Research Focus

Problem and Hypothesis

Determining the available power of a wind farm under curtailment is complicated as the wake losses are different than in normal operation. In the hypothesis it is presumed that by using existing wake models and augmenting them to include curtailment as an input, this difference in wake loss can be calculated accurately.

Continuing...

133

14.1 Research Focus, Continued

Research
Boundaries

Although the future goal of the algorithm is to accurately determine the available power of a wind farm for all types of wind conditions and any wind farm layouts, the following main boundaries were set in this research:

- Only turbine clusters of straight rows were considered and only wind conditions along that straight line were modelled.

    - This made wake model implementation relatively simple, avoiding the need for partial wake calculations. However, the algorithm only needs the output of the wake model calculation and is thus also expandable to other wind farm layouts and wind directions.

- Only sub-rated wind conditions were validated.

    - This allowed wind speed determination using the power curve. If, however, accurate wind speed signals at the turbine level can be obtained in a different manner, this boundary can be avoided.

- No turbulence models were implemented, but measured local turbulence was used.

    - This is expected to have reduced the error of the algorithm with respect to the version that does include a turbulence model. This needs to be quantified in further study.

- Advanced phenomena like wake meandering and the wind shear are not considered.

    - It is expected to have little effect on the accuracy of the algorithm, but this has not been quantified.

- Only the Jensen and Larsen wake models were tested.

    - Other wake models might prove to be more suitable for this algorithm, which could be investigated in further studies.

14

14.2 Research Results

Applying Wake Models Instantaneously

The application of wake models to determine wind turbine losses instantaneously resulted in accurate power estimations when including a time delay for the wind to travel over the wind farm.

Curtailing Leading Turbine

When curtailing the first turbine in the row, a clear reduced wake effect is observed at the second turbine. This additional power was in the range of 45% to 80% of the power curtailed by the first turbine. Also, the third turbine experienced a small reduction of power, due to the increased wake behind the second turbine. This was in the range of 5% to 40% of the power curtailed by the first turbine in four of the five experiments.

Modelling Downstream Turbines

In experiments with curtailment of only the first turbine, with the wind aligned with the row, no noticeable changes in power were observed from the fourth turbine onward. It is therefore concluded, that the effect of curtailment on changes in the wake more than three turbine positions downstream of the curtailed turbine does not have to be modelled.

Wake Models During Curtailment

In the five experiments where the augmented wake models performed well in normal operation, they also showed an accurate estimation during curtailment for turbine #2. The augmented Jensen wake model showed a maximum relative error of 18% and a maximum absolute error of $40kW$ with respect to the measurement data. The augmented Larsen wake model showed an error double in size. However, due to the working of the Larsen wake model the recommendation is not made to continue study of the Jensen wake model only. The Larsen wake model allows more sophisticated calibration to optimize its accuracy, which was not done in this research after the experiments.

Continuing…

14

14.2 Research Results, Continued

Algorithm Performance Second Turbine	The current best practice of using the gross available power method (ignoring the reduced wake effect) for available power determination led to errors between 60% and 100% for the second turbine in the performed experiments. Using the algorithm with the augmented Larsen wake model reduced this error to the range of 10% to 40% . Using the algorithm with the augmented Jensen wake model reduced the error even further to the range of 1% to 20%.

Algorithm Performance All Turbines	The algorithm showed less improvement for determining the available power of the whole row of turbines. This is mainly due to large errors in the wake modelling of the third turbine. In three of the five experiments the algorithm performed better than the gross available power method for both augmented wake models and in these cases using the Larsen wake model performed better than using the Jensen wake model. In an other experiment only the augmented Larsen wake model performed better and in one experiment neither wake model yielded better results. The large error introduced for the available power calculation of the third turbine needs to be mitigated in order to achieve more consequent results, see the recommendations in the next chapter.

Evaluation Hypothesis	The hypothesis is accepted to be true for the modelling for the second turbine, but for the third turbine the algorithm needs to be improved.

14

15

RECOMMENDATION FOR FURTHER RESEARCH

During this research several uncertainties and limitations were encountered that could have a negative influence on accuracy or uncertainty of the algorithm. This chapter provides several recommendations to improve on the reduction of those uncertainties and limitations. First, recommendations are discussed to improve the quality of the measurements with respect to the data available for this research. Second, several recommendations are stated to either improve the accuracy of the model. Finally, some recommendations of new or extended studies are presented.

15.1 Improvement of Validation Data

Measurements
The measurement data available for this research comprised of $1Hz$ sampling data measured at the turbine. However, the sonic sensor had an error too large for direct use, so the power production data in combination with the power curve was used. But, to determine the turbulence the sonic sensor had to be used. When accurately calibrated meteorological measurement instruments or lidars are available the uncertainty of the data signal lowers considerable.

Continuing…

137

15.1 Improvement of Validation Data, Continued

Wind Conditions

A disadvantage of using a real size wind farm is that the research is dependent on the wind conditions occurring during the experimental phase. When using wind tunnels as in [35], the wind conditions can accurately be defined and the validation can be performed over a larger span of parameters and with a finer step size. This has the following advantages:

- More wind speeds can be considered.

- For each wind speed setting several turbulence intensities can be tested.

- Different farm layouts and wind directions can be tested.

- The surface roughness can be changed.

- The dependency on the turbine design can be studied.

Thrust
Coefficient

In order to determine the thrust coefficient, this research used the thrust curves provided by the turbine manufacturer. However, the accuracy of these curves are difficult to determine. If the thrust coefficient or thrust force can be measured, the uncertainty of the algorithm could possibly be reduced.

15

15.2 Improvement of Algorithm

Using Turbulence Models

It was decided to not use turbulence models in this research, but to use the measured turbulence instead to minimize introducing additional uncertainties and focus modelling the reduced wake effect. However, when applying the algorithm this approach cannot be used and the usage of a turbulence model is required. In the comparative study of Renkema [21] many wake added turbulence models are discussed. It needs to be determined how this will influence the error of the algorithm. Note that not only the turbulence during normal operation, but also the curtailment induced reduction of the increased turbulence intensity during curtailment needs to be modelled, i.e. the height of the yellow bars in figure 11.5.

Continuous Wake Model Calibration

The wake models are now evaluated in a simplistic manner. The free stream turbulence, wind speed and curtailment factor are measured only to determine the wake losses of the whole row of turbines. It might reduce the error - especially for turbine #3 and further downwards - to continuously calibrate the wake models at each turbine by using the measurement data of that turbine.

Using Production Data

In order to determine the reduced wake effect, the algorithm of this research uses the wake models to model both the curtailed as the normal operation to determine the difference. However, the wake models can also be used to model only the normal operation when the wind farm is being curtailed. The measured power of the turbines can be used instead of modelling the curtailed operation. This means that equation 3.2 is replaced with equation 15.1

$$\Delta P_{rw_i} = \hat{P}_{c_i} - P_i \tag{15.1}$$

For this research the results of the algorithm did not improve for any experiment, but when the other parts of the algorithm increase in accuracy this might be the case.

15

15.2 Improvement of Algorithm,   Continued

Alternative Wake Models

In this research only two wake models, namely the Jensen and Larsen wake models, are used for wind speed deficit calculations, as narrowed down in section 5.3 Wake Model Selection . Other engineering wake models, like the mentioned Ainslie and Frandsen wake model could also be tested or the Jensen and Larsen wake model could be improved further. For example, Campagnolo et al found much better results in wind tunnel tests, using the Jensen wake model with a linear or quadratic wake expansion coefficient, instead of the original constant wake expansion. [36] Also, the kinetic wake model by Bastankhah et al, assuming a Gaussian shape of the wake, showed better results than the original Jensen wake model comparing to experimental and LES data. [37] Moreover, CFD wake models could possibly be used, if they are tabulated beforehand to maintain fast algorithm processing.

Time-Varying Wake Model

When manually finding the right time delay between the turbines, it was found that it was not constant for the whole time span of the experiment and reference period. For example, peaks in power production of turbine #1 at $20s$ and $30s$ would qualitatively appear at turbine #2 at $100s$ and $120s$ and at turbine #3 at $200s$ and $250s$. This gives rise to the need of a time-varying wake model estimating the wind speed at downstream turbines at the right time. For downstream turbines the data of all upstream turbines is available for continuous calibration.

Continuing…

15

15.2 Improvement of Algorithm, Continued

Correction for
Increase RPM

In the analysis of the experiments it was found that turbine #2 not only produces more power during curtailment, but during the transient response the rotational speed of its rotor also increases. This leads to part of the additional available power in the wind flowing towards the acceleration of the rotor instead of the measured electricity production. In appendix C it is investigated with simple calculations if this could be corrected for. It showed that it could result in a improvement in the range of 40% to 65%, considering the calculation of the available power in the wind during the transient.

15.3 Extended Research

Future Power Prediction

When studying the power production data of the turbines, it was found that disturbances found in the first turbine can often be found (although smaller) in the second turbine and even further downstream. Considering that there is a time delay between the same wind hitting these turbines, a prediction could be made on the power production in the very near future. For wind farm Westermeerwind this time delay was between one and two minutes per turbine, depending on the wind speed.

Transient Response

This research focused on determining the steady state response of the turbines during curtailment. However, it was found that the transient response to reach this steady state was one minute and to reach normal conditions after the experiment was two minutes. Considering that a power transfer unit (PTU) in The Netherlands is fifteen minutes, when curtailing for just $1PTU$, 20% of the response is the transient response. Further study can determine if this transient response can easily be calculated or an adjustment to the proposed algorithm can be made to include the power production during the transient response of the turbines.

15

NOMENCLATURE

List of Abbreviations

AFPE	Available farm power estimator
APE	Available power estimator
CFD	Computational fluid dynamics
pp	Percentage points
MOI	Mass moment of inertia
PRP	Power responsible party
PTU	Power transfer unit
RWE	Reduced wake effect
RMS	Root mean square
rpm	Rotations per minute
SCADA	Supervisory control and data acquisition
SSW	South south west wind direction (210°)
TRD	Transient response duration
TSO	Transmission system operator

List of Symbols

θ	Blade pitch angle	$[°]$
μ_u	Mean wind speed	$\left[\frac{m}{s}\right]$
ρ	Air density	$\left[\frac{kg}{m^3}\right]$
σ_u	Standard deviation of the wind speed	$\left[\frac{m}{s}\right]$
ϕ	Relative humidity	$[-]$
ω	(Rotor) rotational speed	$\left[\frac{rad}{s}\right]$
A	(Swept rotor) area	$[m^2]$
a	(Axial) induction factor	$[-]$
C_P	Power coefficient	$[-]$
C_T	Thrust coefficient	$[-]$
$C_{T_{i_{curtailed}}}$	Thrust coefficient of turbine i during curtailment	$[-]$
c_i	Curtailment factor	$[-]$
D	Rotor diameter	$[m]$
d_i	Wind speed deficit as a ratio of turbine i versus the leading turbine	$[-]$
d_{c_i}	Wind speed deficit as a ratio of turbine i during curtailment	$[-]$
i and j	Indices of turbines	$[-]$
k_i	Wake decay factorof turbine i for the Jensen wake model	$[-]$
N	Number of turbines	$[-]$
$\mathscr{P}(u)$	Power production according to the power curve	$[W]$
P_i	Power production of turbine i	$[W]$
P_{AWF}	Available power of the wind farm including the RWE	$[W]$
P_{GA}	Gross available power of the wind farm excluding the RWE	$[W]$
ΔP_{rw}	The difference in power production due to the RWE	$[W]$
p	Pressure of air	$[Pa]$
p_w	Pressure of water vapour	$[Pa]$
R	Rotor radius	$[m]$
R_0	Gas constant of air	$\left[\frac{J}{kgK}\right]$
R_w	Gas constant of water vapour	$\left[\frac{J}{kgK}\right]$
r	Radial position, offset from position along turbine line	$[m]$
T	Temperature	$[K]$
TI	Turbulence intensity	$[-]$
t_{delay}	Time delay for wind to travel between two neighbouring turbines	$[s]$
u	Wind speed	$\left[\frac{m}{s}\right]$
u_1	Wind speed in far wake	$\left[\frac{m}{s}\right]$
u_{hub}	Wind speed at hub height	$\left[\frac{m}{s}\right]$
u_i	Wind speed at turbine i	$\left[\frac{m}{s}\right]$
V_0	Free-stream wind speed	$\left[\frac{m}{s}\right]$
Δx	Turbine spacing	$[m]$
x	Downstream distance after turbine	$[m]$
z	Elevation	$[m]$
z_{hub}	Hub height	$[m]$

REFERENCES

[1] T. Ackermann, *Energy Sources*, Tech. Rep. (Regeringskansliet, 2008).

[2] Elia.be, *Delivery of downward aFRR by wind farms*, Tech. Rep. October (Elia.be, 2015).

[3] T. G. Bozkurt, G. Giebel, and P. Sorensen, *Possible Power Estimation of Down-Regulated Offshore Wind Power Plants*, Ph.D. thesis, Technical University of Denmark. (2016).

[4] G. Koustas, G. Papaefthymiou, M. Ieee, and B. C. Ummels, *Stochastic Assessment of Opportunities for Wind Power Curtailment*, Power , 1 (2007).

[5] C. Warmer, M. Hommelberg, I. Kamphuis, Z. Derzsi, and J. Kok, *Wind Turbines and Heat Pumps - Balancing wind power fluctuations using flexible demand*, 6th International Workshop on Large-Scale Integration of Wind Power and Transmission Networks for Offshore Wind Farms , 1 (2006).

[6] P. S. Georgilakis, *Technical challenges associated with the integration of wind power into power systems*, Renewable and Sustainable Energy Reviews **12**, 852 (2008).

[7] P. Tielens and D. van Hertem, *Grid Inertia and Frequency Control in Power Systems with High Penetration of Renewables*, Status: Published , 1 (2012).

[8] M. Milligan, P. Donohoo, and D. Lew, *Operating Reserves and Wind Power Integration: An International Comparison*, 9th Annual International Workshop on Large-Scale Integration of Wind Power into Power Systems , 1 (2010).

[9] L. Bird, J. Cochran, and X. Wang, *Wind and Solar Energy Curtailment : Experience and Practices in the United States Wind and Solar Energy Curtailment : Experience and Practices in the United States*, National Renewable Energy Laboratory (NREL) (2014).

[10] F. Díaz-González, M. Hau, A. Sumper, and O. Gomis-Bellmunt, *Participation of wind power plants in system frequency control: Review of grid code requirements and control methods*, Renewable and Sustainable Energy Reviews **34**, 551 (2014).

[11] TenneT, *Volume of settled imbalance, accessed on 2016-01-15,* (2016).

[12] R. N. E. Agency, *Wind SDE+ 2015 (land, meer en dijk), accessed on 2016-01-15,* (2016).

[13] TenneT, *Settlement prices, accessed on 2016-01-15,* (2016).

145

[14] M. S. Thomas Esbensen, Ramakrishnan Krishna, Frank Scheurich, *System for automatic power estimation adjustment,* (2007).

[15] J. W. V. Heemst, *Improving the Jensen and Larsen Wake Deficit Models*, Tech. Rep. (Delft University of Technology, 2015).

[16] Martin O. L. Hansen, *Aerodynamics of Wind Turbines, 2nd edition* (Earthscan London, 2008) p. 192.

[17] B. Sanderse, *Aerodynamics of wind turbine wakes: Literature review*, Tech. Rep. October (Delft University of Technology, The Netherlands, 2009).

[18] N. Troldborg and J. Sørensen, *A simple atmospheric boundary layer model applied to large eddy simulations of wind turbine wakes,* Wind Energy **17**, 657 (2014).

[19] L. Vermeer, J. Sörensen, and A. Crespo, *Wind turbine wake aerodynamics,* Progress in Aerospace Sciences **39**, 467 (2003).

[20] F. Holzäpfel, T. Hofbauer, D. Darracq, H. Moet, F. Garnier, and C. F. Gago, *Analysis of wake vortex decay mechanisms in the atmosphere,* Aerospace Science and Technology **7**, 263 (2003).

[21] D. J. Renkema, *Validation of wind turbine wake models*, Tech. Rep. (Delft University of Technology, The Netherlands, 2007).

[22] B. Hu, *Design of a Simple Wake Model for the Wind Farm Layout Optimization Considering the Wake Meandering Effect*, Tech. Rep. (TU Delft, 2016).

[23] I. Katic, J. Højstrup, and N. Jensen, *A Simple Model for Cluster Efficiency,* European Wind Energy Association Conference and Exhibition , 407 (1986).

[24] T. Göçmen, P. V. D. Laan, P. E. Réthoré, A. P. Diaz, G. C. Larsen, and S. Ott, *Wind turbine wake models developed at the technical university of Denmark: A review,* Renewable and Sustainable Energy Reviews **60**, 752 (2016).

[25] N. O. Jensen, *A note on wind generator interaction*, Tech. Rep. (Risø National laboratory, Roskilde, Denmark, 1983).

[26] J. Ainslie, *Calculating the flowfield in the wake of wind turbines,* Journal of Wind Engineering and Industrial Aerodynamics **27**, 213 (1988).

[27] G. C. Larsen, *A simple stationary semi-analytical wake model*, Tech. Rep. August (DTU, 2009).

[28] S. Frandsen, R. Barthelmie, S. Pryor, O. Rathmann, S. Larsen, and J. Hojstrup, *Analytical modelling of wind speed deficit in large offshore wind farms,* Wind Energy **9**, 39 (2006).

[29] J. Choi and M. Shan, *Advancement of Jensen (Park) Wake Model,* European Wind Energy Conference and Exhibition 2013 , 1 (2013).

[30] Siemens, *Wind Turbine SWT-3.0-108 / SWT-3.2-108 / SWT-3.4-108, accessed on 2016-01-20,* (2006).

[31] F. Technologies, *FT702 ultrasonic wind sensor by FT Technologies,* (2016).

[32] *IEC 61400-1, Ed.1, Wind Turbines-Part 12-1: Power performance measurements of electricity producing wind turbines,* (2005).

[33] G. P. M. O. and v. W. J.W., *Maximum power-point tracking control for wind farms,* Wind Energy **17**, 657 (2014), arXiv:arXiv:1006.4405v1 .

[34] T. Burton, N. Jenkins, D. Sharpe, and E. Bossanyi, *Wind Energy Handbook* (John Wiley & Sons, Ltd, 2011) pp. 1–642.

[35] J. Bartl and L. Sætran, *Experimental testing of axial induction based control strategies for wake control and wind farm optimization,* Journal of Physics: Conference Series **753**, 032035 (2016).

[36] F. Campagnolo, V. Petrovi, C. L. Bottasso, and A. Croce, *Wind Tunnel Testing of Wake Control Strategies,* American Control Conference 2016 , 1 (2016).

[37] M. Bastankhah and F. Porté-Agel, *A new analytical model for wind-turbine wakes,* Renewable Energy **70**, 116 (2014).

[38] J. Jonkman, S. Butterfield, W. Musial, and G. Scott, *Definition of a 5-MW reference wind turbine for offshore system development,* Contract , 1 (2009).

Note: All references are provided with cyan clickable links to the original files in the digital PDF version of this report.

A

DETAILED EXPERIMENTAL RESULTS

In this appendix the measurement results of all experiments are discussed in detail in addition to section 11.2 Experimental Results .

A.1 Experimental Results

Experiment 1   Experiment 1 has been discussed in detail in section 11.2 Experimental Results .

Continuing...

A.1 Experimental Results, Continued

Experiment 2   Figure A.1 shows the data signals for the second experiment, sim-
                      ilar to figure 11.3. The following observations are made:

- During the experiment the available power of turbine #1 is
  constant within a $200kW$ band width.

- The response of turbine #2 shows several power increases
  and decreases - e.g. at $240s$ and $300s$ - which coincide with a
  periodic signal of the pitch angle. This periodic pitch signal
  is visible in figure 11.2 for turbine #1 and for #2. The reasons
  of this small periodic change in blade pitch is not known.

- Turbines #4 to #7 are varying more than $500kW$ during the
  experiment. This effect is expected to be wake meandering.
  This research focuses on the mean power production only.

Figure A.2 shows the overview of all turbines of experiment 2 and is
qualitatively similar to figure 11.4 of experiment 1. Note, however,
the doubled variation of turbines #4 to #6 during the experiment,
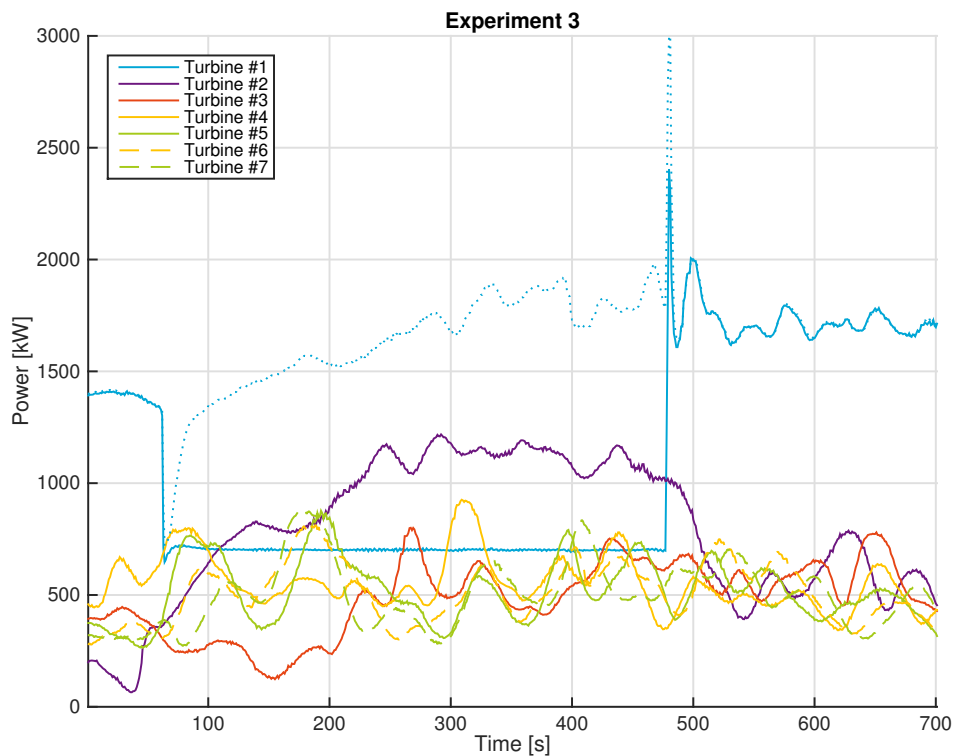due to the increase of the fluctuations.
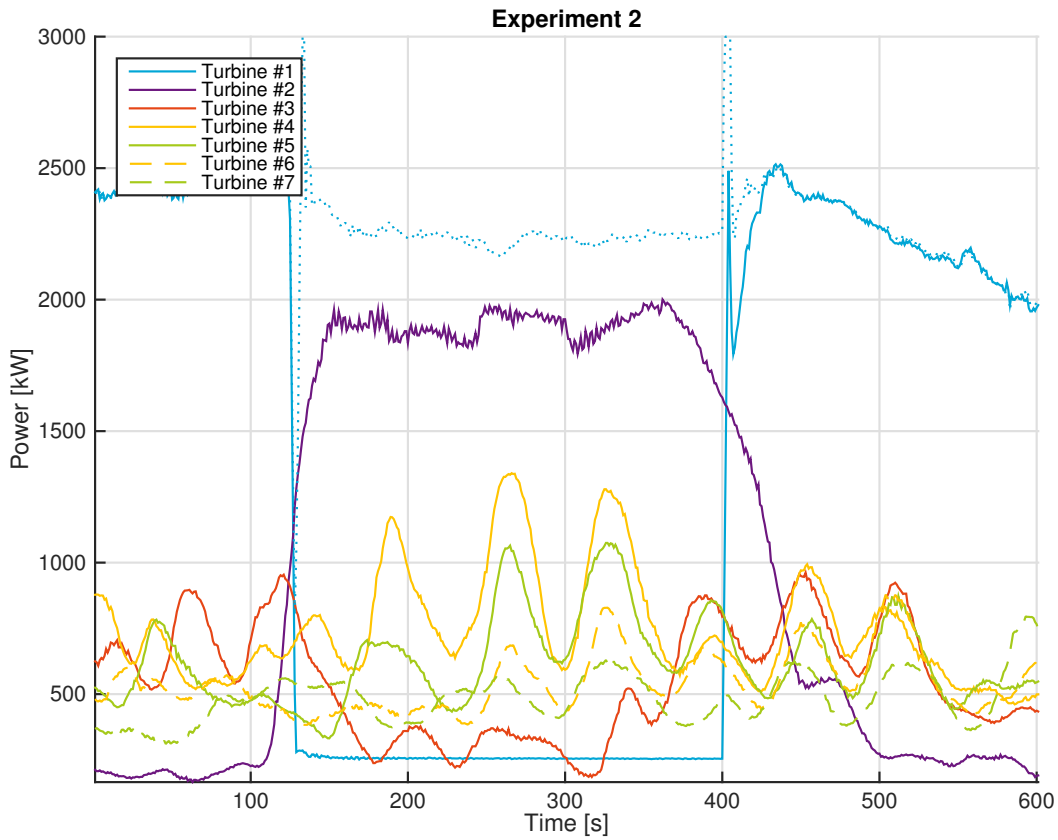
Figure A.1: Power production signal of the first seven turbines as measured during and around curtailment experiment 2. The dotted line shows the available power of the curtailed turbine.
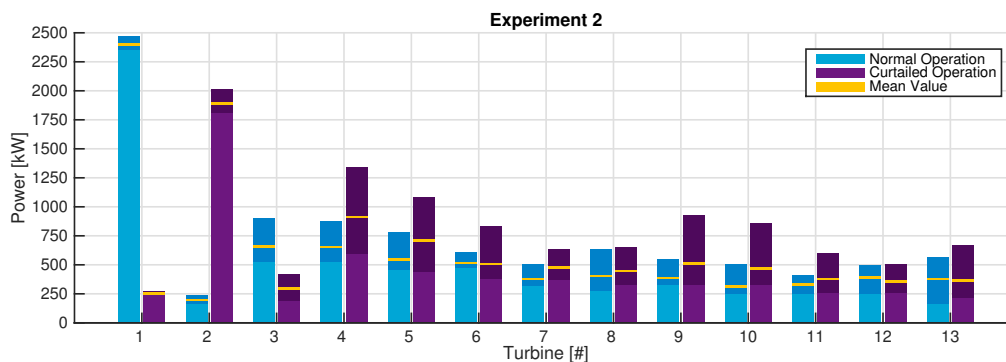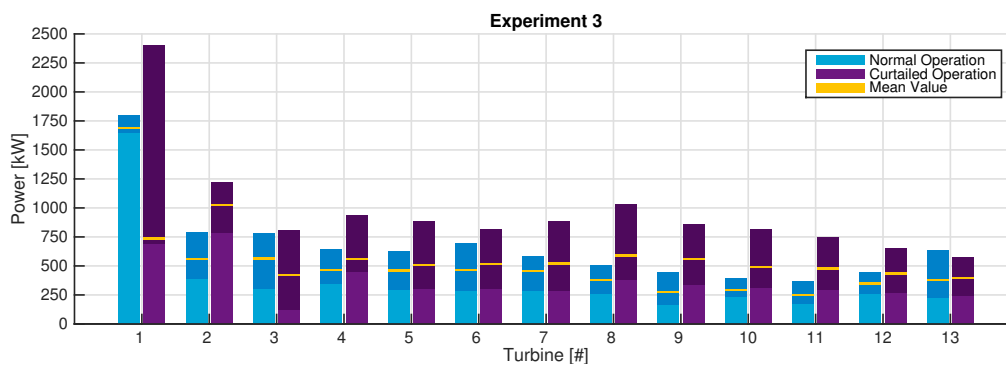

Figure A.2: The power production of all thirteen turbines for the reference period (normal operation) and during curtailment experiment 2. The dark shaded areas indicate the minimum and maximum measured values, while the yellow line shows the mean value.

A.1 Experimental Results, Continued

Experiment 3

Figures A.3 and A.4 show the third curtailment experiment. It is qualitatively similar to the previous experiments, but there are a few differences

- During the experiment the wind speed increased, resulting in an increase in available power from $1,400 kW$ to $1,800 kW$.

- Due to the fixed set-point during curtailment the curtailment percentage changed from 50% to 40%.
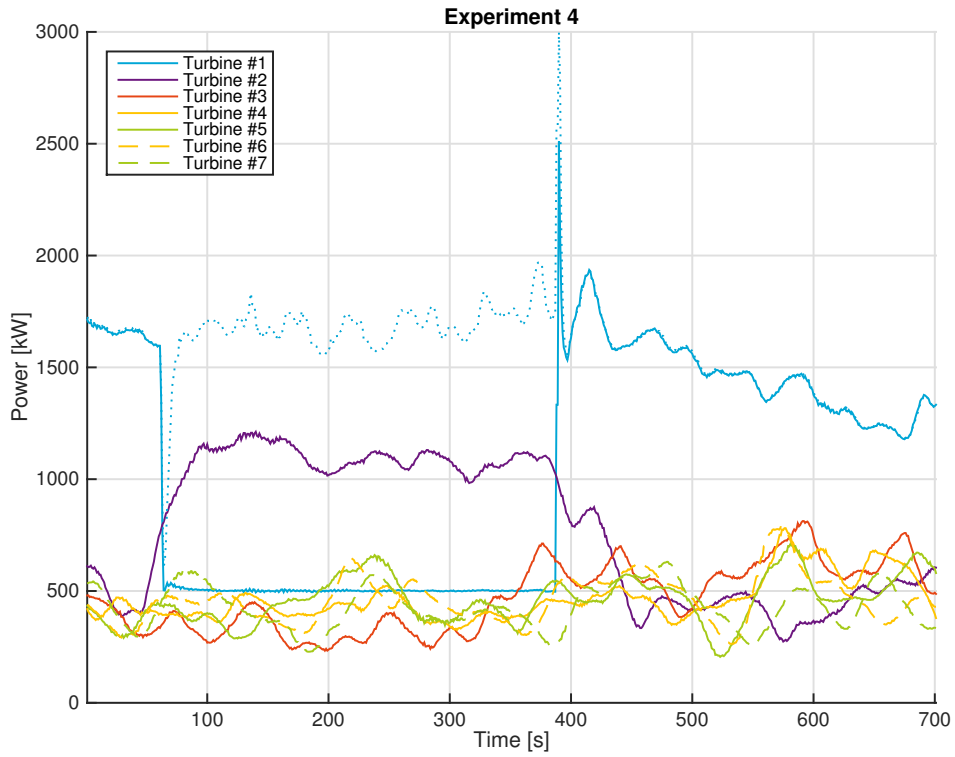

Figure A.3: Power production signal of the first seven turbines as measured during and around curtailment experiment 3. The dotted line shows the available power of the curtailed turbine.
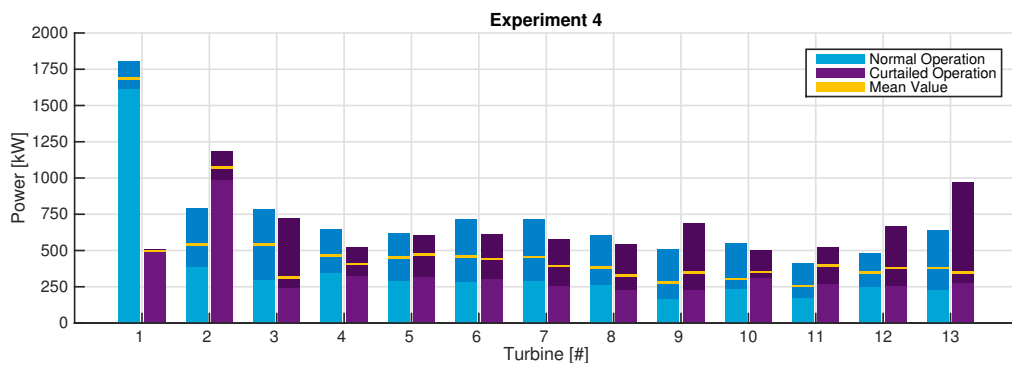
A.1 Experimental Results, Continued

Figure A.4: The power production of all thirteen turbines for the reference period (normal operation) and during curtailment experiment 3. The dark shaded areas indicate the minimum and maximum measured values, while the yellow line shows the mean value.

Experiment 4   Figures A.5 and A.6 show the fourth curtailment experiment. It is qualitatively similar to the previous experiments:

- Turbine #2 increased in power production with $500 kW$.

- Turbine #3 decreased in power production with $200 kW$.

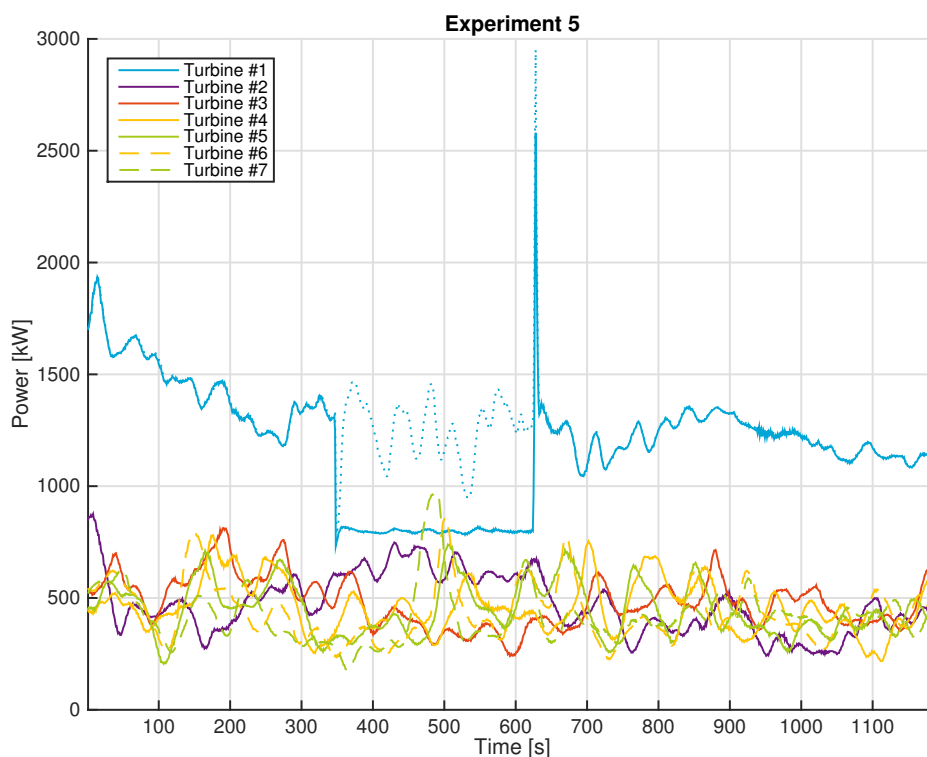- All other turbines have no significant effect.

Figure A.5: Power production signal of the first seven turbines as measured during and around curtailment experiment 4. The dotted line shows the available power of the curtailed turbine.

Figure A.6: The power production of all thirteen turbines for the reference period (normal operation) and during curtailment experiment 4. The dark shaded areas indicate the minimum and maximum measured values, while the yellow line shows the mean value.

A.1 Experimental Results, Continued

Figures A.7 and A.8 show the fourth curtailment experiment. Although the response of the downstream turbines is smaller, the experimental results are qualitatively similar to the previous experiments:

- Turbine #2 increased in power production with $200kW$.

- Turbine #3 decreased in power production with $200kW$.

- All other turbines have no significant effect.

Figure A.7: Power production signal of the first seven turbines as measured during and around curtailment experiment 5. The dotted line shows the available power of the curtailed turbine.
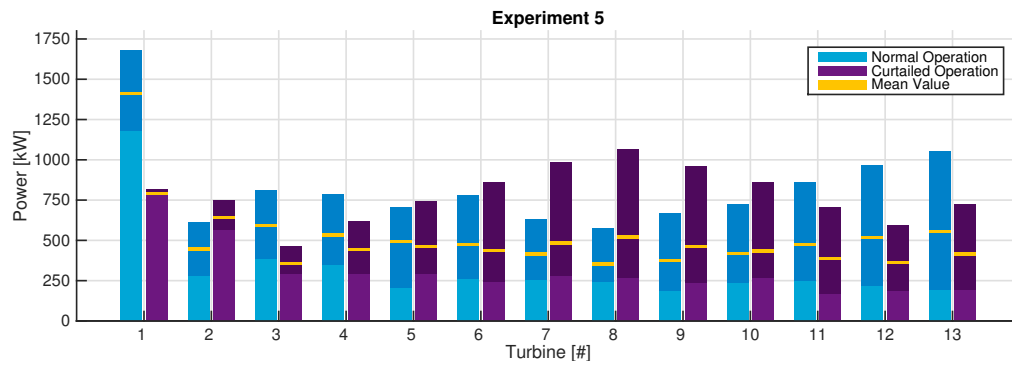
A.1 Experimental Results, Continued

Figure A.8: The power production of all thirteen turbines for the reference period (normal operation) and during curtailment experiment 5. The dark shaded areas indicate the minimum and maximum measured values, while the yellow line shows the mean value.

A.1 Experimental Results, Continued

Experiment 6

Figure A.9 shows the data signals of the sixth experiment. The mean wind speed was $8\frac{m}{s}$ with a maximum deviation of $0.5\frac{m}{s}$ until $620s$. For the last minute the wind speed dropped to $6.8\frac{m}{s}$. This drop can also be observed in the signal of the pitch angle, see figure A.10. Therefore this data is not considered in the analysis. The vertical red lines indicate the limits of the data that was used. This data shows the same qualitative response as the previous experiments.

Figure A.11 shows the overview of the power production of all turbines, except the last two. The total time delay for the last few turbines is more than 15 minutes. However, after 15 minutes a new (rejected) experiment was started, which included curtailing turbines #12 and #13. Therefore these turbines can not be used for analysis. Considering that these deep wake turbines do not provide interesting responses, the experiment is not rejected because of this.
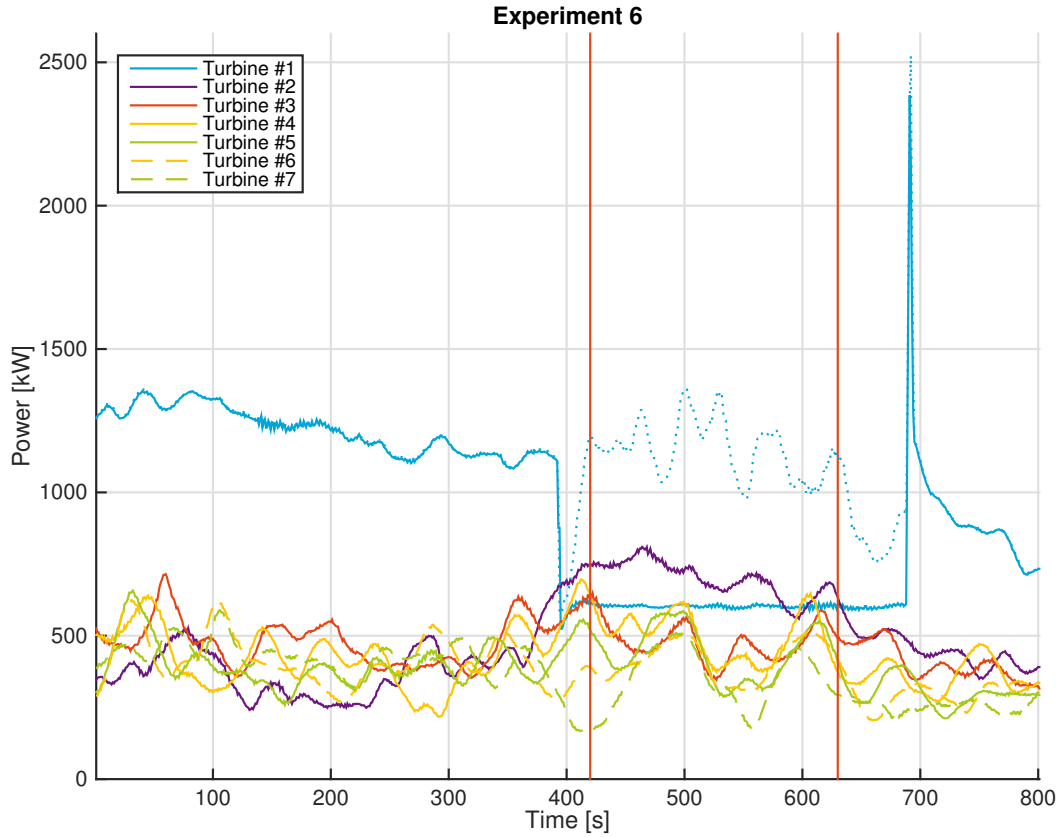
Figure A.9: Power production signal of the first seven turbines as measured during and around curtailment experiment 6. The dotted line shows the available power of the curtailed turbine. The vertical red lines indicate the limits of the used experiment data.
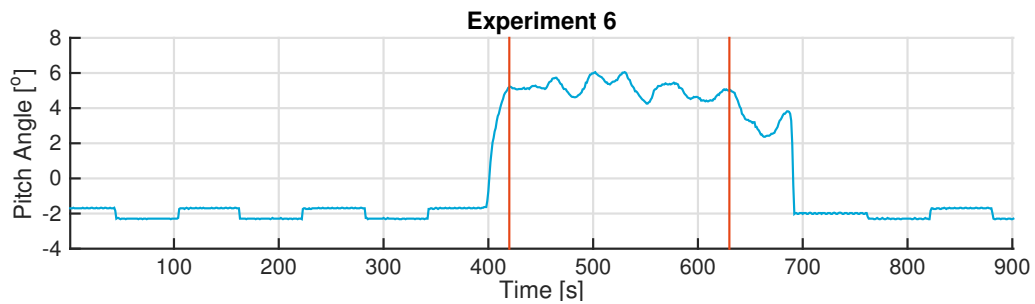

Figure A.10: Pitch angle of turbine #1 corresponding to experiment 6. The vertical red lines indicate the limits of the used experiment data.

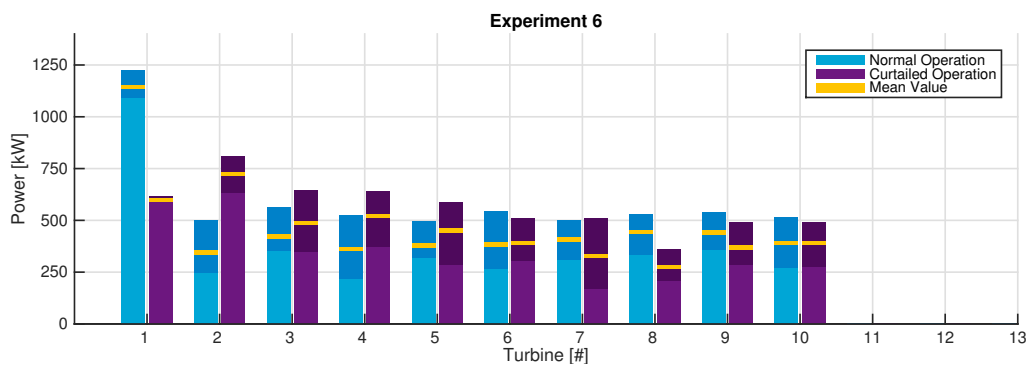# A.1 Experimental Results, Continued

Figure A.11: The power production of all thirteen turbines for the reference period (normal operation) and during curtailment experiment 6. The dark shaded areas indicate the minimum and maximum measured values, while the yellow line shows the mean value.

A.1 Experimental Results, Continued

Experiment 7   The seventh experiment was performed for 15 minutes. Figure
                A.12 shows the data signals of the power of the first five turbines
                smoothed over $30s$ by a moving average to improve readability.
                The following observations are made:

- The available power signal of turbine #1 shows rated power
  for a long period during the experiment. This is expected to
  be an overestimation of the actual power similar as in exper-
  iment 1.

- Figure A.12 shows that the available power is not at rated
  power between $1300s$ and $1500s$, leaving these $200s$ avail-
  able for validation purposes.

- The data of turbine #3 and further downstream indicate
  wake meandering similar to experiment 2. This meander-
  ing made it difficult to accurately shift the data signals of the
  far downstream turbines (#5+) in time. This might impair
  the comparison of the far downstream turbines.

Figure A.14 shows the overview of the response of all turbines.
Note that the suspected wake meandering has an influence on the
minimum and maximum observed power per turbine. Also, due to
the meandering and difficulty of properly aligning the data signals
of the downstream turbines, the value of the comparison of the far
downstream turbines is low. However, qualitatively similar results
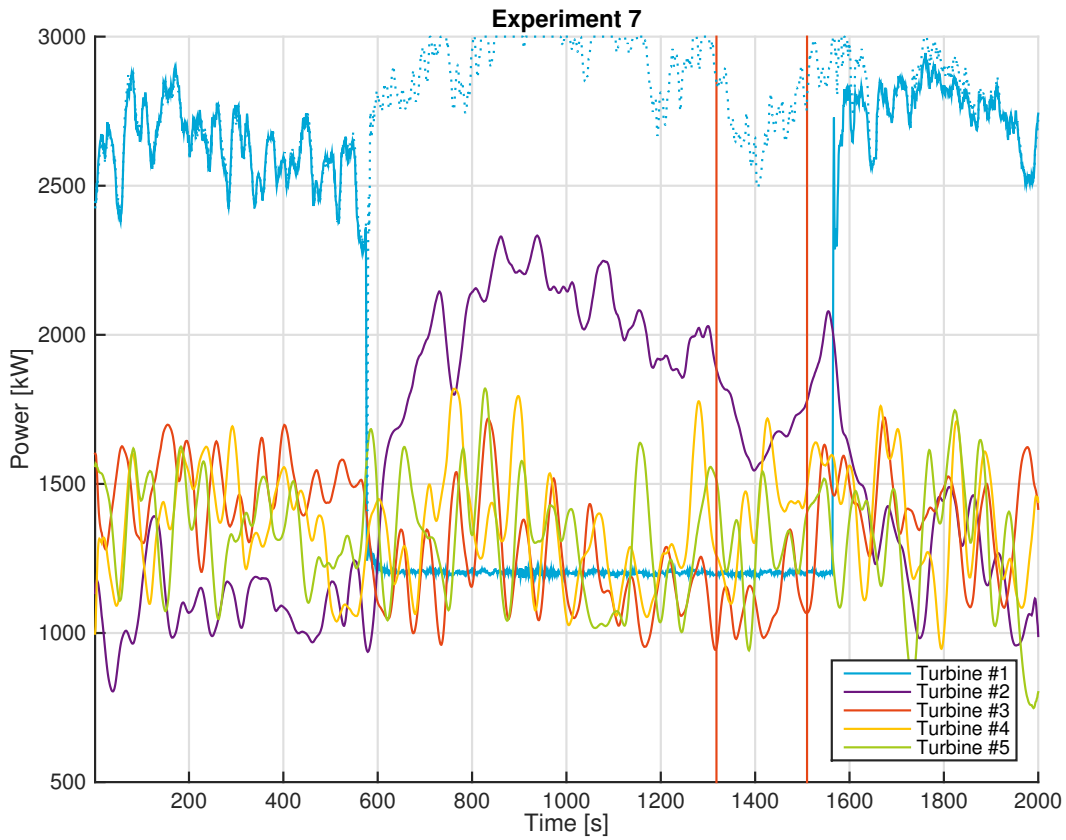are found as in the other experiments, especially for the turbines
#1 to #3.

Figure A.12: Power production signal of the first seven turbines as measured during and around curtailment experiment 7. The dotted line shows the available power of the curtailed turbine. The vertical red lines indicate the limits of the used experiment data.
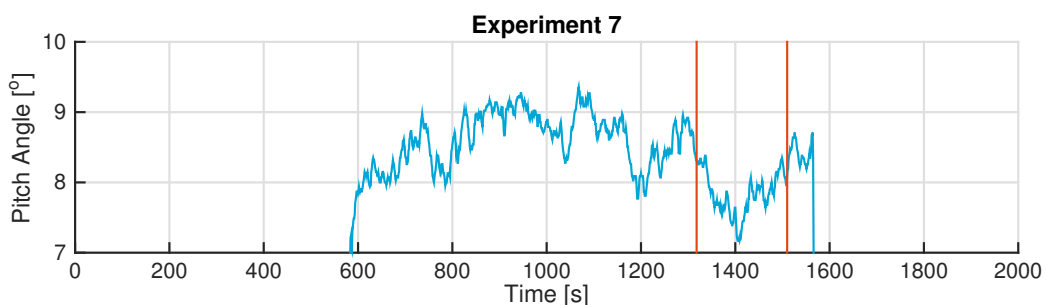

Figure A.13: Pitch angle of turbine #1 corresponding to experiment 7. The vertical red lines show the limits of the used experiment data.
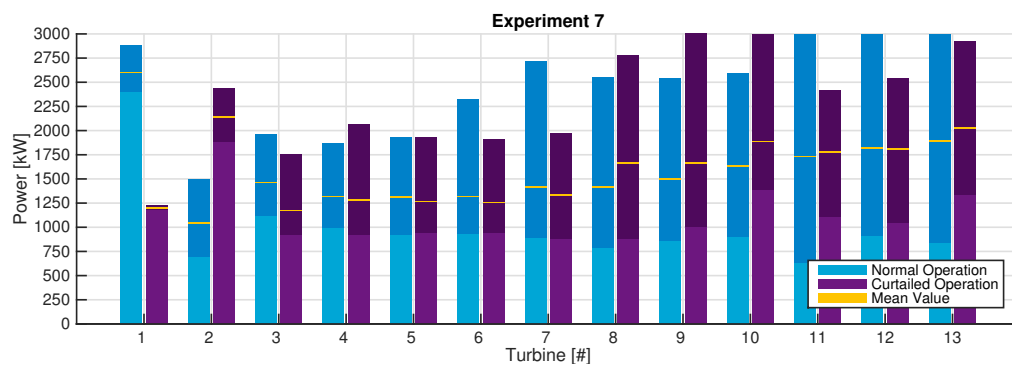
A.1 Experimental Results, Continued

Figure A.14: The power production of all thirteen turbines for the reference period (normal operation) and during curtailment experiment 7. The dark shaded areas indicate the minimum and maximum measured values, while the yellow line shows the mean value.

B

DETAILED MODELLING RESULTS

In this appendix the measurement results of all experiments are discussed in detail in addition to section 12.2 Results for Turbine #2 .

B.1 Results for Turbine #2

Experiments 1 to 3

Experiments 1, 2 and 3 have been discussed in detail in section Results for Turbine #2.

Continuing. . .

163

B.1 Results for Turbine #2, Continued

Experiment 4   Figure B.1 shows the modelling of experiment 4. The following observations are made:

- Both before and after the experiment the models perform well in modelling the production of turbine #2.

- The APE provides a reasonable signal as it stays between the values before and after the experiment.

- During the experiment the augmented Jensen wake model overestimates and the augmented Larsen wake model underestimates the power production of turbine #2.

  - The augmented Jensen wake model has an error of 13%.

  - The augmented Larsen wake model has an error of -12%.

  - The augmented Jensen and Larsen wake model thus have a comparable performance.

- The modelling of the normal operation is reasonable, as it stays between the normal operation before and after the experiment.
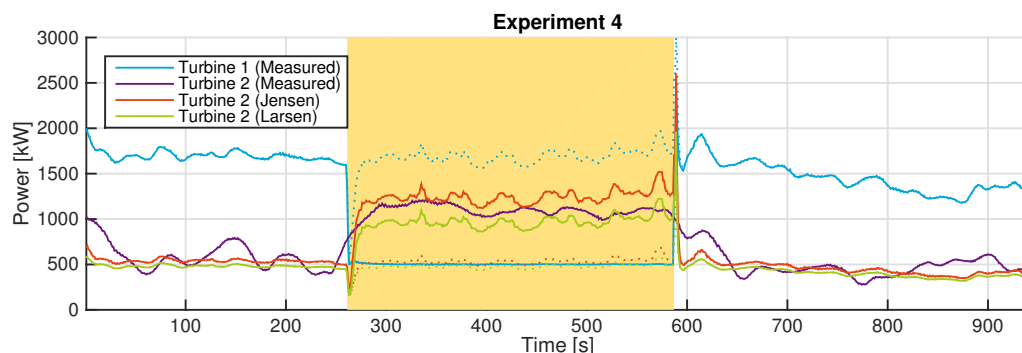

Figure B.1: Power production signal of turbine #1 and #2. The dotted line of turbine #1 indicates the APE-signal. The dotted line of the wake models indicate the power production modelling if no curtailment is applied to the augmented models. The experiments are indicated by the yellow shaded area.

B.1 Results for Turbine #2, Continued

Experiment 5   The following observations are made for experiment 5 in figure B.2

- The APE provides a reasonable signal as it stays between the values before and after the experiment. However, it does have a more intermittent shape than in the reference period.

- For both augmented wake models the effect of the intermittency of the APE signal (via the calculation of the curtailment factor) is visible.

- During the experiment the augmented Jensen wake model overestimates and the augmented Larsen wake model underestimates the power production of turbine #2.

    - The Jensen wake model has an error of 8.2%.
    - The Larsen wake model has an error of −21%.

- The modelling of the normal operation is reasonable, as it stays between the normal operation before and after the experiment. The intermittency of the APE signal is also visible in the modelling of the normal operation.
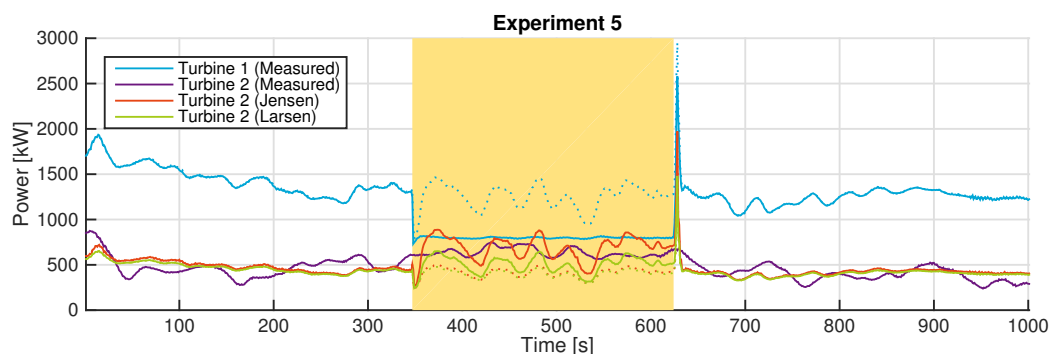

Figure B.2: Power production signal of turbine #1 and #2. The dotted line of turbine #1 indicates the APE-signal. The dotted line of the wake models indicate the power production modelling if no curtailment is applied to the augmented wake models. The experiments are indicated by the yellow shaded area.

B.1 Results for Turbine #2, Continued

Experiment 6

Figure B.3 shows the modelling of experiment 6. The following observations are made:

- Before the experiment the models perform well in modelling the production of turbine #2, but after the experiment both models have an error between $100KW$ and $250kW$.

- The APE provides a reasonable signal as it stays between the values before and after the experiment. However, it does have a more intermittent shape than in the reference period.

- During the experiment both augmented wake models underestimate the power production of turbine #2.

  - The Jensen wake model has an error of -5.7%.
  - The Larsen wake model has an error of -35%.

- The modelling of the normal operation is reasonable, as it stays between the normal operation before and after the experiment.
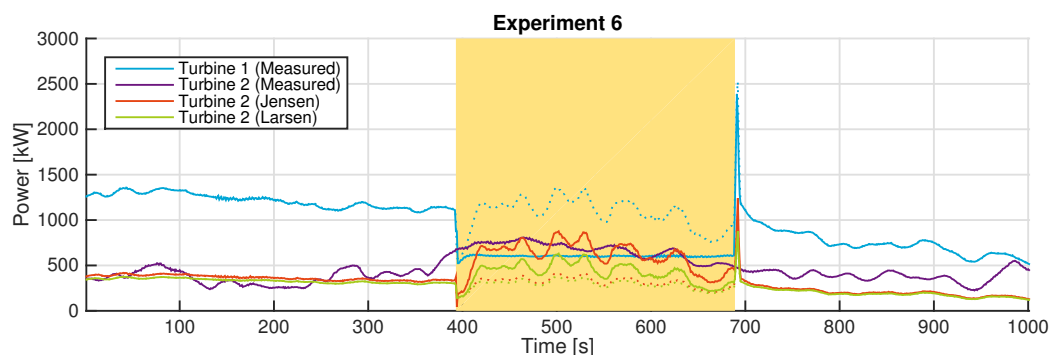

Figure B.3: Power production signal of turbine #1 and #2. The dotted line of turbine #1 indicates the APE-signal. The dotted line of the wake models indicate the power production modelling if no curtailment is applied to the augmented models. The experiments are indicated by the yellow shaded area.

B.1 Results for Turbine #2, Continued

Experiment 7

During experiment 7 the turbine #1 operated at rated power for a long time. This analysis only focuses on a time set when the turbine was operating below rated power. The following observations are made:

- Both before and after the experiment the Jensen wake model performs well in modelling the production of turbine #2, but the Larsen wake model has an error between $200KW$ and $300kW$.

- The APE provides a reasonable signal as it stays between the values before and after the experiment. However, it does have a more intermittent shape than in the reference period.

- During the experiment both wake models underestimate the power production of turbine #2.

  – The augmented Jensen wake model has an error of 15%.

  – The augmented Larsen wake model has an error of -11%.

  – During the experiment the augmented Jensen wake model overestimates and the augmented Larsen wake model underestimates the power production of turbine #2.

- The modelling of the normal operation is reasonable, as it stays between the normal operation before and after the experiment.
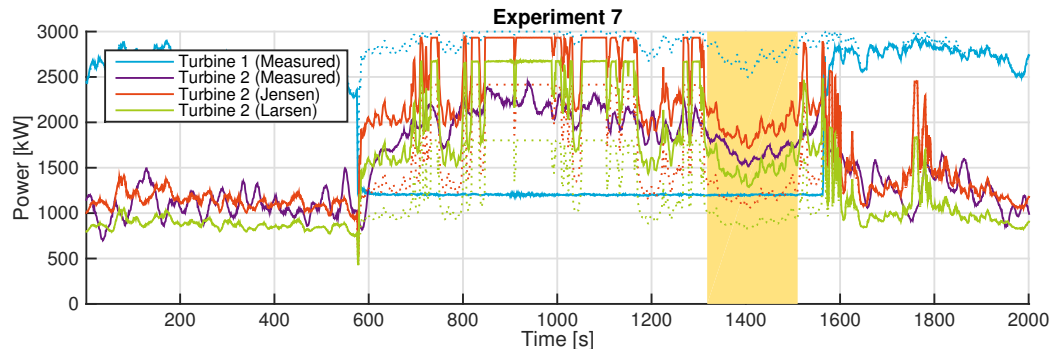
Figure B.4: Power production signal of turbine #1 and #2. The dotted line of turbine #1 indicates the APE-signal. The dotted line of the wake models indicate the power production modelling if no curtailment is applied to the augmented models. The experiments are indicated by the yellow shaded area.

C

INTERESTING RESULTS OUTSIDE THE SCOPE OF THIS REPORT

During the data analysis of the experiments several interesting results or phenomena were encountered that did not contribute to the goals of this research directly. However, these results are briefly described as they might be useful for further research.

C.1 Transient Response

Transient Response

In figure 11.3 it can be observed that the new steady state of the curtailed turbine #1 is research within several seconds. However, the transient response duration (TRD) of the downstream turbine #2 is much slower, both when reaching its new steady state value due to the curtailment of turbine #1 (TRD 1) and when reaching the normal production after the experiment (TRD 2).

Continuing...

C.1 Transient Response, Continued

Observations

The following observations are made when studying the transient response time:

- TRD 1 is in the range of $40s$ to $60s$.

- TRD 2 is in the rang of $70s$ to $130s$.

- The sum of TRD1 and TRD2 is in the range of $130s$ to $170s$.

Dependency Curtailment

No significant dependency of the TRDs was found with respect to the curtailment factor of turbine #1. For TRD 1 and TRD 2 a coefficient of determination of 0.7 and 0.3 was found, respectively. Also using the normal power and the power reduction did not reveal significant dependencies.

Turbine Control Dependency

As will be studied in the next section, the duration of the transient response is not only dependent on the reduced wake effect, but also on the control strategy of the turbine. Operating at higher wind speeds generally happens with higher rotational speeds of the rotor. Due to the acceleration of the rotor during TRD 1 less energy is available for electricity generation. During TRD 2 the rotor decelerates and additional power is available aside from the wind power, which elongates the time to return to the normal operation level.

C.2 Correction Kinetic Energy Rotor

Inertia Rotor

A disadvantage of using the power production to calculate the wind speed using the power curve method, is that sudden changes in wind speed are not observed, due to the inertia of the rotor. For example, the turbulence of the wind does not result in the same fluctuations in the power generation. Similarly, when the wake reduction due to curtailment hits the next downstream turbine, its power will not increase instantaneously.

Increase
Rotational Speed

When the increase of wind speed - due to the reduced wake effect - is available for a while, the increased thrust force will lead to a higher power production. However, at higher wind speeds wind turbines generally operate at higher rotational speeds. Therefore, some part of the additional energy in the reduced wake will go to accelerating the rotor and is therefore not available as wind power for the turbine. In this section it is studied if a correction factor is feasible to correct for this additional power during the transient response of downstream turbines.

Increase
Rotational
Energy

The kinetic energy of a rotating object can be calculated using equation C.1, where I refers to the rotational moment of inertia of the object and ω to the rotational speed in rad. The rotational speed of the rotor for the turbine of Westermeerwind, is estimated in appendix E to be $19 Mkgm^2$. The increase of rotational energy of turbine #2 between the steady state responses of the two operation modes of turbine #1 can therefore be calculated, using equation C.2.

$$E_{rot} = \frac{1}{2} I \omega^2 \tag{C.1}$$

$$\Delta E_{rot} = \frac{1}{2} I \left(\omega^2_{curtailed} - \omega^2_{normal} \right) \tag{C.2}$$

Continuing…

C.2 Correction Kinetic Energy Rotor,   Continued

Power
Production
During Transient

Because the upwards transient response of turbine #2 is not instant, there is a loss of power production during the transient. However, after the curtailment experiment, turbine #2 does not instantly go instantly back to its original production, resulting in extra power production. This is visualized in figure C.1, which is the data of experiment 2. The upper figure shows the power production of turbine #2, where the shaded are is either the missed power with respect to the steady state during curtailment or the extra power with respect to normal production.

Comparison
Approach

Figure C.1 also shows the increase of the rotational speed, where the shaded areas indicate the difference with respect to the steady state values. Especially for the right tail it is clear that indicating the exact period of the transient response if very difficult. By integrating the power of the shaded area in the upper figure and comparing it with the result of equation C.2 it can be seen if the loss or extra power is due to the difference in rotational speed. Equation C.2 results in a difference in rotational energy of $18MJ$. The area of the left tail of equals $27MJ$ and the area of the right equals $42MJ$.

Conclusion

For the upwards transient response of turbine #2 67% of the missed power is due to the increase of the rotational speed of the rotor. Including this effect in the available power calculation of the algorithm is therefore considered reasonable. For the downwards transient response, however, this effect is 42%, which could be due to the longer duration of the response. Including this effect is considered reasonable as well, but further study to the transient response is need to be able to model is better.
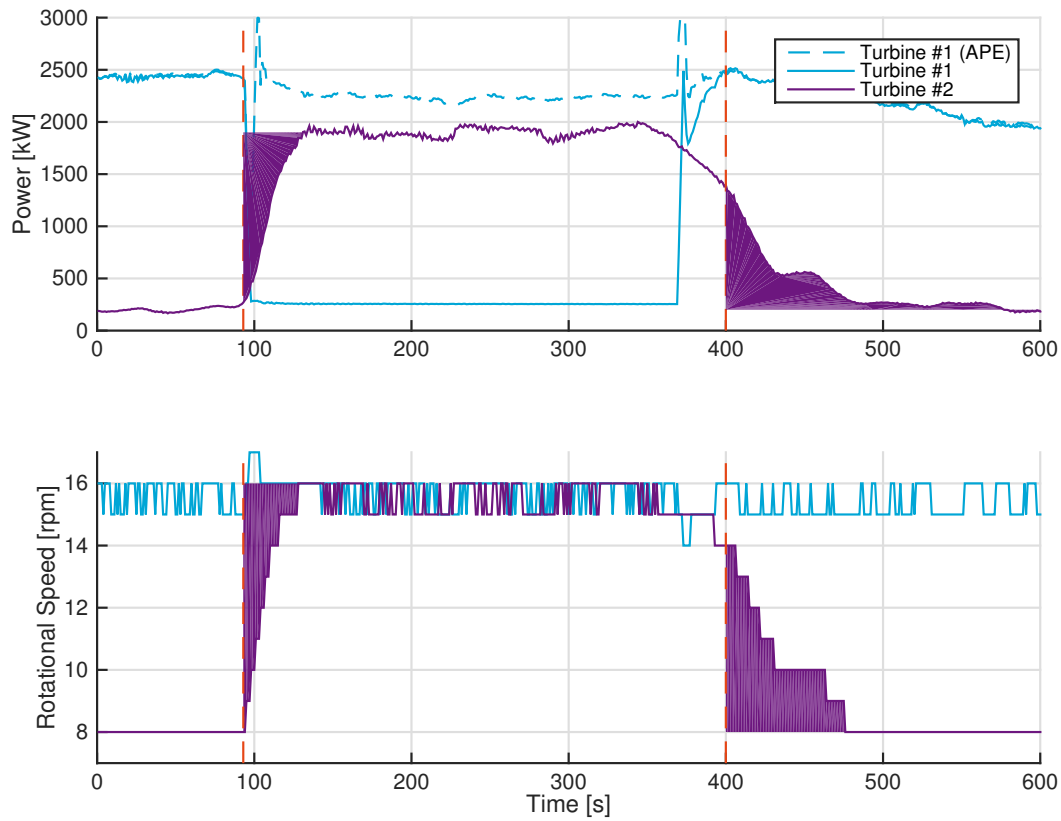
Figure C.1: The measured power production and rotational speed of turbine #1 and #2 during experiment 2. The shaded area in the upper figure indicate the missed or extra power production during the transient response of turbine #2. The shaded area of the lower figure indicate the difference in the rotational speed with respect to the steady state values.

D

DETERMINING ERROR OF THE TURBULENCE INTENSITY

In this appendix the error will be determined by calculating the turbulence intensity using both the power production and the sonic sensor.

D.1 Error Derivation

<div></div>

Error Wind Speed

As mentioned, the accuracy of the sonic sensor is $\pm 0.5 \frac{m}{s}$. In this appendix the resulting error on the turbulence intensity (TI) is determined as a result of this uncertainty of the wind speed data signal.

<div></div>

Calculating TI

The TI is calculated as a function of the sample standard deviation and the mean wind speed as in equation D.1. The effect of the error on these variables need to be determined first.

$$TI = \frac{s_u}{\bar{u}} \tag{D.1}$$

Continuing…

D.1 Error Derivation, Continued

Error of Mean
Wind Speed

First, the effect of the error on the mean wind speed is studied. This can be done by adding the term Δu_i, which is the error of each measurement, see derivation D.2. In the last step of this derivation the assumption is made that every experiment has the highest possible error that the sensor can have: Δu. As shown in figure 8.4 this is $0.5 \frac{m}{s}$.

$$
\begin{aligned}
\hat{\bar{u}} &= \frac{1}{N} \sum (u_i \pm \Delta u_i) \\
&= \frac{1}{N} \sum u_i \pm \frac{1}{N} \sum \Delta u_i \\
&= \bar{u} \pm \Delta u
\end{aligned}
\tag{D.2}
$$

Continuing…

D.1 Error Derivation, Continued

Error of Standard Deviation

Second, the effect of the error on the standard deviation can be calculated. In the definition of the standard deviation, see the first line of derrivation D.3, and error is taken into account for every measurement u_i. Also, the mean wind speed as calculated from the sensor is used. However, the actual mean wind speed is required for the definition. Therefore an additional error has to be added, resulting from equation D.2.

$$
\begin{aligned}
\hat{s}_u &= \sqrt{\frac{1}{N-1} \sum \left(u_i - \hat{\bar{u}} + \Delta u_i\right)^2} \\
&= \sqrt{\frac{1}{N-1} \sum (u_i - \bar{u} + 2\Delta u_i)^2} \\
&= \sqrt{\frac{1}{N-1} \sum \left[(u_i - \bar{u})^2 + 4\Delta u_i^2 + \Delta u_i (u_i - \bar{u})\right]} \\
&= \sqrt{\frac{1}{N-1} \sum (u_i - \bar{u})^2 + \frac{1}{N-1} \sum 4\Delta u_i^2 + \frac{1}{N-1} \sum \Delta u_i (u_i - \bar{u})}
\end{aligned}
\tag{D.3}
$$

The sum $\sum (u_i - \bar{u})$ goes to zero following the definition of calculating the average. For large values of N one can also simplify the second ther in the equation, assuming worst cases $\Delta u_i = \Delta u = \pm 0.5 \frac{m}{s}$.

$$
\frac{1}{N-1} \sum \Delta u_i^2 = \frac{N\Delta u^2}{N-1} \approx \Delta u^2
\tag{D.4}
$$

This leads to standard deviation including the measurement error on the wind speed as follows.

$$
\begin{aligned}
\hat{s}_u &= \sqrt{\frac{1}{N-1} \sum (u_i - \bar{u})^2 + 4\Delta u^2} \\
&= \sqrt{s_u^2 + 4\Delta u^2}
\end{aligned}
\tag{D.5}
$$

Continuing…

D.1 Error Derivation, Continued

Error of the TI   Implementing these results into equation D.1 allows to determine the error of the turbulence intensity due to the error in wind speed measurements.

$$
\begin{aligned}
\hat{T}I &= \frac{\hat{s}_u}{\hat{\bar{u}}} \\
&= \frac{\sqrt{s_u^2 \pm 4\Delta u^2}}{\bar{u} \pm \Delta u}
\end{aligned}
\tag{D.6}
$$

The error of the turbulence intensity can now be calculated.

$$
\begin{aligned}
error_{TI} &= TI - \hat{T}I \\
&= TI - \frac{\sqrt{TI^2 \bar{u}^2 \pm 4\Delta u^2}}{\bar{u} \pm \Delta u}
\end{aligned}
\tag{D.7}
$$

Alternative
Method Using
Power Curve

An improvement can be made by using the mean wind from the power curve as explainend in section 8.1 Measurement Context . Due to the turbulence and rotor inertia this method does not return the mean wind speed instantaneously. However, when using enough data points it does converge to the mean wind speed.

Continuing…

D.1 Error Derivation, Continued

Error of the TI Power Curve Method

The error of this hybrid turbulence intensity calculation can be determined by implementing $\hat{\bar{u}} = \mathscr{P}^{-1}(P + \Delta P) = \bar{u} + \Delta u_P(u)$. The error in the power measurement (ΔP) has a maximum of 0.2% of the power production. Another error, is from the power curve itself. This has been determined by DTU on its Høvsøre test facility. It depends on the wind speed, but is commonly lower than 1% above $8\frac{m}{s}$. Figure D.1 shows the error of this method due to these two errors. It can be seen that the error in estimating the mean wind speed is much lower than using the sonic sensor. The final estimation of the error is stated in equation D.8, see figure D.2.

$$error_{TI,\mathscr{P}^{-1}} = TI - \frac{\sqrt{TI^2 \bar{u}^2 \pm (\Delta u + \Delta u_P(u))^2}}{\bar{u} + \Delta u_P(u)} \tag{D.8}$$

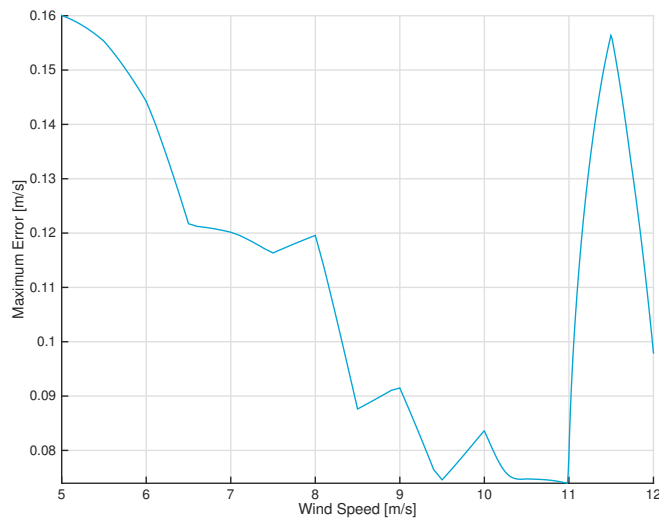Figure D.1: Error of the wind speed using the power curve method
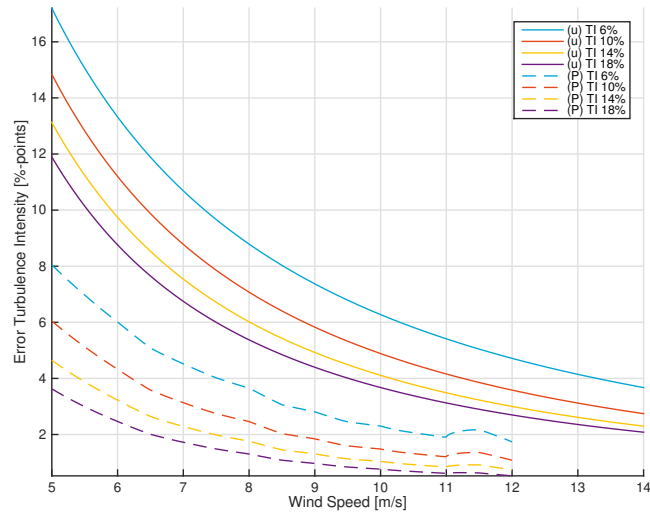
D.1 Error Derivation, Continued

Figure D.2: Absolute error in %-points of the turbulence intensity for different actual values of the the turbuelence intensity using sonic sensor for mean (u) or the power curve (P)

Continuing…

D.1 Error Derivation, Continued

Comparison Methods

Both methods are shown in figure D.2 for several values of the actual turbulence intensity. Two conclusions can be drawn.

1. The method of using the power curve (P) performs better than using the sonic sensor (u) for the mean wind speed.

2. The error is still considerable is most of the domain, but from about $7\frac{m}{s}$ the error is smaller than $3.2\% - points$ for more than 10% of turbulence.

Note that in this analysis always the worst case (maximum error) is assumed.

Conclusion

As long as the validation is not performed at low wind speeds, using the turbulence intensity with this method is deemed reasonable. It has to be tested how sensitive the wake models are to the turbulence intensity in order to set error limits on the wake effect.

E

DETERMINING MOMENT OF INERTIA ROTOR

In this appendix the moment of inertia of the rotor is estimated as part of the suggested kinetic correction of appendix C.

E.1 Moment of Inertia

Moment of
Inertia

In order to quantify the inertial response of the rotor on an increase of incoming wind speed, the mass moment of inertia (MOI) of the rotor - drive train assembly needs to be determined. This assembly consists of the following heavy parts:

- Hub

- Generator (rotating part) and shaft

- Blades

Continuing. . .

E.1 Moment of Inertia,   Continued

Hub

From back of the envelope calculations and a report from NREL [38], a significant difference in the order of magnitude for the mentioned parts were found. For the 5 MW NREL, the hub weighs $57t$ and has a MOI of $0.12 \cdot 10^6 kg m^2$. The dimensions of the hubs are comparable, but the weight of the hub of the SWT-3.0-108 of this research is $32t$ [30]. Linearly adjusting for this weight, results in a MOI of $0.07 \cdot 10^6$. Using a simple solid disk of with a radius of $4.2m$ results is the same MOI.

Generator

The NREL report mentions a MOI of the generator drive train of $0.53 \cdot 10^6 kg m^2$, however no weights and dimensions are given. Also, it considers a turbine with a gearbox. The rotating part of the direct drive generator of the SWT-3.0-108 weighs about $40t$ and is approximated by a ring with an outer radius of $2.1m$ and inner radius of $1.7m$. This results in a MOI of $0.15 \cdot 10^6 kg m^2$, which seems reasonable comparing with the NREL report.

Blades

From blade measurement reports of Ventolines BV the average centroid and weight of the blades were determined. An average MOI due to the Steiner term was estimated to be $3.4 \cdot 10^6 kg m^2$ per blade. The MOI of the blade around its centroid was calculated by modelling the blade as two infinite thin but rigid rods starting at the centroid. The weight of the blade is split evenly over these two rods. This results in a total MOI of $6.2 \cdot 10^6 kg m^2$ per blade.

Conclusion

From the analysis above it can be concluded that the three blades contribute to more than 97% of the total MOI. Combining the MOI of the hub, generator and the three blades equals $19 kg m^2$.